

FRONTS IN THE INDIAN OCEAN SECTOR  
OF  
SOUTHERN OCEAN

THESIS SUBMITTED TO THE  
COCHIN UNIVERSITY OF SCIENCE AND TECHNOLOGY  
FOR THE DEGREE  
OF  
DOCTOR OF PHILOSOPHY  
IN  
PHYSICAL OCEANOGRAPHY

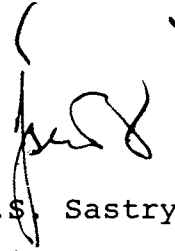
*BY*  
**HARILAL B. MENON, *M. Sc.***

PHYSICAL OCEANOGRAPHY DIVISION  
NATIONAL INSTITUTE OF OCEANOGRAPHY  
GOA – 403 004

FEBRUARY, 1990

C E R T I F I C A T E

This to Certify that this thesis is an authentic record of research work carried out by **Shri Harilal B. Menon**, M.Sc. under my supervision and guidance in the Physical Oceanography Division of National Institute of Oceanography and no part of this has previously formed the basis for the award of any other Degree or Diploma to any University.



Dr. J.S. Sastry  
(Supervising Teacher)

Deputy Director and Head,  
Physical Oceanography Division,  
National Institute of Oceanography

Dona Paula,  
GOA - 403 004.

## P R E F A C E

In recent years an increased attention has been paid on frontal research in different parts of the World Ocean. Fronts in the Southern Ocean are of planetary scale nature and our attempts to study them are hampered by the remoteness of the oceanic area as well as by the environmental difficulties for working in the Southern Ocean. Except in the Drake Passage, the earlier investigations were of opportunity type in the sense that during a cruise an oceanic front was unexpectedly discovered, resulting only in a brief investigation of the frontal phenomenon. However, in the recent past, more systematic investigations have been carried out using highly sophisticated instruments in the Atlantic and Pacific Sectors of the Southern Ocean. Though some efforts were also made to examine fronts in the Indian Ocean sector, the information is still fragmentary.

In the coming years, the research covering the dynamics of the fronts and their effects on biological, acoustic and atmospheric processes will be intensified. Therefore, it is felt that a detailed account of frontal characteristics in the Southern Ocean from the archived

data might be useful as a baseline information before accelerating our efforts to understand the influence of fronts.

The present thesis is an outcome of the work carried out on fronts in the Indian Ocean sector of Southern Ocean.

The thesis is divided into seven Chapters. Chapter I consists of introduction to oceanic fronts in general with special relevance to those in the Southern Ocean. Details of data used and the methods of analysis adopted in the present study have been given in Chapter II. The hydrographic property distributions at selected meridians are presented in Chapter III and the zonal volume flux at different fronts has been dealt in Chapter IV. The importance of the Southern Ocean fronts as productive zones is shown in Chapter V. The major characteristics of Southern Ocean fronts such as their mean location, width, the gradients in hydrographic properties across them and their contribution to ACC in the western and eastern regions of the Indian Ocean sector of the Southern Ocean are discussed in Chapter VI. Finally the last Chapter VII includes the summary and conclusion arrived at.

# C O N T E N T S

	Page No.
PREFACE	i - ii
Acknowledgement	iii - V
List of Figures	Vi - iX
List of Tables	X
CHAPTER - I Introduction	1
1.1 Oceanic Fronts and General Characteristics	2 - 6
1.2 Southern Ocean Circulation and Fronts	7 - 8
1.2.1 Antarctic Circumpolar Current	8 - 9
1.2.2 Antarctic Convergence (Antarctic Polar Front)	9 - 12
1.2.3 Sub-Tropical Convergence (Sub-Tropical Front)	12 - 14
1.2.4 Sub-Antarctic Convergence (Sub-Antarctic Front)	14 - 15
1.3 Studies in the Indian Ocean sector of Southern Ocean	15 - 17
CHAPTER - II Data and Methods of Analysis	18 - 19
2.1 Identification of fronts	19 - 22
2.2 Methods to identify fronts from surface observation data	22 - 23
2.3 Data used	23 - 24
2.4 Computation of zonal volume flux	24 - 28
2.5 Computation of heat content	28 - 29

	Page No.
CHAPTER - III Hydrographic properties along different meridians	30- 31
3.1 Temperature distribution	31
3.1.1 Along 20°E	31 - 33
3.1.2 Along 30°E	33 - 34
3.1.3 Along 35°E	34 - 35
3.1.4 Along 40°E	35 - 36
3.1.5 Along 45°E	36
3.1.6 Along 55°E	36 - 37
3.1.7 Along 85°E	37 - 38
3.1.8 Along 95°E	39
3.1.9 Along 100°E	39-40
3.1.10 Along 105°E	40-41
3.1.11 Along 110°E	41
3.1.12 Along 115°E	41-42
3.2 Salinity	42- 43
3.2.1 Along 20°E	43
3.2.2 Along 30°E	43- 44
3.2.3 Along 35°E	45
3.2.4 Along 40°E	45 - 46
3.2.5 Along 45°E	46
3.2.6 Along 55°E	46 - 47
3.2.7 Along 85°E	47 - 48
3.2.8 Along 95°E	48
3.2.9 Along 100°E	48 - 49

		Page No.
3.2.10	Along 105°E	49
3.2.11	Along 110°E	49 - 50
3.2.12	Along 115°E	50
3.3	Thermosteric anomaly	50
3.3.1	Along 20°E	50-51
3.3.2	Along 30°E	51
3.3.3	Along 35°E	51-52
3.3.4	Along 40°E	52
3.3.5	Along 45°E	52
3.3.6	Along 55°E	53
3.3.7	Along 85°E	53- 54
3.3.8	Along 95°E	54
3.3.9	Along 100°E	54 - 55
3.3.10	Along 105°E	55
3.3.11	Along 110°E	55
3.3.12	Along 115°E	56
3.4	Heat content	56-58
CHAPTER - IV Zonal volume flux at frontal zones		59-60
4.1	Along 20°E	60-62
4.2	Along 30°E	62-63
4.3	Along 35°E	63-64
4.4	Along 40°E	64- 65
4.5	Along 45°E	65-66
4.6	Along 55°E	66-67

	Page No.	
4.7	Along 85°E	67-69
4.8	Along 95°E	69-70
4.9	Along 100°E	70-71
4.10	Along 105°E	71-72
4.11	Along 110°E	72-73
4.12	Along 115°E	73-76
CHAPTER - V Fronts and Productivity		77
5.1	Classification of waters into different regimes	78-80
5.2	Fronts in the western region of the study area	80
5.2.1	Sub-Tropical Front (STF)	80-81
5.2.2	Antarctic Polar Front (APF)	81
5.3	Fronts in the eastern region of the study area	81-82
5.3.1	Sub-Tropical Front (STF)	82-83
5.3.2	Sub-Antarctic Front (SAF)	83
5.3.3	Antarctic Polar Front (APF)	83-84
5.4	Meridional distribution of surface chl. <u>a</u>	84
5.4.1	Along 20°E (Between Africa and Antarctica)	84-85
5.4.2	Along 110°E (Between the western Australia and Antarctica)	85-86
5.5	Mean distribution of chl. <u>a</u> in different water regimes	86
5.5.1	In the western region	86-87
5.5.2	In the Eastern region	87-88



	Page No.
CHAPTER - VI Discussion	89-90
Fronts in the Indian Ocean sector of Southern Ocean	
6.1 Sub-Tropical Front (STF)	90-92
6.2 Sub-Antarctic Front (SAF)	92-94
6.3 Antarctic Polar Front (APF)	94-98
6.4 Volume Transport	98-104
6.5 Productivity at the frontal zones	105-108
6.6 Heat content associated with the front	108-109
CHAPTER - VII Summary and Conclusion	110-118
REFERENCES	119-133

## LIST OF FIGURES

- Fig. 1.1 Bathymetry of the study area
- Fig. 1.2 Movement of watermasses in the Southern Ocean
- Fig. 1.3 Regime of surface currents in the Indian Ocean sector of Southern Ocean.
- Fig. 2.1 Map showing the station positions of selected twelve hydrographical sections
- Fig. 3.1.1 Vertical section of temperature along 20°E
- Fig. 3.1.2 Vertical section of temperature along 30°E
- Fig. 3.1.3 Vertical section of temperature along 35°E
- Fig. 3.1.4 Vertical section of temperature along 40°E
- Fig. 3.1.5 Vertical section of temperature along 45°E
- Fig. 3.1.6 Vertical section of temperature along 55°E
- Fig. 3.1.7 Vertical section of temperature along 85°E
- Fig. 3.1.8 Vertical section of temperature along 95°E
- Fig. 3.1.9 Vertical section of temperature along 100°E
- Fig. 3.1.10 Vertical section of temperature along 105°E
- Fig. 3.1.11 Vertical section of temperature along 110°E
- Fig. 3.1.12 Vertical section of temperature along 115°E
- Fig. 3.2.1 Vertical section of salinity along 20°E
- Fig. 3.2.2 Vertical section of salinity along 30°E
- Fig. 3.2.3 Vertical section of salinity along 35°E
- Fig. 3.2.4 Vertical section of salinity along 40°E
- Fig. 3.2.5 Vertical section of salinity along 45°E

- Fig. 3.2.6 Vertical section of salinity along 55°E
- Fig. 3.2.7 Vertical section of salinity along 85°E
- Fig. 3.2.8 Vertical section of salinity along 95°E
- Fig. 3.2.9 Vertical section of salinity along 100°E
- Fig. 3.2.10 Vertical section of salinity along 105°E
- Fig. 3.2.11 Vertical section of salinity along 110°E
- Fig. 3.2.12 Vertical section of salinity along 115°E
- Fig. 3.3.1 Vertical section of thermosteric anomaly along 20°E
- Fig. 3.3.2 Vertical section of thermosteric anomaly along 30°E
- Fig. 3.3.3 Vertical section of thermosteric anomaly along 35°E
- Fig. 3.3.4 Vertical section of thermosteric anomaly along 40°E
- Fig. 3.3.5 Vertical section of thermosteric anomaly along 45°E
- Fig. 3.3.6 Vertical section of thermosteric anomaly along 55°E
- Fig. 3.3.7 Vertical section of thermosteric anomaly along 85°E
- Fig. 3.3.8 Vertical section of thermosteric anomaly along 95°E
- Fig. 3.3.9 Vertical section of thermosteric anomaly along 100°E
- Fig. 3.3.10 Vertical section of thermosteric anomaly along 105°E
- Fig. 3.3.11 Vertical section of thermosteric anomaly along 110°E
- Fig. 3.3.12 Vertical section of thermosteric anomaly along 115°E
- Fig. 3.4.1 Variation of heat content at different fronts along 20°E
- Fig. 3.4.2 Variation of heat content at different fronts along 30°E
- Fig. 3.4.3 Variation of heat content at different fronts along 35°E

- Fig. 3.4.4 Variation of heat content at different fronts along 40°E
- Fig. 3.4.5 Variation of heat content at different fronts along 45°E
- Fig. 3.4.6 Variation of heat content at different fronts along 55°E
- Fig. 3.4.7 Variation of heat content at different fronts along 85°E
- Fig. 3.4.8 Variation of heat content at different fronts along 95°E
- Fig. 3.4.9 Variation of heat content at different fronts along 100°E
- Fig. 3.4.10 Variation of heat content at different fronts along 105°E
- Fig. 3.4.11 Variation of heat content at different fronts along 110°E
- Fig. 3.4.12 Variation of heat content at different fronts along 115°E
- Fig. 4.1 Zonal volume flux along 20°E
- Fig. 4.2 Zonal volume flux along 30°E
- Fig. 4.3 Zonal volume flux along 35°E
- Fig. 4.4 Zonal volume flux along 40°E
- Fig. 4.5 Zonal volume flux along 45°E
- Fig. 4.6 Zonal volume flux along 55°E
- Fig. 4.7 Zonal volume flux along 85°E
- Fig. 4.8 Zonal volume flux along 95°E
- Fig. 4.9 Zonal volume flux along 100°E
- Fig. 4.10 Zonal volume flux along 105°E
- Fig. 4.11 Zonal volume flux along 110°E

- Fig. 4.12 Zonal volume flux along 115°E
- Fig. 4.13 Zonal volume flux across different meridians in the Indian Ocean sector of Southern Ocean and its components associated with various fronts (STF, SAF and APF)
- Fig. 5.2.1 Latitudinal locations of surface and subsurface observation of three fronts
- Fig. 5.4.1 Meridional distribution of surface chlorophyll. a along 20°E
- Fig. 5.4.2 Meridional distribution of surface chlorophyll. a along 110°E
- Fig. 5.5.1 Surface chlorophyll. a distribution in the western region
- Fig. 5.5.2 Surface chlorophyll. a distribution in the eastern region
- Fig. 6.1 Schematic diagram showing the dynamic nature of the fronts in the study area

## LIST OF TABLES

- Table 2.1 Details of data used
- A Hydrographic data
  - B Expendable Bathy-Thermograph (XBT) data
  - C Surface temperature data
- Table 2.2 Details of Chlorophyll a data used
- Table 5.2.1 Fronts in the western region of the Indian Ocean sector of Southern Ocean
- Table 5.3.1 Fronts in the eastern region of the Indian Ocean sector of Southern Ocean

# *CHAPTER - I*

## INTRODUCTION

The remote position of the Southern Ocean conceals the general knowledge about the processes occurring in the high latitudes. The Southern Ocean has been recognized as an ocean area of special global relevance only after Discovery I (1925 - 1930) expeditions by British oceanographers, laying the foundation of our knowledge of the Southern Ocean. Not only <sup>does this</sup> ~~the~~ ocean with a zonal flow around the globe linking ~~ing~~ the three major oceans, but it also initiates the deep ocean circulation through the deep Antarctic Convection (bottom water formation), which in turn, maintains the main thermocline throughout the world ocean. This deep convection further causes the Southern Ocean to act as a largest ~~t~~ heat sink, thus forming a strong link between ocean and atmosphere. The permanent convergences or fronts (Antarctic Polar Front - APF and Sub Tropical Front - STF) in the Southern Ocean are responsible for the intermediate depth circulation of the world ocean. The sources of Antarctic Intermediate Water and Central Watermasses are APF and STF. The Southern Ocean is an important study area for understanding the world's climate and its changing conditions, as planetary scale fronts play an important role <sup>in</sup> ~~to~~ controlling meridional heat flux from lower to higher latitudes.



### 1.1 Ocean Fronts and general characteristics:

An oceanic front is a sharp boundary zone between adjacent watermasses of dissimilar properties. It is recognised by the discontinuity in the properties of watermasses in the horizontal direction. The fronts are characterised with gliding and sliding of watermasses of different densities.

Fronts are important in the study of the oceanic dynamics. Interacting with atmosphere, fronts generate atmospheric disturbances. Large scale fronts have significant role in controlling weather and climate. Hence an understanding of their cause and effect is necessary in forecasting global climate. The design of fishing strategies for maximum yields involves a detailed knowledge of the locations of oceanic fronts which are normally associated with higher biological productivity. Pingree and Mardell (1981) reported biological enhancement at tidal fronts in the shelf seas around the British Islands. The northern edge of the subtropical convergence has been associated with a high fishery resource (Planke, 1977). As a region of convergence, fronts concentrate pollutants. Cadavers, small boats and swimmers can also be trapped into them. A

knowledge on the locations of fronts is necessary to design the marine based discharge outfalls and for the agencies charged with search and rescue operations.

Oceanic fronts generally have large surface gradients either in temperature or salinity or both. The thermal and haline gradients can reinforce each other forming strong density fronts or they can compensate each other resulting in the weak density gradients or density compensated fronts. The density fronts are persistent and strong baroclinic zones associated with geostrophic jets. On the other hand density compensated fronts are weak baroclinic zones and are marked by the interleaving of different watermasses along surfaces of constant density. Since fronts are generally associated with sharp thermohaline gradients together with jet-like flows, they can be sources of recoverable thermal and haline energy, and also they can be the sources of mechanical energy.

Few theoretical investigations have been carried out in the field of oceanic frontal dynamics as compared to the intense research done in the case of atmospheric fronts. For a two layer model of a stationary front, Welander (1963) investigated the upwelling features along a frontal interface. Orlanski (1969) <sup>and</sup> Orlanski and Cox (1972) studied

the baroclinic instability and applied this model to the Gulf Stream front. After applying the theory in the natural case, Rao et al. (1971) found that the meanders of Gulf Stream between Miami and Hatters were unstable baroclinic waves. This model predicted average vertical motion of the order of 0.1 cm/s with a maximum value up to 1 cm/s.

A frontal interface between two watermasses is in slanting position, indicating a current shear across it. The shear depends on the slope of the interface, the Coriolis parameter and the difference in density, and can as a first approximation be expressed by the Wittee-Margules equation

$$\Delta v = \frac{g}{f} \cdot \frac{\Delta \rho}{\rho} + g \alpha$$

where  $\Delta v$  is the shear,  $\Delta \rho$  is the density difference,  $g$  is the gravity,  $f$  is the Coriolis parameter and  $\alpha$  the slope of the interface. If the slope and density difference are known from the hydrographic data, a rough estimate of the shear can be obtained.

In the ocean the probable mechanisms for the formation of fronts are horizontal shearing motion, horizontal and vertical deformation fields, differential vertical motion, surface friction, turbulent wind mixing and non-uniform

buoyancy fluxes (heating and cooling, precipitation and evaporation, river runoff, ice melt, ice brine etc). Rao and Murthy (1973) developed a theoretical model to understand the motions near the frontal zone. But the model results showed fronts as regions of divergence nature rather than convergence, thus contradicting all the field observations.

Witte (1902) and Voorhis (1969) indicated that the mixture of two watermasses at the fronts had density greater than that of either watermass, since the equation of state is nonlinear. Voorhis (1969) further stated that the turbulence due to mixing of two watermasses could result in a surface discontinuity for a longer time. The velocity with which water sinks at the front is maximum and the flow field at the front has an intense horizontal shear normal to it as water from both sides of the front are coming closer to it. Such shears are common for large scale fronts but minimal for small scale fronts. On the basis of hydrographic studies on fronts, Cromwell and Reid (1956); Knauss (1957); Voorhis and Hersey (1964); Katz (1969) and Voorhis (1969) found that the fronts were associated with sharp gradient in temperature and hence termed as thermal fronts. Horne (1978) suggested the manifestation of a front even in the presence of diffusion.

Oceanic fronts are classified into several categories. These are fronts forming (i) at subtropical convergence (Sub Tropical Front - STF), Subantarctic convergence (Sub Antarctic Front - SAF) and Antarctic Convergence (Antarctic Polar Front - APF) with planetary scale (ii) at the edges of major western boundary currents in association with intrusion of warm water of tropical origin into higher latitudes and (iii) at shelf break between the coastal and deep sea waters. In the coastal areas of pronounced upwelling, fronts also form as suggested by Collins et al. (1968); Bang (1973) and Mooers et al (1976). Coastal plume fronts form at the lateral and leading edges of river discharges (Ryther et al., 1967; Gibbs, 1970; Wright and Coleman, 1971 and Garvine and Munk, 1974). The zones of horizontal gradients in continental seas and around island banks represent the boundary between the tidally mixed nearshore waters and stratified deeper offshore waters. The equatorial fronts forming in response to the winds were studied by Wyrtki (1966). The equatorial front in the eastern Pacific Ocean separates the cold saline waters of the Peru Current from the warm fresher tropical waters (Pak and Zaneveld, 1974).

## 1.2 Southern Ocean Circulation and Fronts:

The southern extent of the world ocean was established for the first time by James Cook after his historic voyage to Antarctica in the 18th Century (1772-1773). Germans had acquired some knowledge about the circumpolar water and the convergence zones in the early 19th century. However, vigorous investigations were started on the Southern Ocean only around the middle of 20th century as a part of the International Geophysical Year (1957-1958). For the first time, mechanical bathythermograph data provided a high resolution picture of the thermal structure of frontal zones and indicated the existence of eddies within them (Wexler, 1959). The presence of high meridional temperature gradient in the surface waters around 50°S, first reported by Meinardus (1923) during German South Polar Expedition during 1901-1902, had drawn the attention of several investigators as a favourite study topic of the Southern Ocean. The earlier studies to explain the circumpolar nature of the Southern Ocean and its convergence zones were mainly limited to its Atlantic sector and were those of Brennecke (1921); Drygalski (1926); Deacon (1933); Sverdrup (1933); Wüst (1933, 1935) and Mosby (1934). In the Pacific Ocean sector of the Southern Ocean, convergence nature was studied by

Midttur and Natvig (1957); Burling (1961) and Gordon (1967a). But in the Indian Ocean sector the information is largely of fragmentary nature and it is known only in the southwestern (Gordon and Goldberg, 1970; Wyrтки, 1971) and in the Australian (Gordon and Rodman, 1977) sectors.

### 1.2.1 Antarctic Circumpolar Current:

Several studies of both earlier and recent type made by Deacon (1933, 1937, 1945, 1964, 1976, 1977, 1979, 1982, 1983, 1984) indicated that the circulation in the Southern Ocean is dominated by an eastward flowing Antarctic Circumpolar Current (ACC) extending to the deeper depths with a transport of the order of 125 SV (1 SV =  $10^6$  cm<sup>3</sup>/s). Waters in the south are ~~more~~ denser than in the north and hence the flow is predominantly ~~of~~ baroclinic in nature. Gordon (1971b) indicated that the surface velocity of ACC is generally less than 30 cm/s with lesser vertical shear. ACC is associated with a baroclinic structure resulting from the surfacing of the main thermocline (Wyrтки, 1973).

The frictional stress due to westerly winds combined with the Coriolis force gives rise to a northward component - Antarctic Surface Water (ASW). Current meter records coupled with the hydrographic observations in the Drake Passage

established that ACC was strongly baroclinic (Nowlin et al., 1977; Bryden and Pillsbury, 1977). Several transport estimates on ACC were made using the data collected in 1975 under International Southern Ocean Studies (ISOS) Programme. These established a reliable value of 125 Sv as the total transport of ACC. However, the ISOS studies were mainly concentrated in the Drake Passage and in the southeast off New Zealand (Gordon, 1967; Reid and Nowlin, 1971; Foster, 1972 and Bryden and Pillsbury, 1977). The processes which maintain the Antarctic Circumpolar Current have not yet been identified. Hidaka and Tsuchiya (1953) applied basic ideas regarding general ocean circulation to the Southern Ocean by treating it as a wind driven circulation in a zonal annulus. Four major mechanisms namely: (i) Drag due to bottom topography (Munk and Palmen, 1951) (ii) Thermodynamic effects (Fofonoff, 1955) (iii) Non-zonal dynamics (Stommel, 1957) and (iv) Freshwater discharge from Antarctic continent (Barcilon, 1966, 1967) were considered. While deriving the Southern Ocean circulation, Stommel (1957) pointed out the difficulty in considering the circumpolar current as mainly zonal, since coefficients of viscosity needed to maintain an overall equilibrium with wind field should be much greater than those generally accepted.



### 1.2.2 Antarctic Convergence (Antarctic Polar Front):

The surface waters in the Antarctic zone south of Antarctic Convergence generally have temperature less than  $2^{\circ}\text{C}$  (Gordon et al., 1977a). The surface temperature in this zone varies from  $-1.9^{\circ}\text{C}$  to  $1^{\circ}\text{C}$  in winter and from  $-1.9^{\circ}\text{C}$  to  $4^{\circ}\text{C}$  in summer while salinity is normally less than 34.5‰. Antarctic surface waters are thus considered as cold freshwaters with both higher oxyty and nutrient content (Whitworth and Nowlin, 1987). Below Antarctic surface waters, temperature increases with depth to around  $1^{\circ}\text{C}$  due to spreading of Circumpolar Deep Waters (CDW) from north. The CDW is also identified by the salinity maximum (Deacon, 1933, 1937a and Wust, 1936) and is embed<sup>d</sup> in the depth range of 500 to 1000 m (Gordon and Molinelli, 1975). Fifty per cent of the total volume transport of ACC comprises of CDW and the properties of CDW vary considerably along the axis of ACC (Gordon and Rodman, 1977). The ~~most~~ warm<sup>est</sup> and saltiest Circumpolar Deep Water is found south of Africa, whereas the ~~most~~ cold<sup>est</sup> and freshest deep water is encountered in the Drake Passage (Georgi, 1981a).

↳ Preferably give a global map of each place

Oceanographic surveys in the Southern Ocean during recent years, especially those carried out on board ELTANIN

enhanced our picture of thermohaline stratification, watermasses and fronts. The Antarctic polar front splits into two - primary and secondary ones, due to the complexity of thermal structure (Gordan, 1967, 1971). In his study Gordon (1971) noticed a double frontal structure at the Antarctic Polar Front (APF) in the south Pacific and suggested the possible mechanism of its formation as due to either wind or bottom topographic effects.

There was a bit <sup>of</sup> confusion in the beginning among scientists regarding the nomenclature of Antarctic convergence (AC). The AC in the Atlantic Ocean was observed for the first time by Meinardus (1923). Later Schott (1926) named it as "Meinardus line". Subsequently, Defant (1928); Wust (1928); Deacon (1933, 1937a); Mackintosh (1948) and Houtman (1964) described it as Polar Front. Gordon (1971) in his extensive studies used the nomenclature "Antarctic Polar Front" consistently referring to the meeting place of the two water bodies (Antarctic Surface Waters and Subantarctic Waters).

Polar frontal zone is a narrow transition zone separating the Antarctic and Subantarctic regions (Gordon 1971a). At the polar frontal zone, the cold surface waters of Antarctic origin slips below and mixes with the warmer water. Strong eddies and interleaving of cold and warm

waters are observed at the Antarctic Polar Front (Gordon et al., 1977b; Georgi, 1978 and Joyce et al., 1978).

A statistical analysis of all the data available since 1956 in the Indian Ocean between Africa and Antarctic continents was made by Lutjeharms (1979). The results show that the meso-scale disturbances in the Southern Ocean are not homogeneous in their characteristics. These disturbances are dependent on topographical features, such as mid ocean ridges and are dominant in the vicinity of Agulhas Front and the Antarctic Polar Front. Investigations on the dynamics of the fronts and the circulation in the Indian Ocean sector of the Southern Ocean south of Africa have been made by Taylor et al. (1978); Lutjeharms et al. (1981); Lutjeharms and Emery (1983); Lutjeharms and Walters (1985) and Lutjeharms (1985); Lutjeharms and Foldvik (1986).

### **1.2.3 Sub-Tropical Convergence (Sub-Tropical Front):**

During the Meteor voyage (1925-1927) scientists noticed another sharp thermal gradient around 41°S southeast of Cape Town (along 22°E). The convergence (Sub Tropical Front STF) associated with this gradient is a transition zone between cold less saline subantarctic waters and warmer subtropical saline waters. In his extensive studies in the

Southern Ocean, Wüst (1933) observed a temperature change of  $9.1^{\circ}\text{C}$  within 5 to 6 miles. Bohnecke (1938) suggested the name 'West Wind Drift Front' to the subtropical front. In the New Zealand sector, the STF approximately follows  $15^{\circ}\text{C}$  surface isotherm in summer and  $10^{\circ}\text{C}$  surface isotherm in winter and surface salinity isopleth of 34.75‰ (Garner, 1959). But the examination of historical data (Zillman, 1970) on the basis of 43 crossings across the Southern Ocean revealed patches of more saline water reaching upto  $48^{\circ}\text{S}$ . The STF shifts to the south in the western regions of the oceans, where warmer tropical water is carried southwards by the Brazil Current, the Agulhas Current and East Australian Current in the Atlantic, Indian and Pacific Oceans respectively. Deacon (1982) noted that it was the position at which Ekman drift was found decreasing rapidly and he further indicated that this boundary was around  $42^{\circ}\text{S}$  in South Atlantic. The STF in the Indian Ocean region south of Africa is a wide tumultuous front with variable planetary waves and eddy shedding out (Lutjeharms, 1981a) and is positioned at  $42^{\circ}\text{S}$  (Lutjeharms and Valentine, 1984).

Subantarctic zone extending between STF and APF is a continuous band around the Antarctic continent except at the Drake Passage. Both temperature and salinity increase to the north, attaining a maximum gradient at about 300 km north of

the polar frontal zone (Gordon et al., 1977a). The subantarctic surface water is warmer with a temperature range of 11.5-13°C in winter and 14.5-16°C in summer and is saltier than the Antarctic zone waters (Molinelli, 1979). At the northern part of the ACC, it is influenced by the adjacent subtropical gyres as well as by air-sea exchanges along its circumpolar path (Whitworth and Nowlin, 1987). Below the surface layer is a halocline that marks the transition to Antarctic Intermediate Water - a salinity minimum layer between 400 and 1000 m formed by mixing of Antarctic and subantarctic surface waters at the Antarctic polar frontal zone (Deacon, 1933; Wüst, 1936; Deacon, 1937a; Callahan, 1972 and Emery 1977).

McCartney (1977) hypothesizes that the Antarctic Intermediate Water is an extreme type of subantarctic mode water formed by atmospheric effects on the surface waters north of polar front. But the conventional view is that the primary source of the Antarctic Intermediate Water is a product of cross frontal mixing in the vicinity of polar front (Gordon et al., 1977a, 1977b; Molinelli 1978, 1981).

#### 1.2.4 Sub-Antarctic Convergence (Sub-Antarctic Front):

A third front, subantarctic front (SAF), in addition to STF and APF, was postulated first on theoretical grounds by Ivanov (1959, 1961) and the same was observed south of New Zealand by Burling (1961). In the region between Australia and Antarctica, Zillman (1970) described the Sub Antarctic Front as the most prominent feature of the SST decrease exceeding horizontal thermal gradients of both STF and APF. Emery (1977) described that SAF was an intense convergence zone within the subantarctic region and the northern edge of the convergence is associated with a temperature of 8°C and salinity 34.5‰. Sievers and Emery (1978) were of opinion that a similar structure of front exists in Drake Passage. Lutjeharms et al. (1981) hinted the existence of such a front below <sup>South of</sup> Africa. They also stated that it was manifested as a subsurface temperature gradient lying between 3 and 5°C at about 40°S. This feature occurs over the width of Pacific Ocean as well as south of Australia but its existence was doubtful in the west Atlantic and west Pacific Oceans (Edwards and Emery, 1982).



FIG. 1.1 BATHYMETRY OF THE STUDY AREA

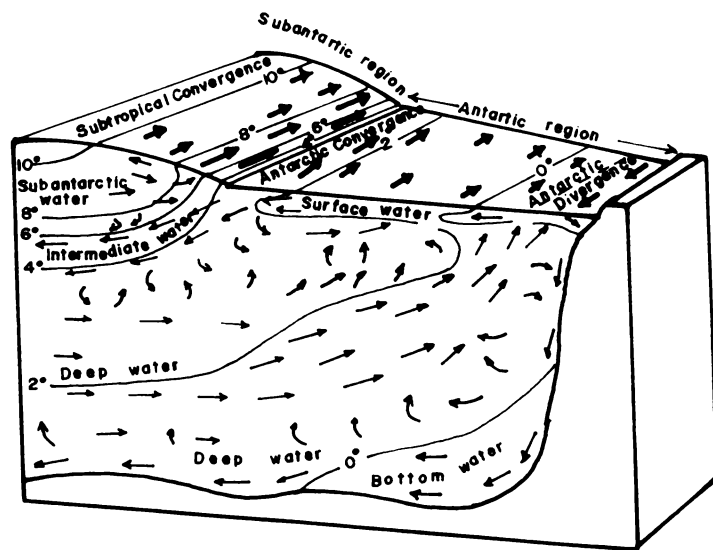


FIG. 1.2 Movement of watermasses in the Southern Ocean. (After Sverdrup et al. 1942).



### 1.3 Studies in the Indian Ocean sector of Southern Ocean:

Systematic oceanographic observations in the Indian Ocean sector of the Southern Ocean were made for the first time as a part of the International Indian Ocean Expedition (IIOE) during 1960 - 1965 - a major effort made by oceanographers of 25 nations employing a total of 44 research vessels. A detailed report incorporating all the results of physical oceanographic data was brought out in the form of atlas by Wyrcki (1971). However, there was no major emphasis on the Southern Ocean sector during this expedition. After IIOE observations, efforts have been made in the western and eastern regions of the Indian Ocean sector of Southern Ocean. These were not of International nature but were carried out as a part of the research programme of National Research Institute for Oceanology, South Africa and the United States Antarctic Research Programme of National Science Foundation. The Indian Ocean sector received little attention compared to those of Pacific and Atlantic oceans. Detailed observations on the frontal structures in the western most region of the Indian Ocean sector of the Southern Ocean were made by Lutjeharms et al. (1986) on board S.A. Agulhas and Polar Sirkel South of Africa. The physical oceanography of the Southeastern part of Indian Ocean sector of Southern Ocean has been

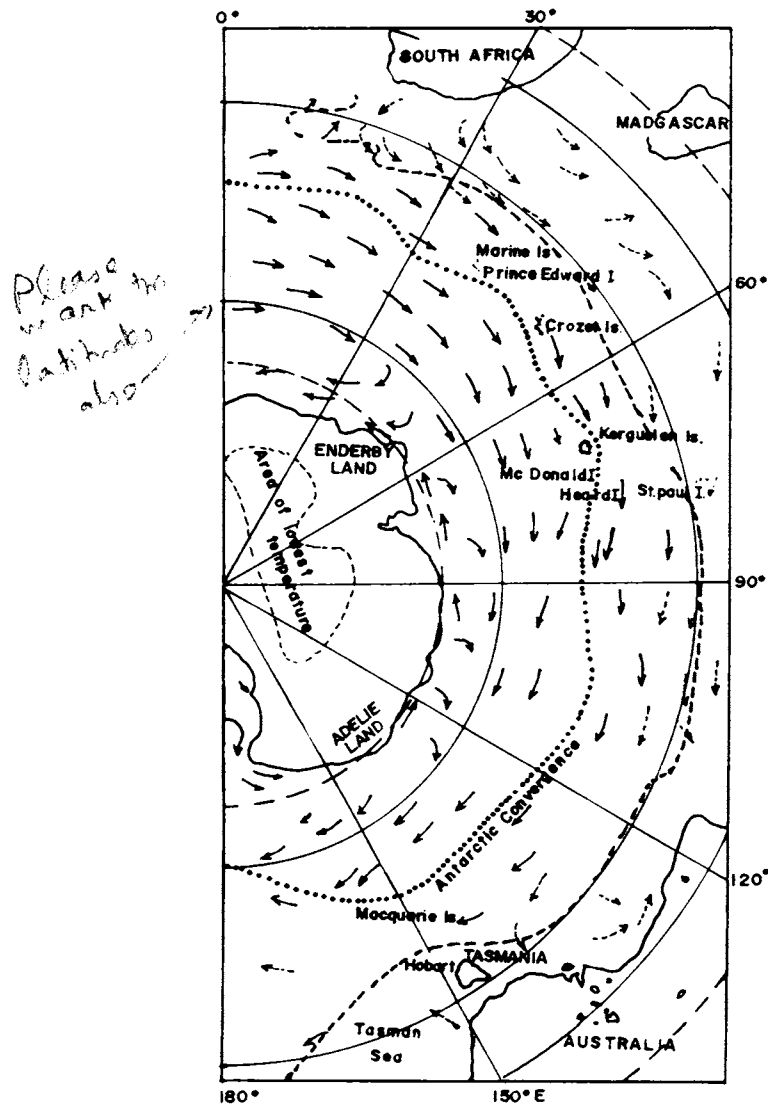


FIG.1.3 Regime of surface currents of the Indian Ocean sector of Southern Ocean.(After Tchernia 1980)

studied from the data of ELTANIN cruise as a part of the polar programmes of the National Science Foundation (NSF) and the results were incorporated in the form of reports (Anonymous 1970, 1971). In the eastern region of the Indian Ocean sector of the Southern Ocean observations on the frontal structure were made during Australian oceanographic cruises in addition to the Eltanin programme. The Australian data were published by the Commonwealth Scientific and Industrial Research Organisation of Australia (1962, 1963a,b, 1966a,b, 1967a,b,c,d, 1968a,b, 1972). India had begun her Antarctic research since 1981 and started oceanographic research component concentrating studies on the watermass structure in the southwestern region of the Indian Ocean sector of Southern Ocean (Raju and Somayajulu, 1983; Gupta and Qasim, 1983 and Naqvi, 1986). Except these studies of fragmentary nature in the Indian Ocean sector of Southern Ocean, no comprehensive efforts have been made to understand the fronts and associated processes. In view of this, the author is tempted to study in detail the different characteristics of planetary scale fronts in the above area.

✓  
to what extent you could study?

# ***CHAPTER - II***

## Data and Methods of Analysis

A significant increase in gradient in sea surface temperature was noticed at two places in the Southern Ocean by Meinardus (1923) and Schott (1935) while proceeding northward from Antarctic continent. The Discovery expedition in late 1930's established the presence of a sharp gradient in temperature across Antarctic Convergence and further brought out the distinct characteristics of maritime climate north and south of it.

Deacon (1937a) based on Nansen bottle cast and Mackintosh (1946) on thermograph data sets mentioned a surface discontinuity - Antarctic Polar Front (APF) - closer to the latitude where the Antarctic waters in association with a temperature minimum make a sharp descent at about 200 m depth below the warm Subantarctic surface Waters. The density discontinuity layer slopes steeply below 200 m where the temperature minimum sinks (Koopman, 1953; Wexler, 1959; Wyrski, 1960; Ostapoff, 1962a; and Taylor et al., 1978).

An abrupt change in sea surface temperature in the horizontal direction <sup>is</sup> encountered <sup>ed</sup> at APF whereas both temperature and salinity are seen drastically changing at STF. It is possible to form a density front at STF depending

upon the intensity of thermohaline gradients. Accordingly geostrophic flow in association with the baroclinic zone generates across STF.

## 2.1 Identification of Fronts

Different methods have been suggested to identify Antarctic Polar front due to its varying description. Deacon (1933, 1937a,b) considered APF at a location where maximum surface thermal gradient prevailed while at subsurface it was located at the northern limit of the Antarctic Bottom Water. Mackintosh (1946) stated that at the surface there would be a larger gradient in temperature at APF but at the subsurface the position of temperature minimum at 200 m depth could be located as APF. Eventhough Garner (1958) agreed with the surface expression of APF as stronger gradient in temperature but its subsurface expression was represented at the northern limit of the subsurface temperature inversion.

The surface expression of APF could be identified by larger temperature gradient while at subsurface, it was located at the northern limit of 1°C isotherm in the temperature minimum layer (Burling, 1961). Since salinity is more conservative than temperature, the axis of the

circumpolar salinity minimum belt at 200 m was considered as the position of APF (Ostapoff, 1962b). On the otherhand, Botnikov (1963) suggested APF as the surface position of 2°C isotherm in winter whereas in summer it could be identified as the northern limit of 2°C isotherm of temperature minimum layer. Houtman (1964) pointed out APF as a region where the cold denser Antarctic surface water and warm less saline subantarctic waters meet each other. The identificatin of APF as a larger surface temperature gradient first encountered while proceeding north from the Antarctic continent and whereas at subsurface its position was shown at the northern end of temperature minimum layer (Gordon, 1967a). The most common method adopted in the present study for the identification of the front involves determination of a relatively large drop in surface hydrographic properties in the horizontal direction.

Occasionally APF does not manifest sharp gradient in surface temperature, especially in summer when warming of surface layer obliterates the gradient. For the present study all the sections except 85°E belong to summer. Hence to identify the position of APF in summer the northern limit of 2°C isotherm in the temperature minimum layer is taken as the location of APF. In winter, the position of the strong surface gradient encountered first in the Antarctic zone

while proceeding from south has been considered to represent APF.

STF can be identified from both the temperature and salinity gradients. The temperature drop across STF was seen between 17.9° and 10.6°C in the region <sup>South of</sup> below Africa (Lutjeharms and Valentine, 1984) and the corresponding surface salinity drop was from 35.5 to 34.3‰. (Lutjeharms, 1985). In subtropics intense evaporation causes an increase in salinity with the result that at subtropical convergence salinity gradient exists. The method adopted for identifying STF in the present study is to locate the region where intense thermal and haline gradients occur consistently in the northern part of all the sections.

The front which is found at the most vertically oriented isotherm within a subsurface temperature gradient between 3° and 5°C is termed as Sub-Antarctic Front SAF (Sievers and Emery, 1978). In the present investigation SAF during summer is identified from the large surface gradient in the above mentioned range of temperature while in winter it is taken as the surface gradient between 5° and 9°C. The recent observations of Lutjeharms et al. (1984) in the Indian Ocean sector of the Southern Ocean south of Africa indicated SAF between STF and APF.



Since large variation is seen in the properties of major fronts in the Southern Ocean, a statistical analysis has been done with all the hydrographic, Expendable Bathy Thermograph (XBT) and surface observations data. The various characteristics of each individual front like its middle latitude position, width, range of temperature and salinity with their gradients have been computed during every meridional crossing.

## **2.2 Methods to identify fronts from surface observation data**

The surface temperature data obtained from Japanese Antarctic research expeditions between 38°S and 60°S have been plotted along different meridians. The STF at the surface has been identified as the most prominent thermal front at the northernmost part of the meridional section. The identification of SAF is done by adopting the method of Lutjeharms and Valentine (1984), who have observed that strong surface temperature gradient occurs within the range of 3.5° - 11°C and the latitudinal range of 42° 40' - 49°S in the eastern Atlantic and the western Indian Ocean sectors of the Southern Ocean. Usually SAF corresponds to the steepest horizontal gradient in temperature between STF and APF. The

position of APF is identified according to the definition of Ostapoff (1962b). According to him the APF is identified as the maximum sea surface temperature gradient between 2°C and 6°C.

### 2.3 Data Used:

The hydrographic data collected during the cruises conducted on board research vessel ELTANIN, as a part of the United States Antarctic Research Programme as well as on board research vessels CONRAD & ISLAS ORCADAS by Lamont Doherty Geological Observatory, USA are used for the present study. The surface observations (1967-1985) and subsurface observation (1978-1985) made by research vessels FUJI and SHIRASE under the Japanese Antarctic Research Programme are considered in addition to the above data. The Indian observations made on board FINN POLARIS during 1984 as a part of Indian Antarctic Research Expedition have also been supplemented.

Since the flow in the Southern Ocean is generally of zonal character, the variations in the water properties are expected in the meridional direction. Hence effort has been made to select the maximum possible meridionally oriented sections. In order to achieve more reliable estimates as far

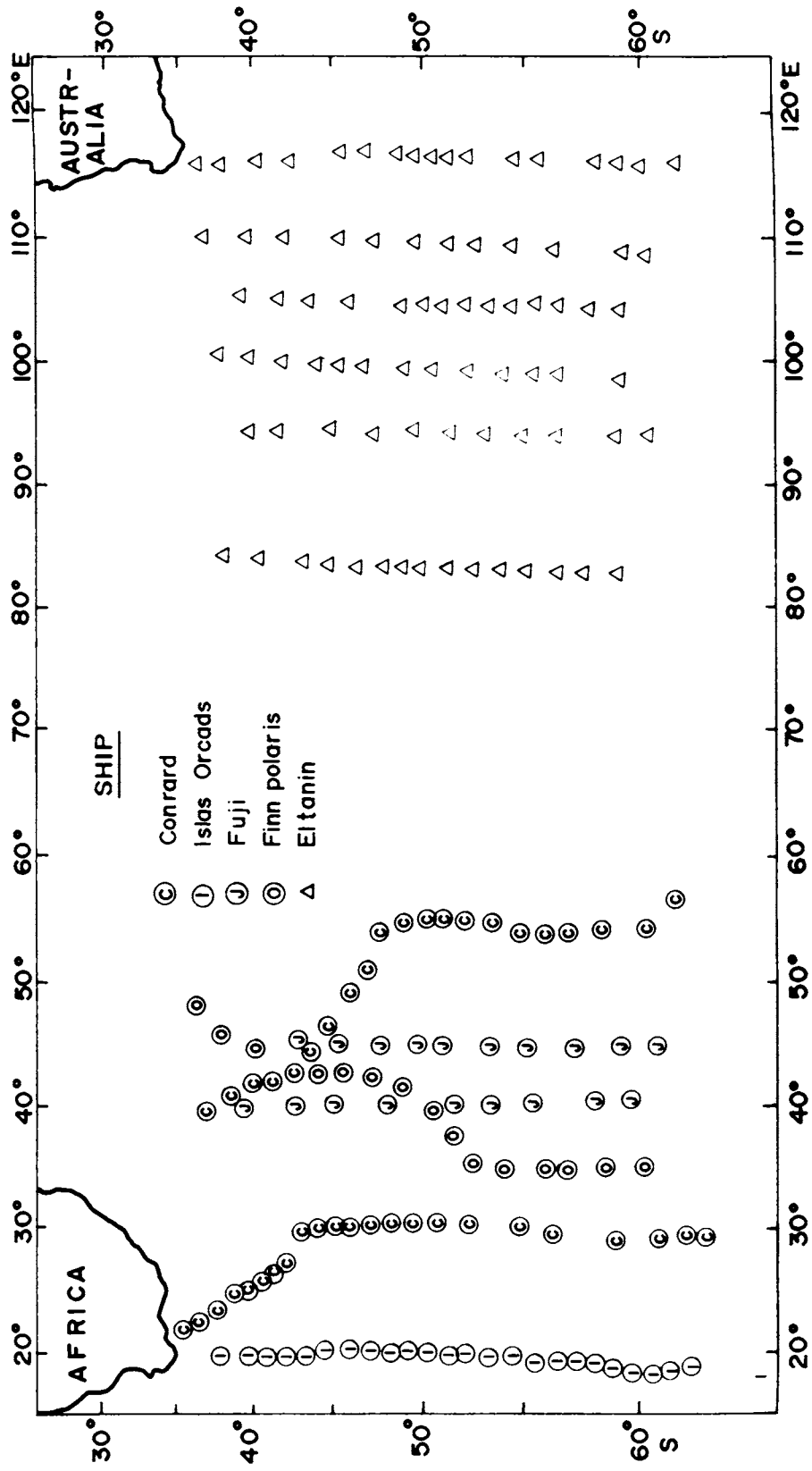


Fig. 2.1 Map showing the station positions of selected twelve hydrographical sections.

TABLE 2.1 Details of data used

## A. Hydrographic data

Sl.No.	Ship	Number of stations used	Period of collection	Symbols used
1.	Eltanin	82	1970 1971 1972	} $\Delta$
2.	Conrad	44	1974	$\odot$
3.	Islas Orcadas	24	1977	$\textcircled{i}$
4.	Fuji	19	1981 1983	} $\textcircled{j}$
5.	Finn Polaris	16	1984	$\textcircled{o}$

## B. Expendable Bathy-Thermograph (XBT) data

1.	Fuji	17	1978-1979
2.	Fuji	57	1979-1980
3.	Fuji	32	1980-1981
4.	Fuji	28	1981-1982
5.	Fuji	28	1982-1983
6.	Shirase	44	1983-1984
7.	Shirase	48	1984-1985

## C. Surface temperature data

1.	Fuji	27	1967-1968
2.	Fuji	35	1972-1973
3.	Fuji	74	1974-1975
4.	Fuji	30	1975-1976
5.	Fuji	35	1976-1977
6.	Fuji	32	1977-1978
7.	Fuji	88	1978-1979
8.	Fuji	45	1980-1981
9.	Fuji	44	1981-1982
10.	Shirase	34	1983-1984
11.	Shirase	48	1984-1985

TABLE 2.2 Details of chl. a data used

---

Sl. No.	Ship	Number of data used (chl. <u>a</u> )	Period of collection
1.	Fuji	36	1967-1968
2.	Fuji	34	1972-1973
3.	Fuji	42	1974-1975
4.	Fuji	39	1975-1976
5.	Fuji	44	1976-1977
6.	Fuji	43	1977-1978
7.	Fuji	148	1978-1979
8.	Fuji	98	1979-1980
9.	Fuji	55	1980-1981
10.	Fuji	40	1981-1982
11.	Shirase	1073	1983-1984
12.	Shirase	3206	1984-1985

---

as possible, meridional sections with stations covered in a single cruise are used. The details of the data used in the present study are given in Table 2.1 and the geographical distributions of twelve selected meridional sections are shown in Fig. 2.1.

Frontal systems are generally considered as areas of higher productivity (Pomazanova, 1980; Jacques and Minas, 1981). An attempt has been made to understand the effect of fronts on productivity in the study area. The details of chlorophyll data that have been used to represent productivity levels at different regions are given in table 2.2.

#### **2.4 Computation of zonal volume flux:**

The frontal characteristics such as temperature and salinity gradients which determine the strength of the front are different at different regions. In order to assess the variation of volume flux associated with the characteristics of the front and its contribution to Antarctic Circumpolar Current (ACC), the zonal volume flux has been computed.

Generally the volume transport is stated as the amount

of water flowing per unit area per unit time. In other words, it is a measure of the volume of water passing through a certain portion of a vertical plane per unit time. If "F" is the flux transported per unit time through a unit area "A" of a vertical plane in the ocean, and if "C" is the component of velocity normal to the plane, then

$$F = A.C$$

Fronts are generally prominent above 1000 m depth in the study area as seen from hydrographic sections. Hence the computation of zonal volume flux has been limited to this depth by taking 1000 db as the reference level. The zonal fluxes at each front are obtained and their contribution to the over all transport of ACC is studied.

In the present study the flux has been estimated by using the method of Montgomery and Stroup (1962). This is done by using the function "Acceleration Potential"  $(\phi_a + \phi_s)$ . The term  $\phi_a$  is the geopotential anomaly relative to the reference depth (1000 m) while  $p$  and  $\sigma$  represent the pressure and specific volume anomaly respectively. Furthermore, this method leads directly to the estimation of geostrophic currents at the chosen isanosteric surface. The geopotential anomaly  $\phi_a$  is defined by vertical integral of

*Is it a subject or a multiplier?*

specific anomaly.

$$\Phi_a = \int_{P=P_0}^{P=P_{1000}} \epsilon \, dp$$

where  $P_0$  and  $P_{1000}$  are the surface pressure (0 db) and the reference pressure (1000 db) respectively. The geopotential anomaly is also represented by changing the variables of integration of the above equation.

$$\Phi_a = \int_{\epsilon=\epsilon_{1000}}^{\epsilon=\epsilon_0} P \, d\epsilon$$

The acceleration potential at an individual hydrographic station is given as

$$\Phi_A = \Phi_a + P\epsilon = \int_{\epsilon_{1000}}^{\epsilon_0} p \, d\epsilon + P_{1000} \epsilon_{1000}$$

where  $\epsilon_0$  and  $\epsilon_{1000}$  are the specific volume anomalies at the surface and reference level. In the upper 1000 m since the pressure term in the anomaly of specific volume is negligible, thermosteric anomaly ( $\epsilon_T$ ) is used in place of specific volume anomaly. The numerical integration has been carried out from the reference level to the surface at each station to yield the acceleration potential.

From the length and mean height of each quadrangle



defined by the given isanosteres and whole degrees of latitudes, the area is calculated. From the area of the quadrangle and the mean velocity of water flowing through it the volume flux is estimated.

The zonal component of geostrophic velocity is calculated from

$$C = \frac{2(\phi_A - \phi_B)}{(f_1 - f_2)L}$$

What are the two signs of sub-samples (A/B)  
They should be

where  $\phi_A$  and  $\phi_B$  are the acceleration potentials at two neighbouring hydrographic stations A & B; L is the distance between the stations. The terms  $f_1 = 2\Omega \sin \phi_1$  &  $f_2 = 2\Omega \sin \phi_2$  are the Coriolis parameters at two stations of latitudes  $\phi_1, \phi_2$ ; where  $\Omega$  is the angular velocity of earth. To represent the volume flux on a T-S-V diagram a novel technique has been adopted. This is achieved by superimposing the vertical section of salinity on corresponding section of thermosteric anomaly. The computed geostrophic volume flux is then divided into each bivariate classes of thermosteric anomaly and salinity on a T-S-V diagram. The estimated flux is

distributed in each classes bounded by salinity interval of 0.1‰ and thermosteric anomaly interval of 10 cl/t. This method gives a quantitative estimate of flow together with its characteristics.

Eastward (+Ve) and Westward (- Ve) fluxes are separately displayed in each classes. The total flux between any two consecutive intervals of thermosteric anomaly is shown at the bottom and that of salinity at the right hand side of the T-S-V diagram.

## 2.5 Computation of heat content

The meridional heat transport of the world ocean is a crucial element of the global climate system (Hastenrath, 1982; and Hollway, 1986). The production of heat transporting eddies <sup>have</sup> ~~have~~ been observed near the well defined oceanic fronts in Southern Ocean (Joyce and Patterson 1977; Peterson et al., 1984 Pillsbury and Bottero, 1984). These frontal eddies are responsible for the effective meridional heat transfer. However, the intensive heat flux across the polar front due to interleaving of adjacent watermasses is minor (Joyce et al., 1978). The intensity of the front and its potential for higher heat flux as well as for the mesoscale eddy turbulence are geographically dependent. The

knowledge on the variations in the heat content of the upper ocean from western to eastern region of the Indian Ocean Sector of Southern Ocean is therefore essential for understanding the global climatic changes.

Heat content computations are limited within the 0-500 m water column as the horizontal extent of front rather than its vertical extent determine the heat storage. The heat content is estimated from the following equation.

$$H = \rho c_p \int_0^z \bar{T} dz$$

where H is the heat content ( $J/m^2$ ),  $\rho$  is the density of water ( $Kg/m^3$ ) and  $c_p$  is the specific heat at constant pressure ( $J/kg/^\circ C$ ). The value ' $\rho c_p$ ' is assumed as a constant ( $0.409 \times 10^7 J/m^3/^\circ C$ ) according to Bathen (1971).

Vertical sections of temperature, salinity and thermosteric anomaly have been presented for each selected meridian. Isotherms are drawn at an interval of  $0.5^\circ C$  while the isohalines and isanosteres are drawn at intervals of 0.1‰ and 10 cl/t respectively. The vertical distribution maps of temperature, salinity and thermosteric anomaly in the Indian Ocean sector of the Southern Ocean are limited to the upper 1000 m water column, as the vertical extent of fronts ~~are~~<sup>is</sup> prominent generally within this depth range.

# ***CHAPTER - III***

## Hydrographic Properties along different meridions

The hydrographic properties of temperature, salinity and density (thermosteric anomaly) are considered to delineate the frontal structures from the different vertical sections (Figs. 3.1.1- 3.1.12). The sections are selected to understand the spatial variations in the characteristics of the front. In the present attempt, thermosteric anomaly is used to understand the combined effects of temperature and salinity on density. The vertical sections are drawn with a vertical to horizontal scale ratio 1 : 2200 and the same ratio has been maintained throughout to depict the features uniformly. The contours are drawn at same interval of 0.5°C, 0.1‰ and 10 cl/t for temperature, salinity and thermosteric anomaly respectively, in order to bring out the maximum details possible from the sections without losing the features.

The vertical sections of temperature and salinity clearly demarcate the fronts. The convergence of the watermasses can be identified from the horizontal gradients of the hydrographic properties. Occasionally nutrient distributions are used to understand the frontal structures, but being a nonconservative property, they are always used in association with hydrographic

properties. Hence only temperature and salinity characteristics are considered for the present study.

### 3.1 Temperature distribution:

Figs. 3.1.1, 3.1.2, 3.1.3, 3.1.4, 3.1.5, 3.1.6, 3.1.7, 3.1.8, 3.1.9, 3.1.10, 3.1.11 and 3.1.12 depict the thermal structures along 20°, 30°, 35°, 40°, 45°, 55°, 85°, 95°, 100°, 105°, 110° and 115°E respectively. Though temperature gradually decreases towards south, its sudden variation in certain regions in the mid-latitudes and slow variation near the high latitudes are the common characteristic features of these sections delineating different zones in between them. In all the sections most prominent feature is the presence of fronts which are narrow regions of sharp horizontal gradients extending upto a depth of about 800 m.

#### 3.1.1 Along 20°E:

The section covers the region between south Africa and Antarctic coast. Proceeding southward, water temperature falls, but the rate of cooling with latitude is highly varied (Fig. 3.1.1). A discontinuity region in watermass distribution is depicted by a strong horizontal



temperature gradient with a drop from  $16^{\circ}$  to  $9^{\circ}\text{C}$  within a distance of two degree latitude. This discontinuity represents the northern limit of the subantarctic region and is known as STF (Sub-Tropical Front). A water body of uniform temperature seen below a seasonal thermocline is called thermostad. In this section a thermostad of temperature  $2.5^{\circ}\text{C}$  is seen between stations 62 and 69. Further proceeding towards south, it is seen that the northern limit of cold Antarctic surface water is delineated by the  $2^{\circ}\text{C}$  isotherm with a sharp descent between stations 65 and 70 suggesting a convection around  $51^{\circ}\text{S}$ . Another noteworthy feature along  $20^{\circ}\text{E}$  is the presence of a shallow thermocline between stations 72 and 83 around 50 m depth.

The presence of dicothermal layer in 100-200 m depth range south of  $51^{\circ}\text{S}$  where cold waters <sup>are</sup> sandwiched between warm waters above and below is remarkable. This layer extends to Antarctic coast. The thickness of this layer is further found to decrease towards south. The topography of dicothermal layer in the Antarctic zone suggests a sinking nature away from the coast.



### 3.1.2 Along 30°E

The hydrographic section along 30°E is at a deviation from the earlier section (Fig. 3.1.2). The prominent feature seen in this section is the weakening of dicothermal layer. Between stations 282 and 283 the Antarctic Convergence is shown by the sharp descent of 2°C isotherm around 58°S whereas same feature was seen at 51°S along 20°E. The dicothermal layer is not only weaker as compared to that at 20°E but it gets dispersed through scooping out of inflated cold pockets (<2°C). This further shows the effect of penetration of eddy turbulence from the north. Between 38° and 44°S, a complex frontal structure is seen unlike the simple one at 20°E. The position of STF is not clear and a double portrayed front is seen channelised by a warm layer bifurcating STF into two portions. The presence of a larger mesoscale eddy in the STF region might have complicated its thermal portrayal. The thermal front with a sharp gradient around 39°S could be taken as the location of STF approximately. Here there is a drop of temperature of about 5.5°C over a latitude of one degree. Eddy generation is possible at the northern most part of the section where Agulhas current retroflex due to the interaction with bottom topography.

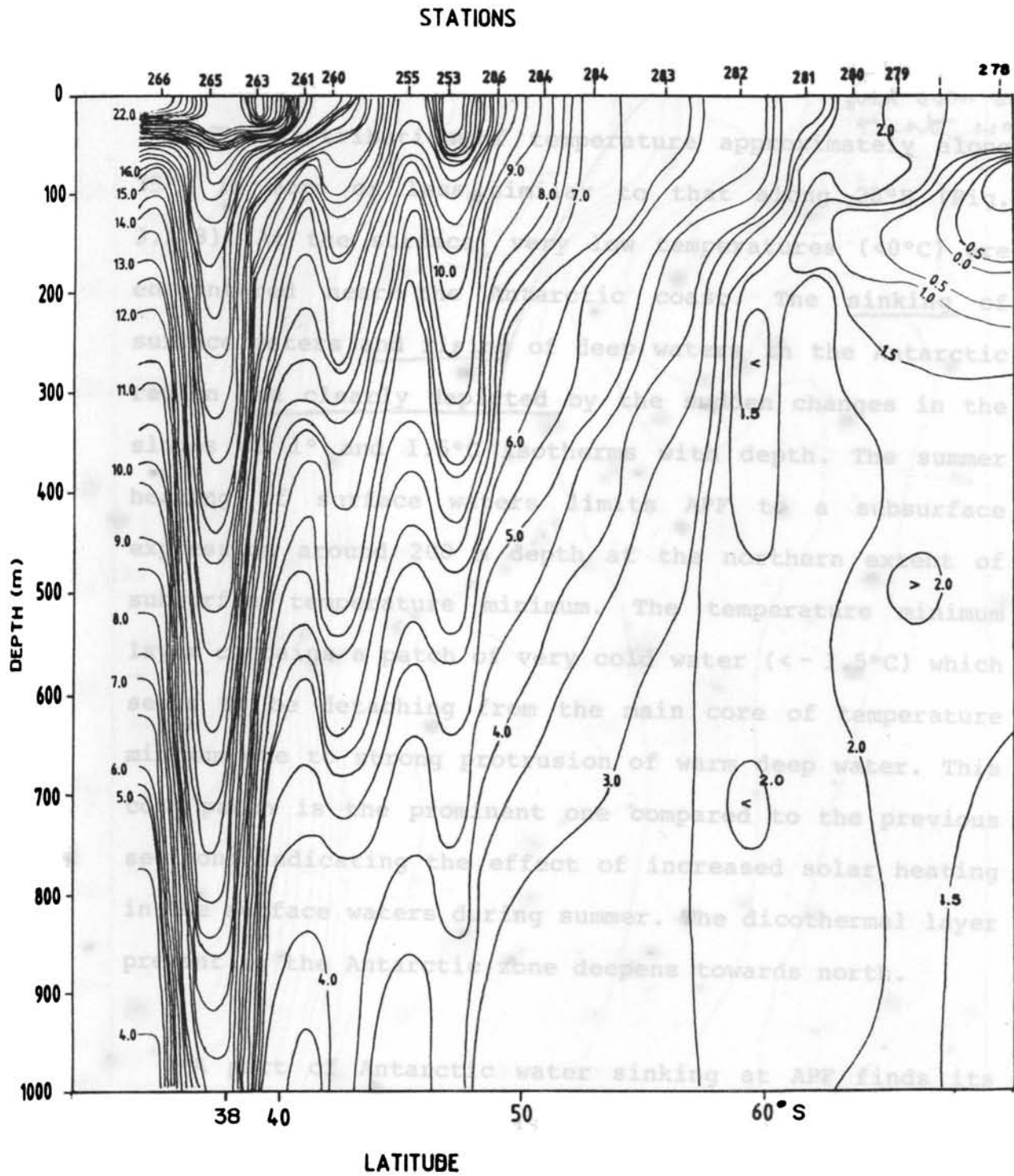


FIG. 3.1.2 VERTICAL SECTION OF TEMPERATURE ( °C-Degree Centigrade )  
ALONG 30°E

[Changes from month to month may be studied to infer dynamic processes.]

### 3.1.3 Along 35°E

→ Is the shape automatically indicative of dynamics? Or it could even be static that way?

The distribution of temperature approximately along 35°E is more or less similar to that along 20°E (Fig. 3.1.3). At the surface, very low temperatures ( $<0^{\circ}\text{C}$ ) are encountered near the Antarctic coast. The sinking of surface waters and rising of deep waters in the Antarctic region are clearly depicted by the sudden changes in the slopes of  $1^{\circ}$  and  $1.5^{\circ}\text{C}$  isotherms with depth. The summer heating of surface waters limits APF to a subsurface expression around 200 m depth at the northern extent of subsurface temperature minimum. The temperature minimum layer contains a patch of very cold water ( $<-1.5^{\circ}\text{C}$ ) which seems to be detaching from the main core of temperature minimum due to strong protrusion of warm deep water. This cold patch is the prominent one compared to the previous sections indicating the effect of increased solar heating in the surface waters during summer. The diathermal layer present in the Antarctic zone deepens towards north.

A part of Antarctic water sinking at APF finds its way further towards north as indicated from the topography of  $2.5^{\circ}$  and  $3^{\circ}\text{C}$  isotherms. The surface waters between stations 7 and 9 also sink in the upper 100 m and later join at STF broadening the subantarctic region. STF is

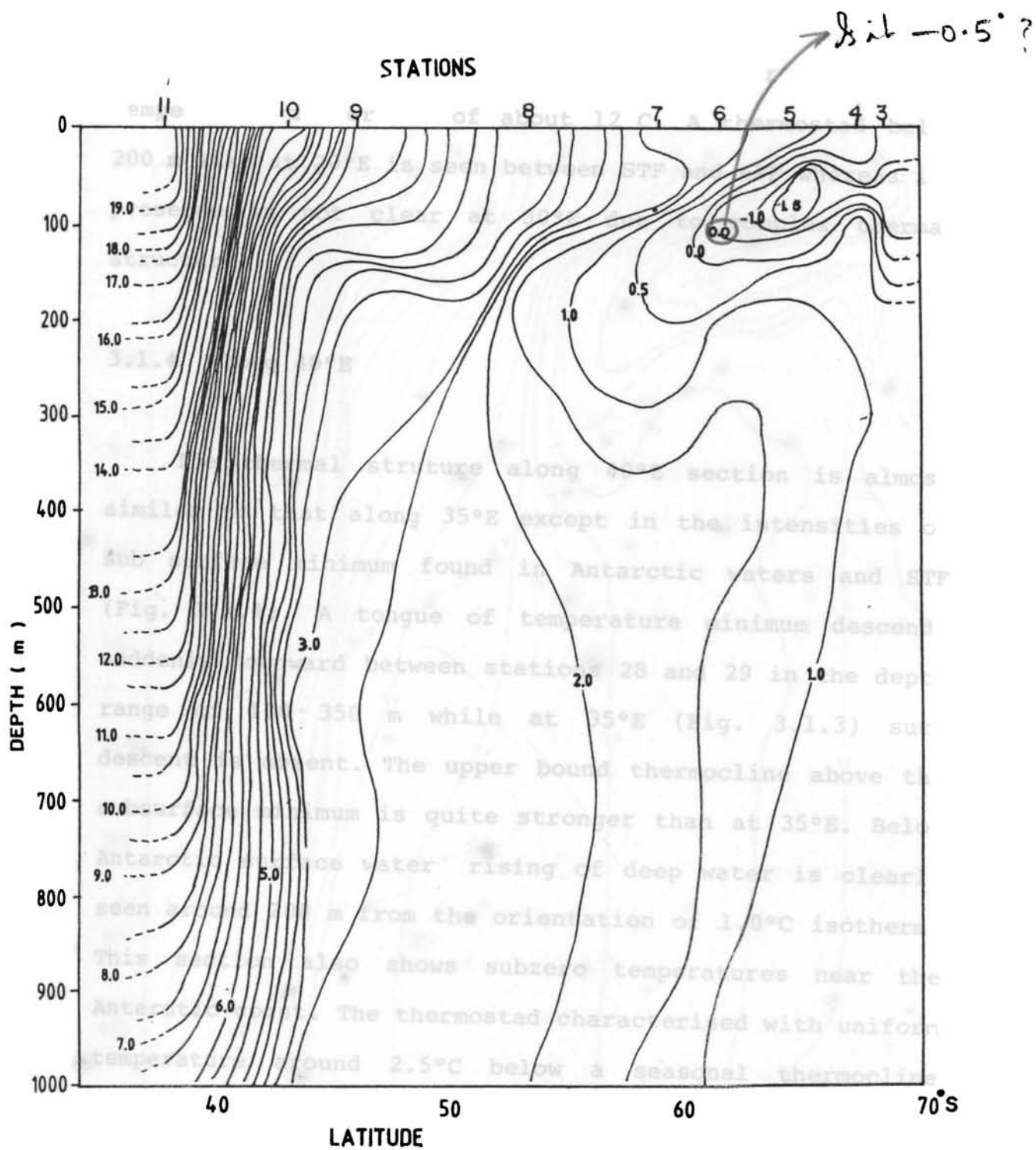


FIG. 3.1.3 VERTICAL SECTION OF TEMPERATURE ( °C-Degree Centigrade )  
ALONG 35°E

quite strong as seen from the steeper horizontal temperature difference of about  $12^{\circ}\text{C}$ . A thermostad below 200 m like at  $20^{\circ}\text{E}$  is seen between STF and APF whereas its presence is not clear at  $30^{\circ}\text{E}$  due to complex thermal structure.

#### 3.1.4 Along $40^{\circ}\text{E}$

The thermal structure along  $40^{\circ}\text{E}$  section is almost similar to that along  $35^{\circ}\text{E}$  except in the intensities of sub surface minimum found in Antarctic waters and STF (Fig. 3.1.4). A tongue of temperature minimum descends suddenly downward between stations 28 and 29 in the depth range of 100-350 m while at  $35^{\circ}\text{E}$  (Fig. 3.1.3) such descent is absent. The upper bound thermocline above the subsurface minimum is quite stronger than at  $35^{\circ}\text{E}$ . Below Antarctic surface water rising of deep water is clearly seen around 200 m from the orientation of  $1.0^{\circ}\text{C}$  isotherm. This section also shows subzero temperatures near the Antarctic coast. The thermostad characterised with uniform temperature around  $2.5^{\circ}\text{C}$  below a seasonal thermocline exists between  $44^{\circ}$  and  $51^{\circ}\text{S}$ . Further towards north, a sudden increase in the water temperature is seen between stations 31 and 32 and this region is identified as STF.

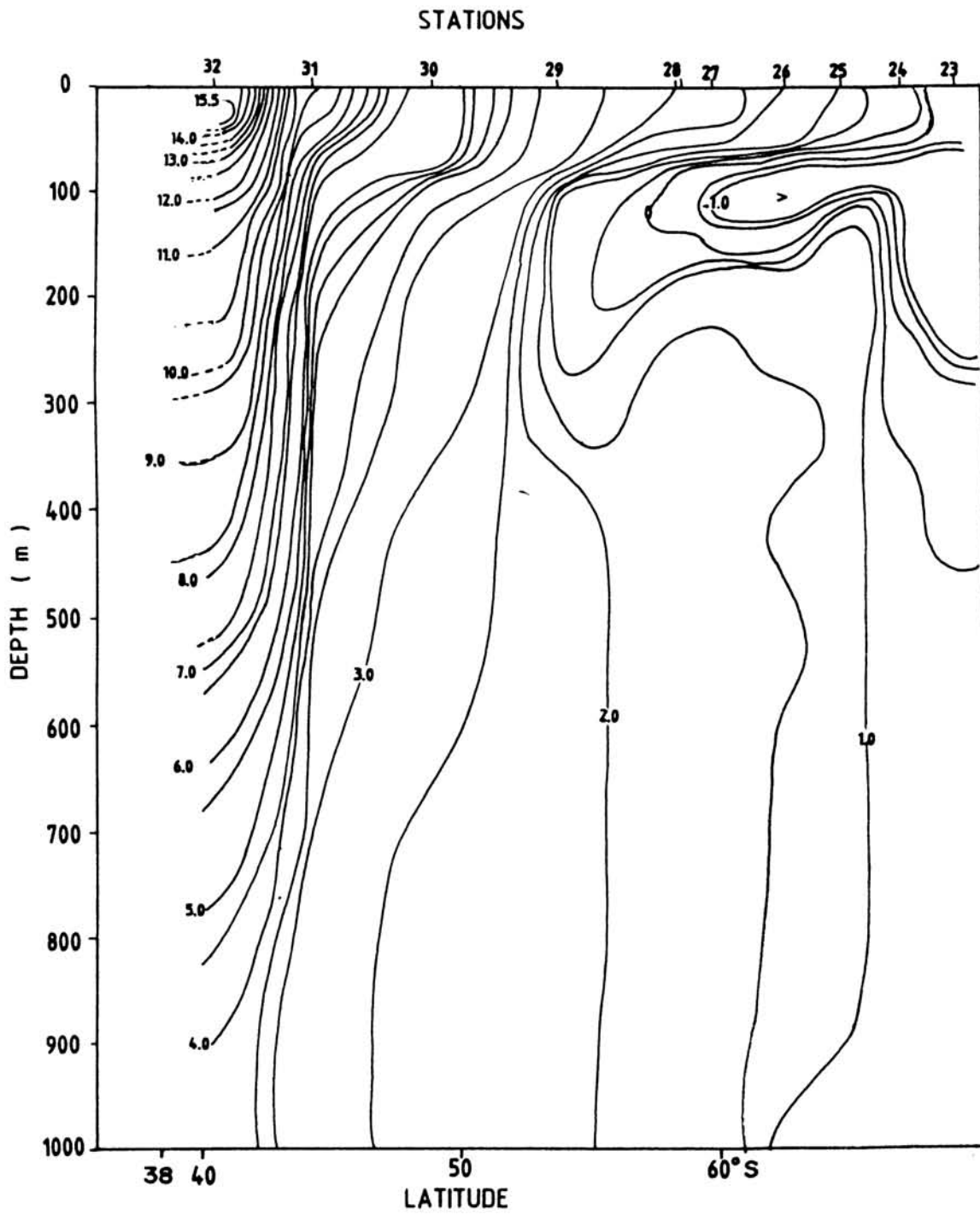


FIG.3.1.4 VERTICAL SECTION OF TEMPERATURE ( °C - Degree Centigrade )  
 APPROXIMATELY ALONG 40°E

### 3.1.5 Along 45°E

This section is limited between 43° and 68°S and as such it does not give enough information about STF (Fig. 3.1.5). However, south of 43°S, the section reveals features of the Antarctic zone. The manifestation of 2°C isotherm suggests the position of APF. A prominent feature along this section is the presence of a thermostad (2.5°C) north of APF. Like previous sections, a tongue of cold water (< -1°C) sinks towards north from the Antarctic region where subzero temperatures are encountered at the surface. The orientation of 1.5°C isotherm suggests that a warmer deep watermass is rising around 65°S.

### 3.1.6 Along 55°E

The thermal structure approximately along 55°E (Fig.3.1.6) shows the presence of the most intensive STF wherein a drop of about 11°C in temperature is observed. The subsurface cold tongue in the Antarctic region is narrow as compared with that at 45°E. The cold Antarctic surface water sinks upto 200 m during its spread from the coast. A layer of homogeneous water is seen above the diathermal layer between stations 246 and 251. The orientation of 2°C isotherm indicates a sharp descent of

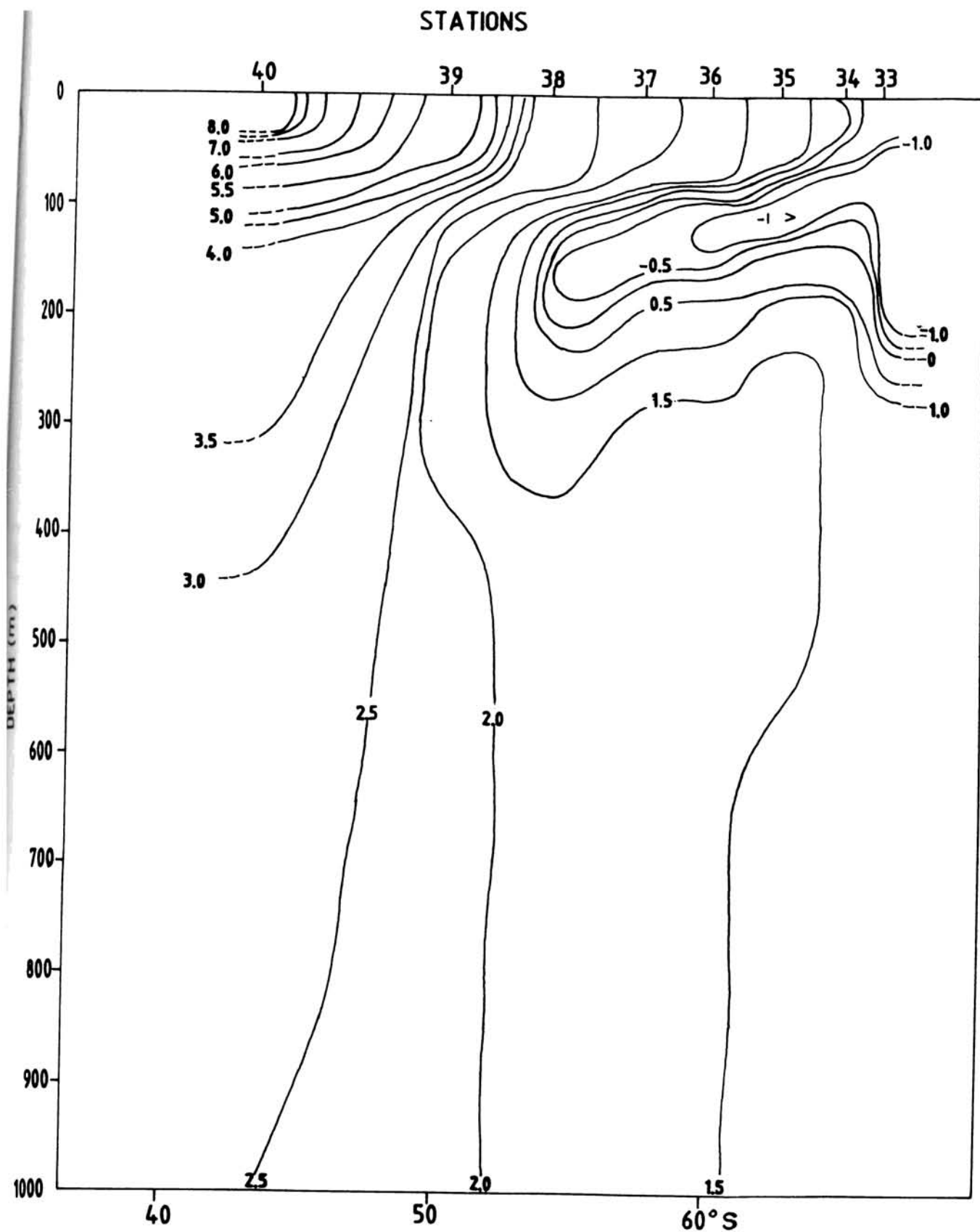


FIG.3.1.5 VERTICAL SECTION OF TEMPERATURE ( °C-Degree Centigrade )  
ALONG 45° E



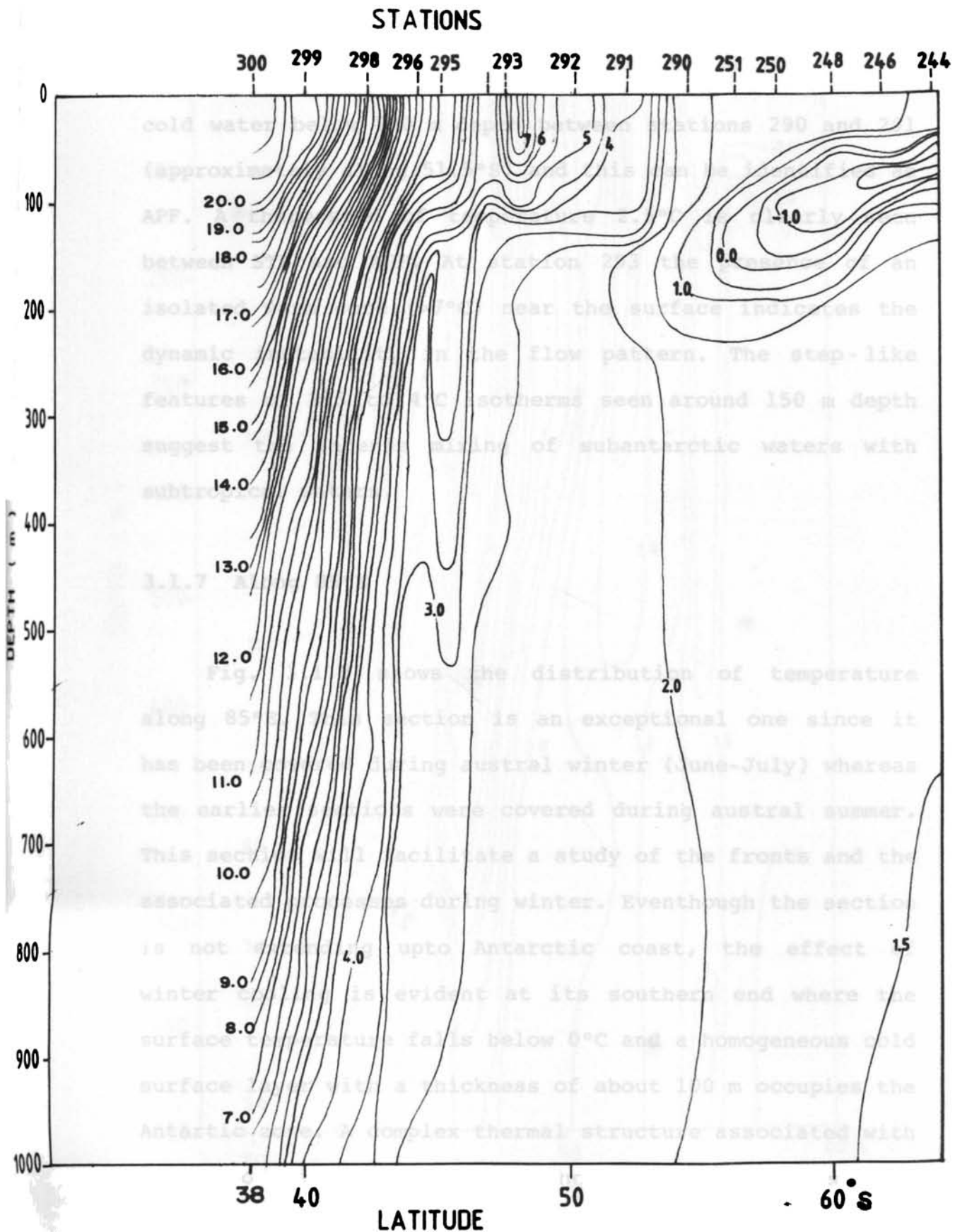


FIG.3.1.6 VERTICAL SECTION OF TEMPERATURE ( °C - Degree Centigrade ) .  
APPROXIMATELY ALONG 55°E

cold water below 200 m depth between stations 290 and 291 (approximately along 51.5°S) and this can be identified as APF. A thermostat of temperature 2.5°C is clearly seen between STF and APF. At station 293 the presence of an isolated warm core (>7°C) near the surface indicates the dynamic instability in the flow pattern. The step-like features of 2.5 to 4°C isotherms seen around 150 m depth suggest the intense mixing of subantarctic waters with subtropical waters.

### 3.1.7 Along 85°E

Fig. 3.1.7 shows the distribution of temperature along 85°E. This section is an exceptional one since it has been covered during austral winter (June-July) whereas the earlier sections were covered during austral summer. This section will facilitate a study of the fronts and the associated processes during winter. Eventhough the section is not extending upto Antarctic coast, the effect of winter cooling is evident at its southern end where the surface temperature falls below 0°C and a homogeneous cold surface layer with a thickness of about 100 m occupies the Antarctic zone. A complex thermal structure associated with deep troughs and ridges in the isotherms is also the characteristics of the Antarctic zone. On the other hand

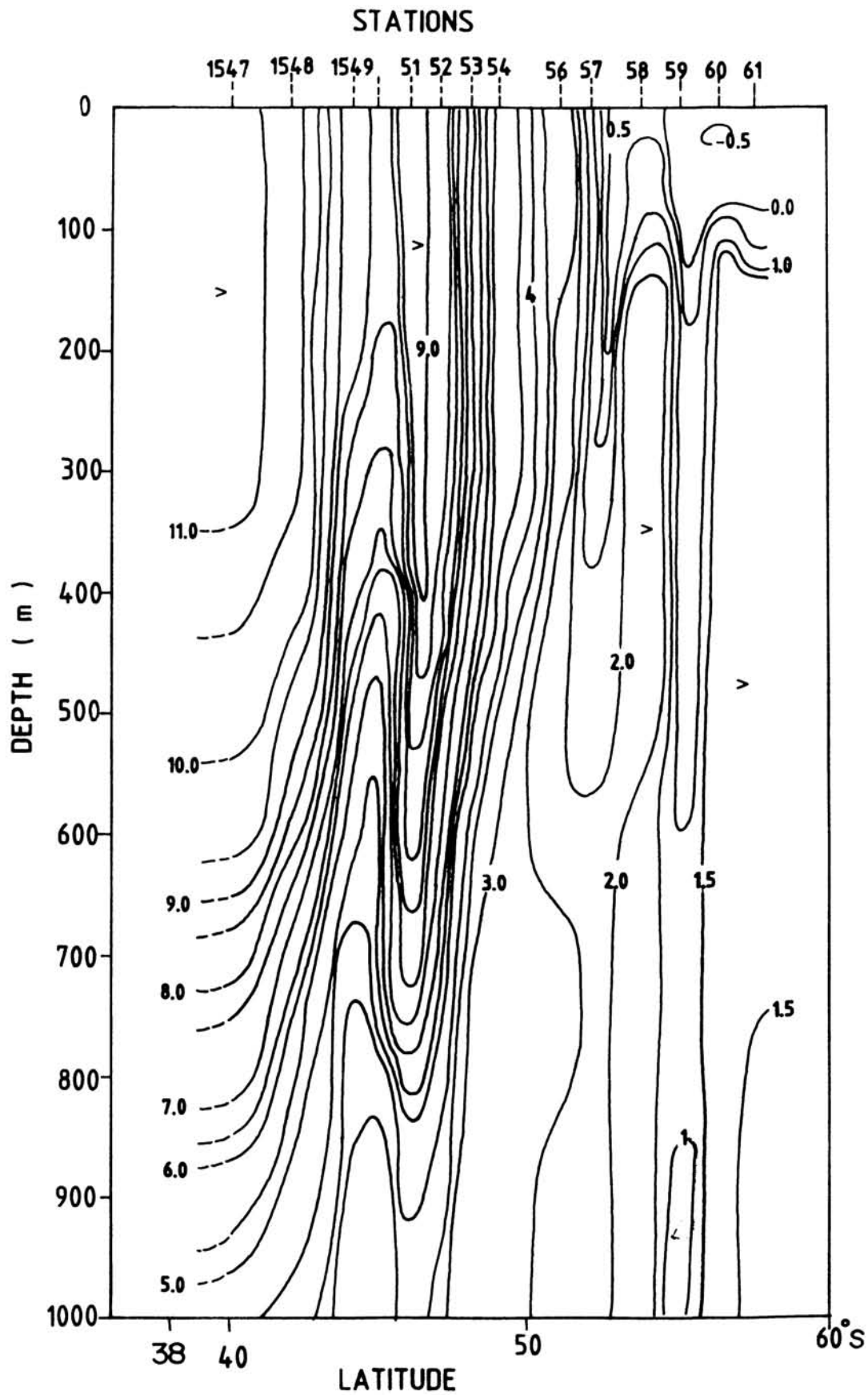


FIG.3.1.7 VERTICAL SECTION OF TEMPERATURE ( °C - Degree Centigrade )  
ALONG 85°E

in the same zone the surface temperature is usually between 1° and 3°C during summer. This gives rise to the positioning of the surface expression of APF directly above its subsurface expression. The trough and ridge like shape of 2°C isotherm between stations 1557 and 1559 suggests a deeper winter convection and the resultant eddy mixing. The thermostat is not well developed along this section. North of APF, another frontal structure with strong thermal gradient is seen around station 1553 extending upto about 900 m depth and is termed as Sub Antarctic Front (SAF) with a drop of about 4°C temperature across it.

Waters on the northern side of SAF are characterised with a complex structure through the presence of isolated warm layers (>9°C) extending upto 400 m. Around 41°S, the surface temperature is found less than 12°C whereas it is higher in the corresponding region as seen from the sections that are covered during summer. STF is quite weak along this section.

### 3.1.8 Along 95°E

The section along 95°E (Fig.3.1.8) has been covered during early summer period. A cold tongue (< -1.5°C) still

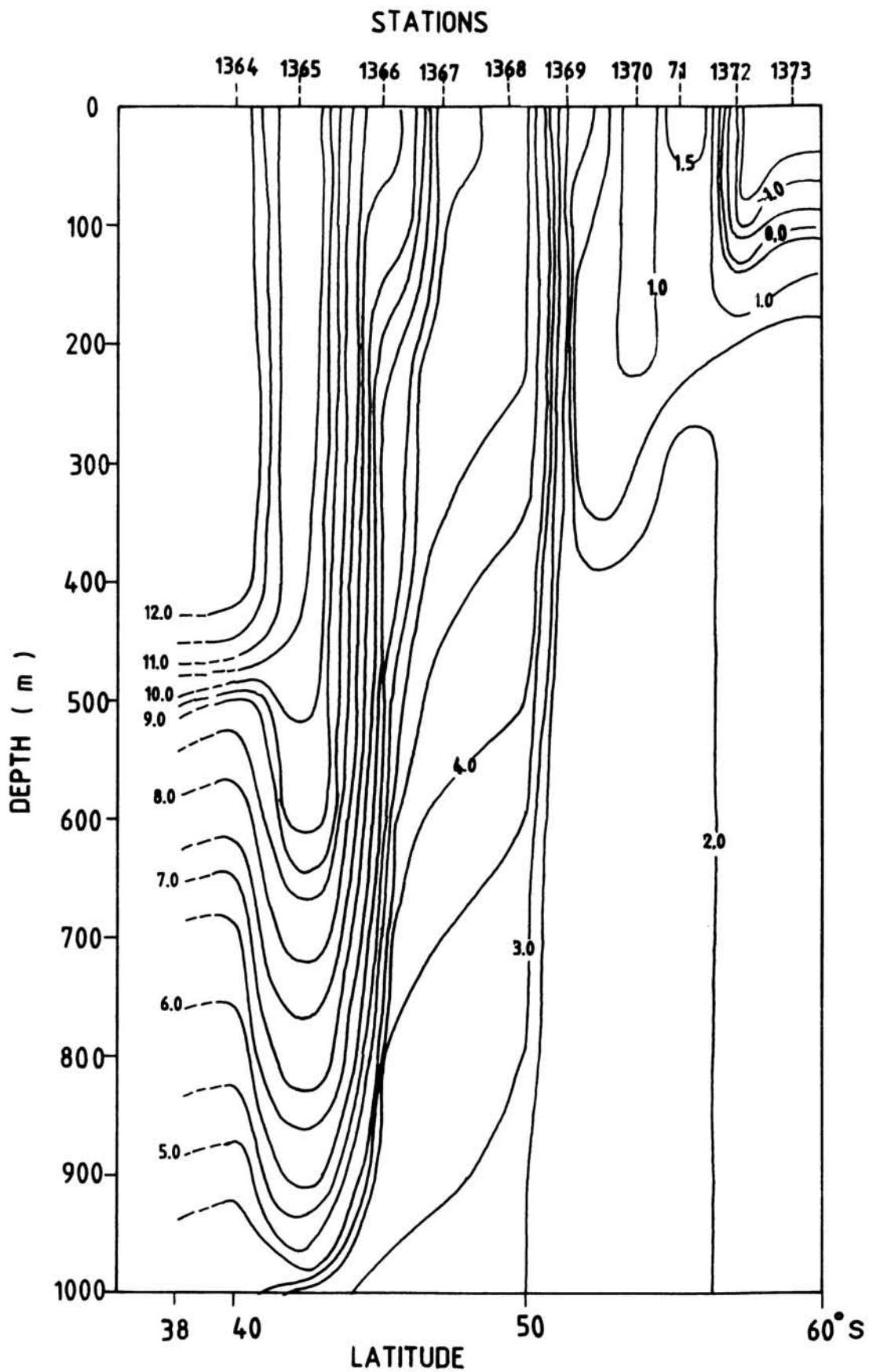


**FIG.3.1.8 VERTICAL SECTION OF TEMPERATURE ( °C - Degree Centigrade ) .  
ALONG 95°E**

prevails at surface near the Antarctic coast as an anomalous situation giving rise to a temporal thermocline with a gradient about  $2^{\circ}\text{C}/100\text{ m}$ . The upward movement of warm North Atlantic Deep Water is indicated around 350 m depth at station 1371 as seen from the orientation of  $2^{\circ}\text{C}$  isotherm. The dicothermal layer does not present in this section like at  $85^{\circ}\text{E}$ , indicating the persistent effect of winter cooling. A degree of bunching of isotherms of  $2.5^{\circ}$  to  $5^{\circ}\text{C}$  in the depth range of 0-400 m between stations 1368 and 1369 shows the existence of a single front instead of two (APF and SAF). The Antarctic Polar Front (APF) is located around  $52^{\circ}\text{S}$  where the  $2^{\circ}\text{C}$  isotherm in the temperature minimum makes a sharp descent upto 450 m. The surface expression of APF almost coincides with its subsurface expression. The structure of STF is of split type with an occurrence of stronger surface gradients on either side of station 1365.

### 3.1.9 Along $100^{\circ}\text{E}$

Hydrographic observations during October were combined to derive thermal structure along  $100^{\circ}\text{E}$  (Fig.3.1.9). A subsurface temperature minimum is clearly evident between stations 1378 and 1379 and its northern limit is the position of APF. Some perturbations such as

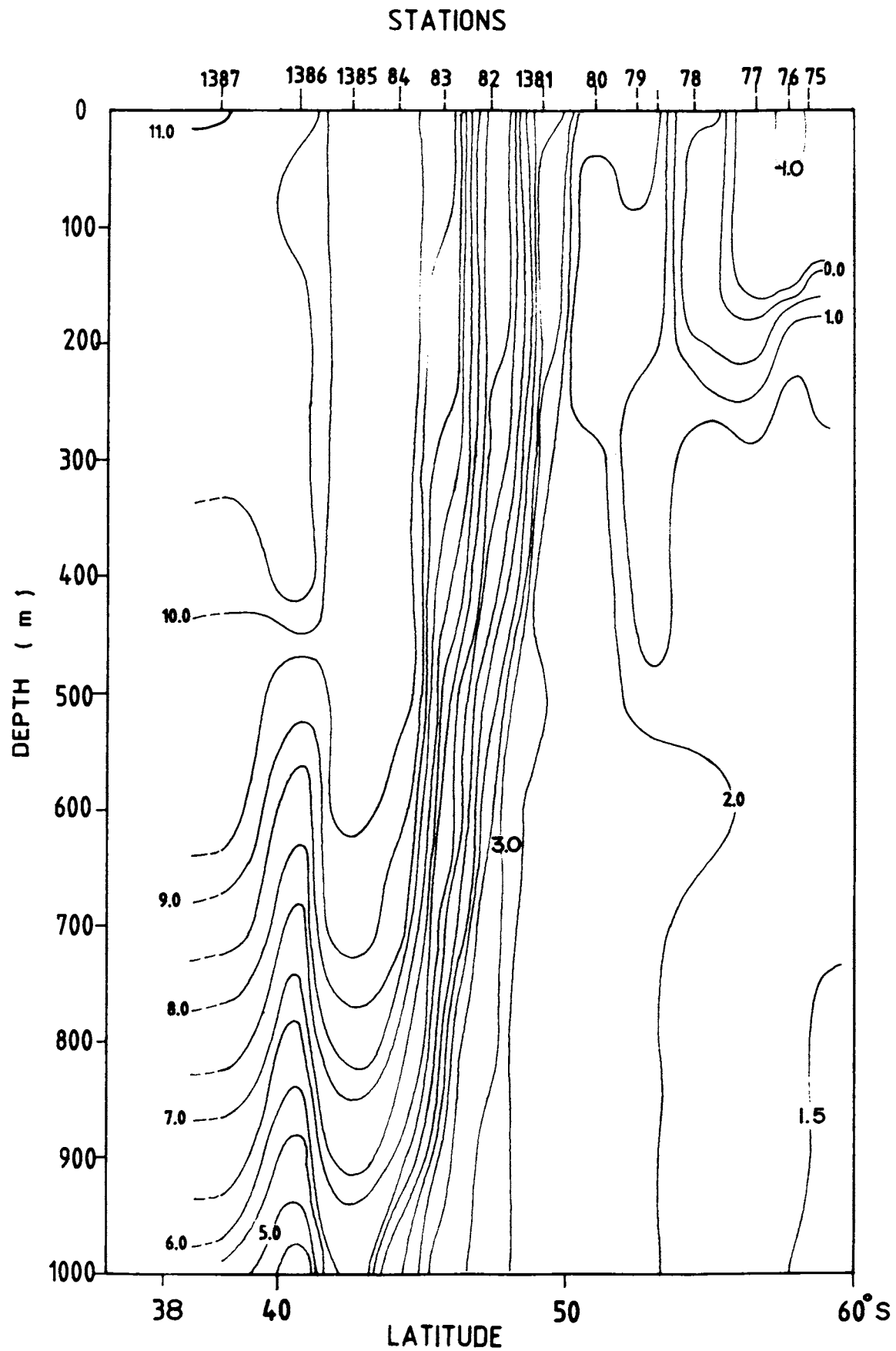


**FIG.3.1.9 VERTICAL SECTION OF TEMPERATURE ( °C - Degree Centigrade )  
ALONG 100°E**

presence of a wedge shape in the orientation of 2°C isotherm can be seen around 600 m depth. This section also shows the occurrence of homogeneous water in the Antarctic zone upto a depth of 200 m below which is bordered by a weak inversion with intensity of about 1°C/100 m. Since it belongs to October month, it shows a gradual surface warming as shown at station 1375. The Sub-Antarctic front is located between stations 1381 and 1382 with a temperature drop of about 3.5°C. STF along this section is very weak. A warm layer divides STF into two parts. The greater part of STF mixes with SAF more prominently below 200 m.

### 3.1.10 Along 105°E

The vertical distribution of temperature along 105°E during November is presented in Fig. 3.1.10. The gradual development of diathermal layer associated with summer heating is clearly depicted in the section. A descent of cold tongue (< -1°C) is also shown in the Antarctic zone. The 2°C isotherm within the temperature minimum sinks around station 1397 and accordingly APF is considered to be located at 49°S. Along this section, SAF is the most intensified front extending upto 1000 m. The presence of



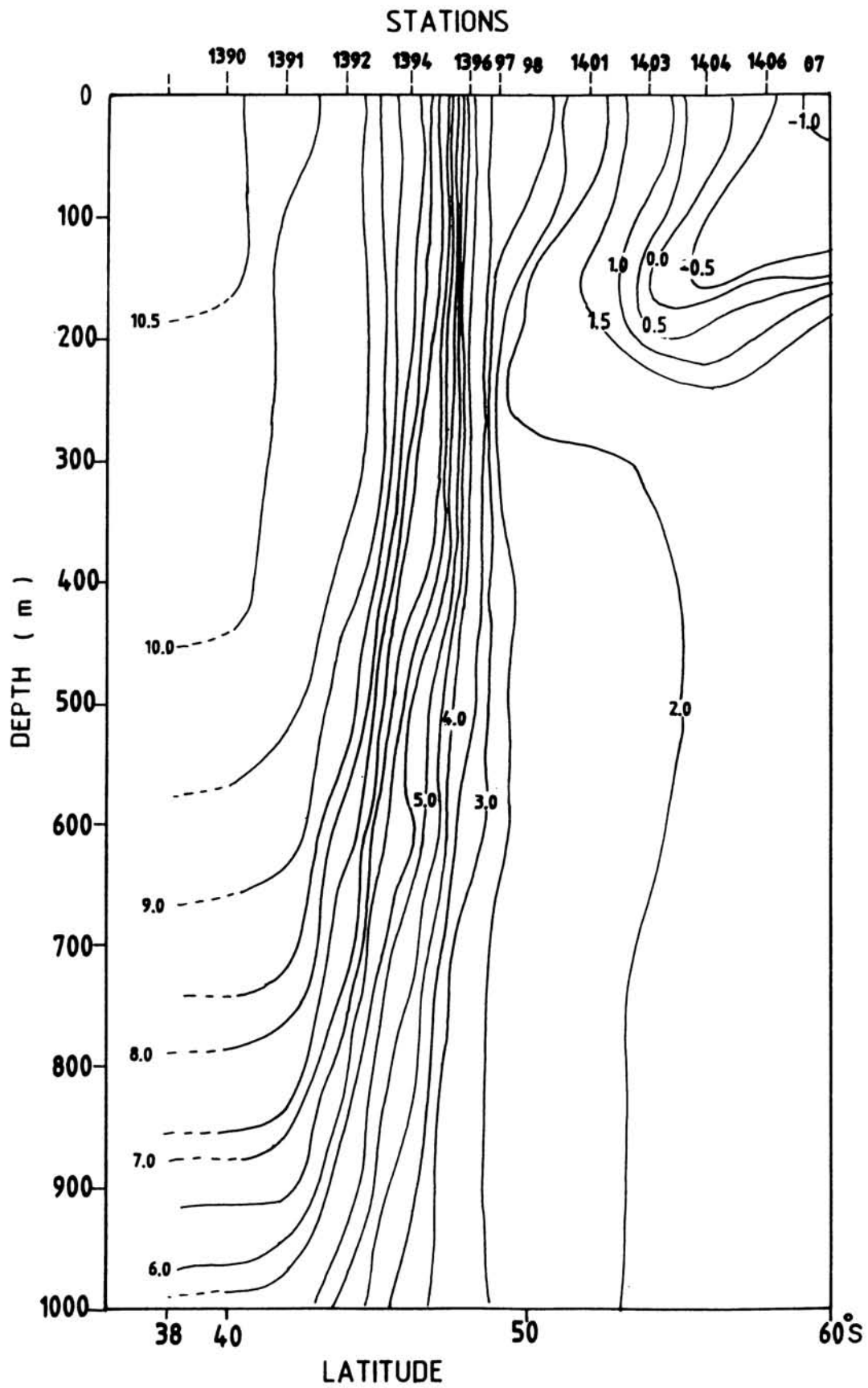


FIG.3.1. VERTICAL SECTION OF TEMPERATURE ( °C - Degree Centigrade ) .  
ALONG 105°E

STF is ambiguous along this section.

### 3.1.11 Along 110°E

The thermal structure along 110°E representing the summer conditions is shown in Fig. 3.1.11. A strong thermal gradient of 1.5°C per one degree latitude is seen extending upto 150 m depth around 60°S. Surface layer of uniform temperature is well depicted between stations 1353 and 1354 extending upto 150 m depth. The 2°C isotherm of the temperature minimum layer makes a sharp descent around station 1351 indicating further the location of APF around 50°S. The ascent of NADW is seen around 300 m between stations 1352 and 1354. Further north, SAF is manifested between stations 1349 and 1351 extending upto 850 m depth. STF is weak along this section.

### 3.1.12 Along 115°E

The distribution of temperature along 115°E is shown in Fig. 3.1.12. The distribution resembles to that along 110°E. A strong thermal front with a temperature difference of about 3°C occurs around 58°S. The 2°C isotherm in the temperature minimum layer sinks between stations 1360 and 1361 and hence the latitude 50°S could

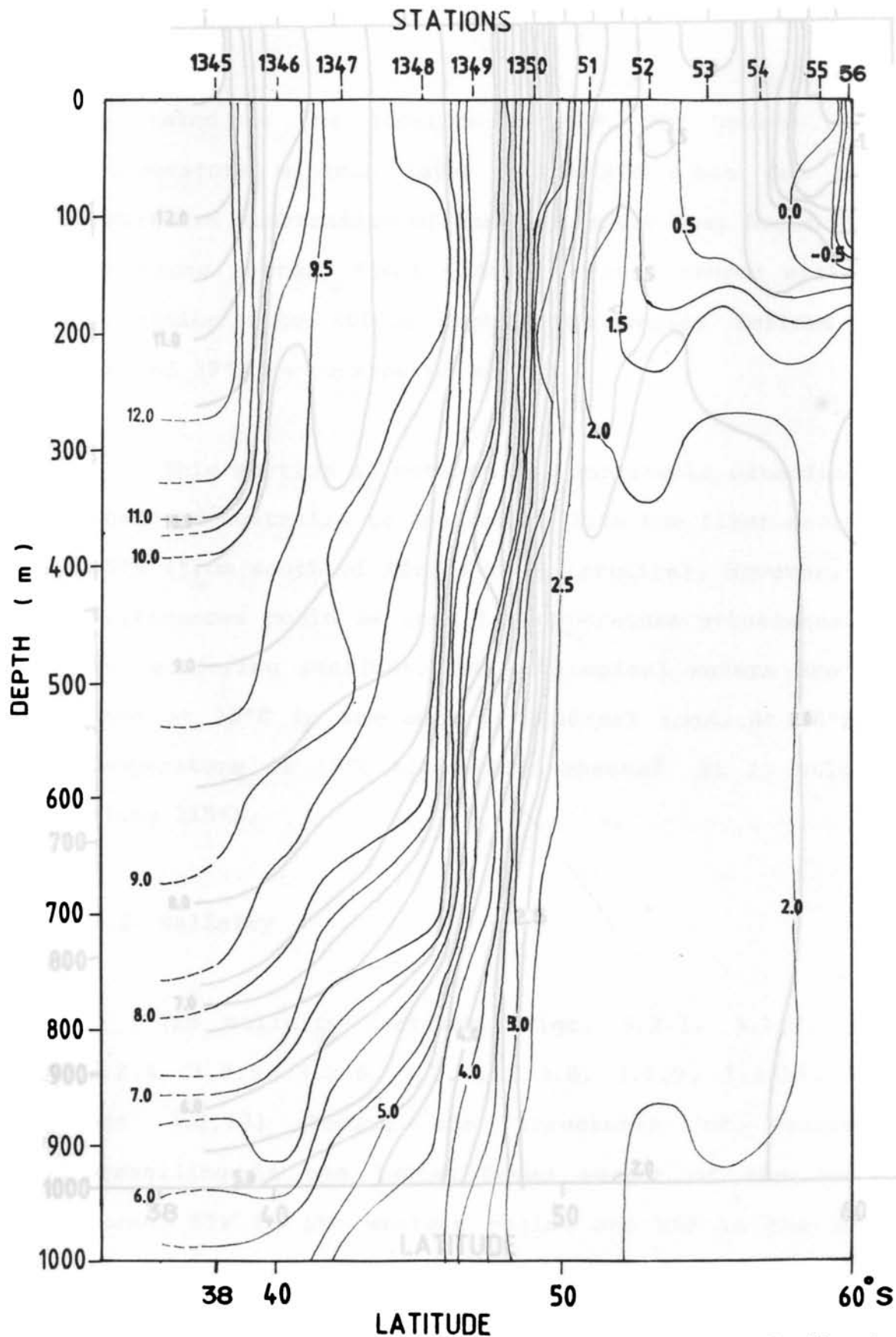


FIG.3.I.II VERTICAL SECTION OF TEMPERATURE ( °C - Degree Centigrade )  
ALONG 110°E

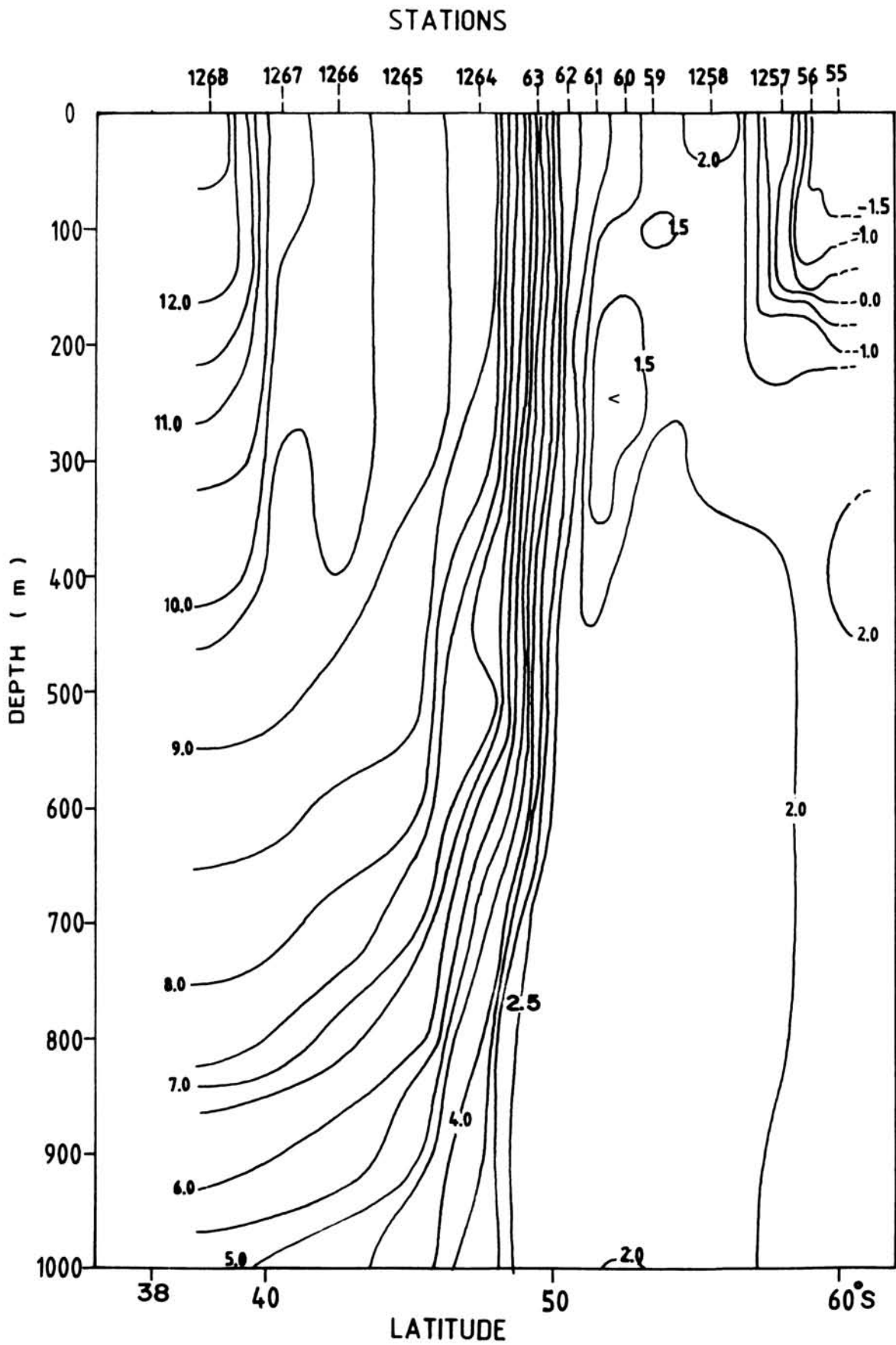


FIG.3.1.12 VERTICAL SECTION OF TEMPERATURE ( °C - Degree Centigrade )  
ALONG 115° E

be taken as the location of APF. The upward tilt of temperature minimum layer below 300 m is due to the southward penetration of North Atlantic Deep Water (NADW). A strong thermal front (SAF) is vivid around station 63 extending upto 900 m depth. The weakly defined front around 39°S is considered as STF.

This section is between two continents extending from south of Australia to Antarctica like the first section at 20°E (from south of Africa to Antarctica). However, large differences could be seen in temperature structures along the bordering sections. The subtropical waters are quite warm at 20°E in the same latitudinal zone. At 38°S, the temperature is 19°C along 20°E whereas it is only 12°C along 115°E.

### 3.2 Salinity

The salinity sections (Figs. 3.2.1, 3.2.2, 3.2.3, 3.2.4, 3.2.5, 3.2.6, 3.2.7, 3.2.8, 3.2.9, 3.2.10, 3.2.11 and 3.2.12) depict the structures of watermasses prevailing in the Indian Ocean sector of the Southern Ocean. STF in the western region and SAF in the eastern region are marked by strong saline gradients. In the

Antarctic zone salinity is generally low due to the processes of melting and continental run off.

### 3.2.1 Along 20°E

The salinity section along 20°E during summer (Fig.3.2.1) shows a salinity range of 33.8-35.5‰ in the surface layer. Near the Antarctic coast, a strong halocline exists from surface to 50 m depth. Between stations 72 and 83, salinity remains uniform below 300 m wherein the high saline waters (>34.6‰) are due to spreading of NADW. The Antarctic Intermediate Water forming at APF is shown by vertical descent of 34.4 to 34.5‰ isohalines around 50°S. There is no clear gradient in salinity at the APF while at STF salinity gradient is prominent with a change of about 1.3‰ within 1.5° latitude.

### 3.2.2 Along 30°E

The salinity section (Fig.3.2.2) during summer shows a large deviation from the previous section. Very low surface salinity (<33.9‰) values are found in the surface layer of Antarctic zone. The halocline shown in the Antarctic coast is weak in comparison with that in

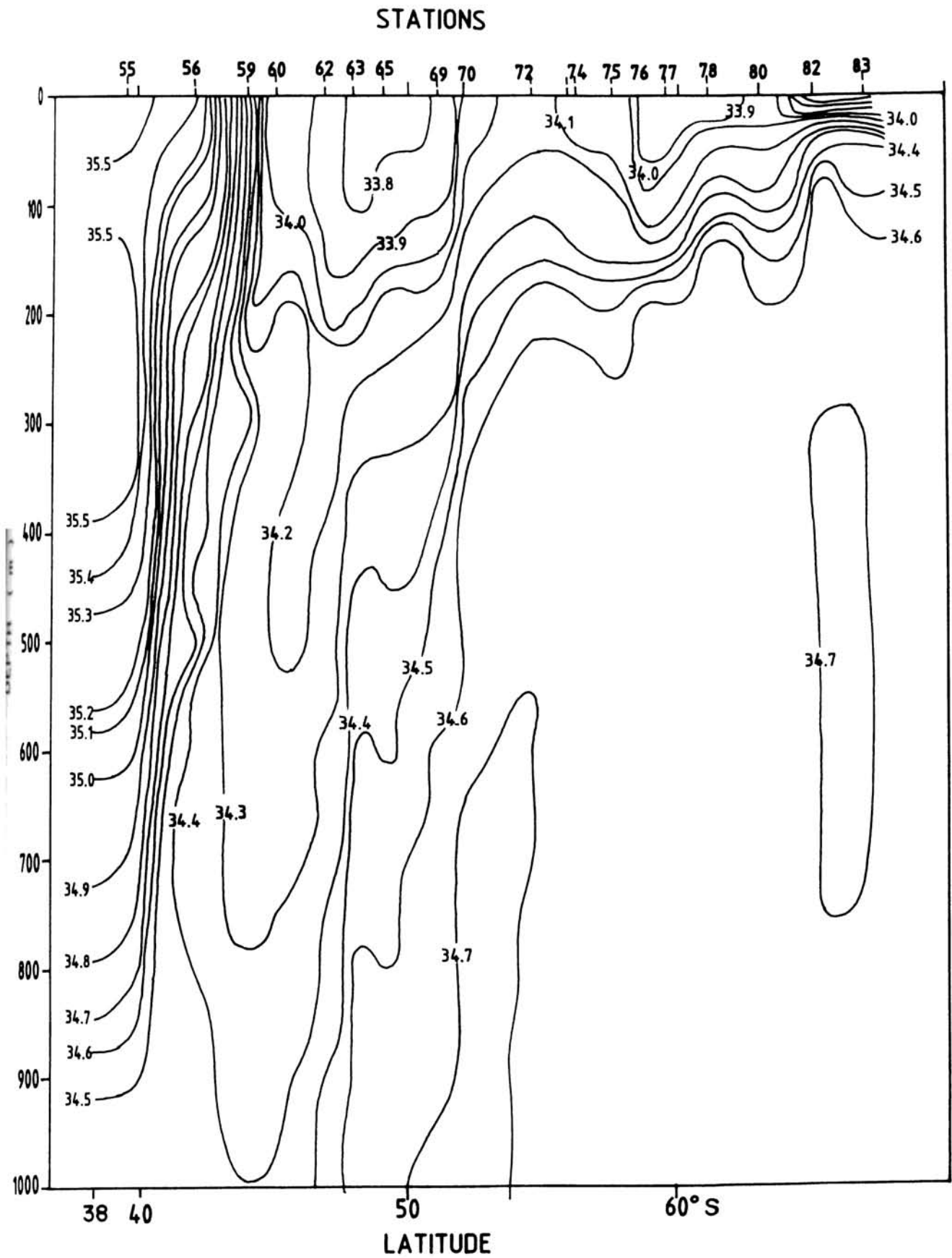


**FIG. 3.2.1 VERTICAL SECTION OF SALINITY ( ‰ - Parts per mille )  
ALONG 20°E**

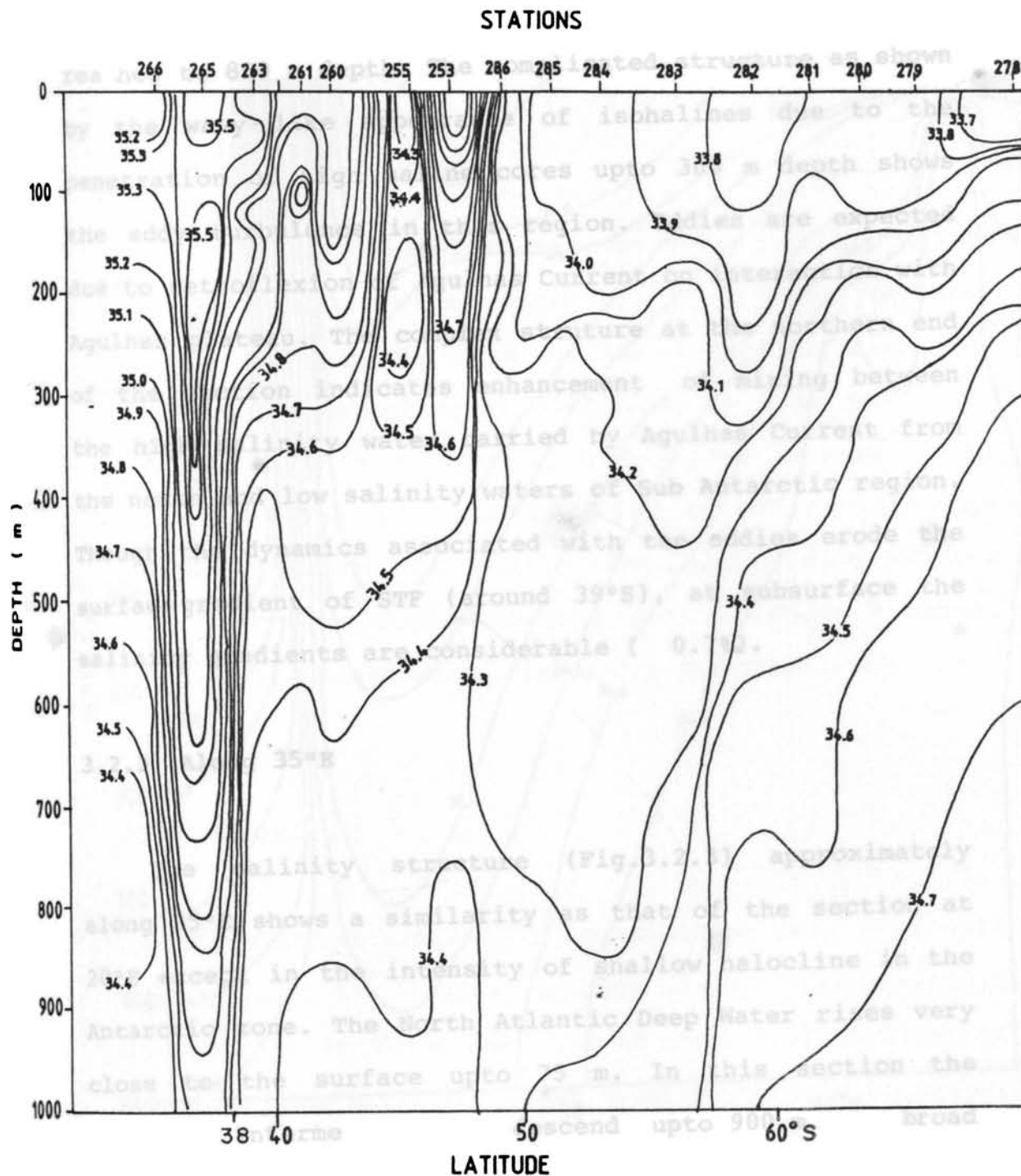


**FIG. 3.2.2 VERTICAL SECTION OF SALINITY ( ‰ - Parts per mille )  
APPROXIMATELY ALONG 30°E**



previous section. The low salinity core associated with Antarctic Intermediate Water is extended upto  $50^{\circ}\text{S}$  and it reaches to 800 m depth. The complicated structure as shown by the wavy-like appearance of isohalines due to the penetration of high saline cores upto 300 m depth shows the eddy turbulence in this region. Eddies are expected due to retroflexion of Agulhas Current on interaction with Agulhas plateau. The complex structure at the northern end of the section indicates enhancement of mixing between the high salinity water carried by Agulhas Current from the north and low salinity waters of Sub Antarctic region. Though the dynamics associated with the eddies erode the surface gradient of STF (around  $39^{\circ}\text{S}$ ), at subsurface the salinity gradients are considerable ( 0.7‰).

### 3.2.3 Along $35^{\circ}\text{E}$

The salinity structure (Fig.3.2.3) approximately along  $35^{\circ}\text{E}$  shows a similarity as that of the section at  $20^{\circ}\text{E}$  except in the intensity of shallow halocline in the Antarctic zone. The North Atlantic Deep Water rises very close to the surface upto 75 m. In this section the Antarctic Intermediate water descends upto 900 m as a broad low salinity tongue around  $43^{\circ}\text{S}$ . Further north, a haline

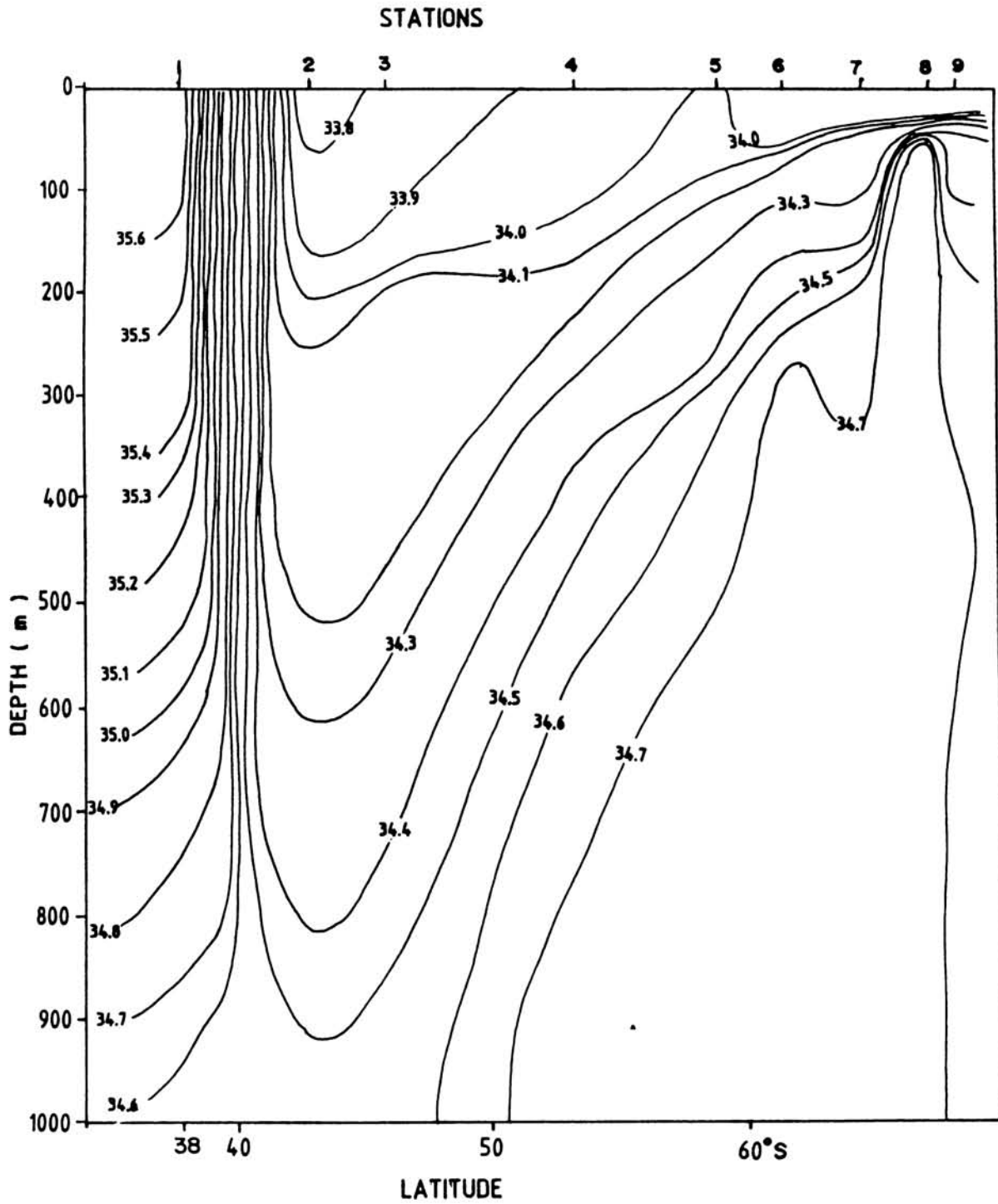


FIG.3.2.3 VERTICAL SECTION OF SALINITY ( ‰ - Parts per mille ) ALONG 35° E

front associated with STF and with a gradient of 1.8‰ per three degree latitude is manifested around 40°S.

#### 3.2.4 Along 40°E

Fig. 3.2.4 represents the vertical distribution of salinity along 40°E. Compared to the previous section, salinity is slightly less in the Antarctic zone. The corresponding halocline in this zone is also weak. The high saline North Atlantic Deep Watermass is seen rising upto 100 m. The water (AIW) formed at APF extends down upto 800 m depth. The haline subtropical front shows a salinity drop of 1.2‰ extending upto about 600 m depth. The salinity structure is closely in resemblance with that of 35°E.

#### 3.2.5 Along 45°E

The section along 45°E is extending only upto 43°S (Fig. 3.2.5). The surface salinity in the region between 43° and 70°S is below 34‰. It is even falls further to 33.6‰ in the Antarctic Zone. Near the Antarctic coast, the halocline is strong with a gradient of 0.6‰ per 50 m. As in the previous section the North Atlantic Deep Water

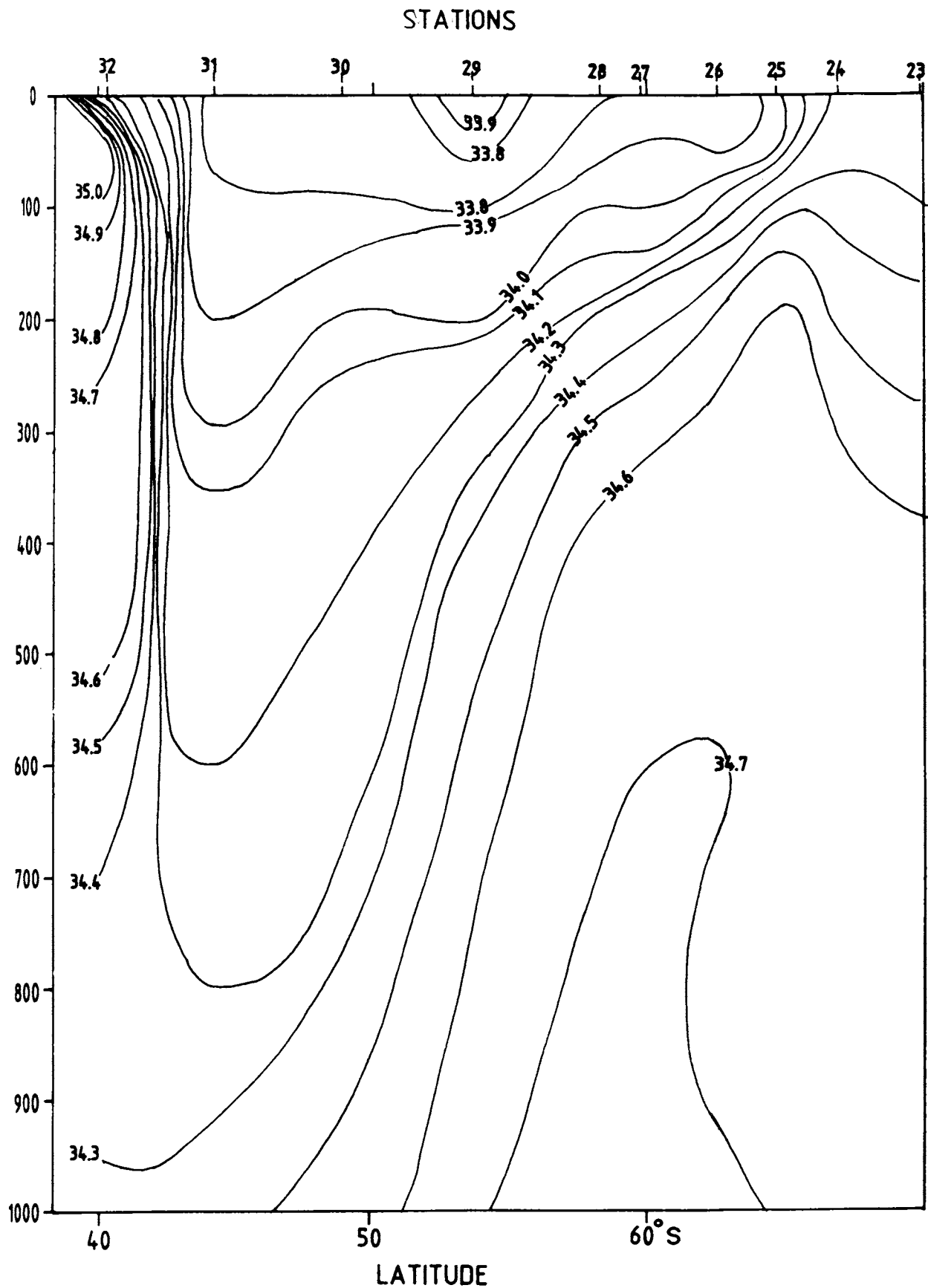
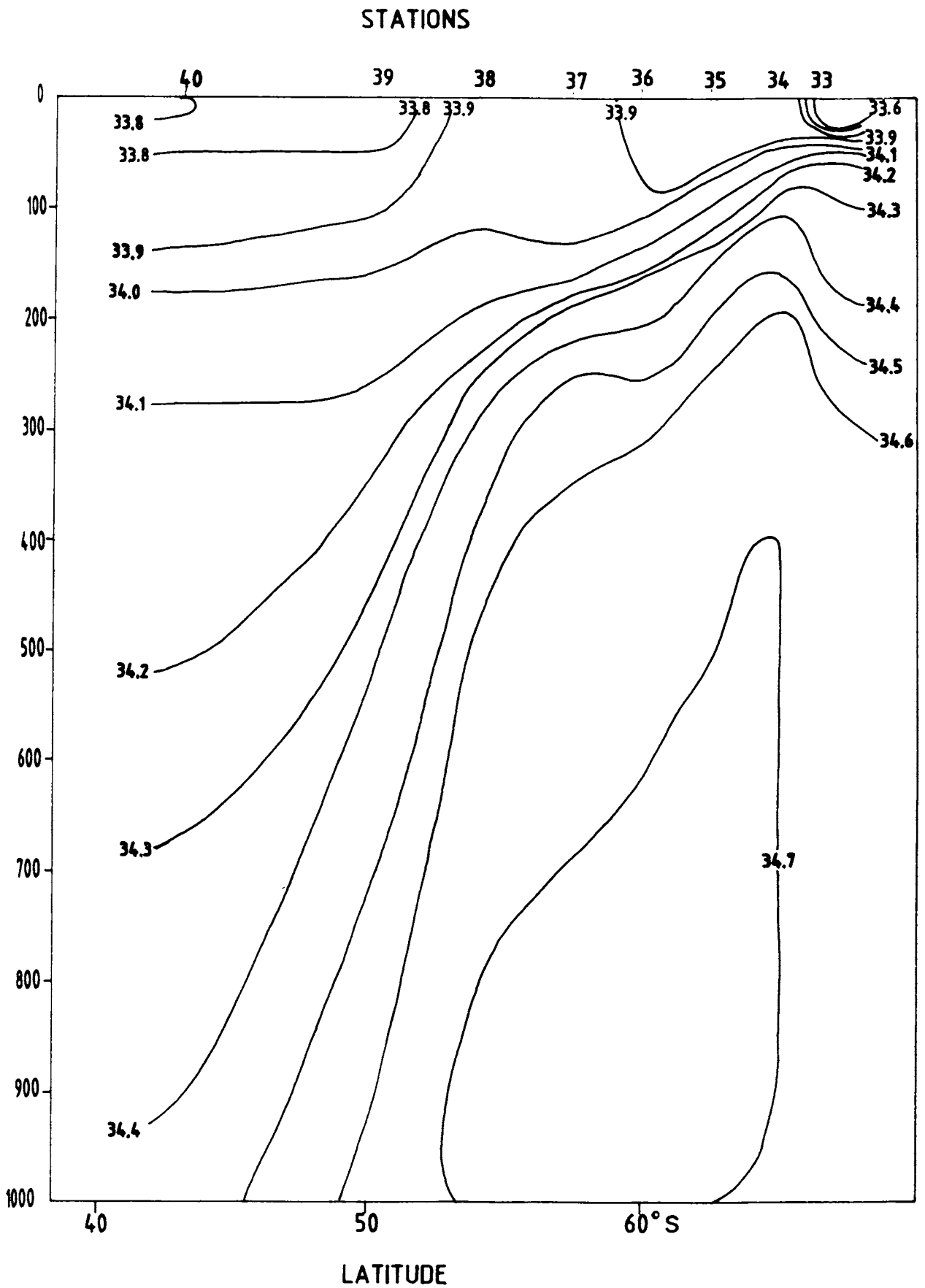


FIG.3.2.4 VERTICAL SECTION OF SALINITY ( ‰- Parts per mille )  
ALONG 40°E



is seen rising upto 100 m depth.

### 3.2.6 Along 55°E

The section approximately along 55°E (Fig.3.2.6) shows on average low surface salinity as compared to that along the section at 40°E. The halocline in the Antarctic Zone is a different one and the Antarctic Intermediate Water sinks more than 1000 m depth. STF is characterised with a strong gradient in salinity (1.7‰ per two degree latitude). Here STF is strong and extends upto 600 m depth.

### 3.2.7 Along 85°E

The winter section (June-July) of salinity along 85°E is depicted in Fig. 3.2.7. The surface salinity ranges from 33.9 to 34.8‰ and this range is much less compared to that in the western region. Unlike in the previous sections the low salinity tongue of Antarctic Intermediate Water descends rather steeply around 49°S. Between stations 1552 and 1553 a haline front with a gradient of 0.6‰ per one degree latitude is depicted and its vertical extent is about 500 m. The presence of this haline front (SAF) is a conspicuous feature in the eastern region of

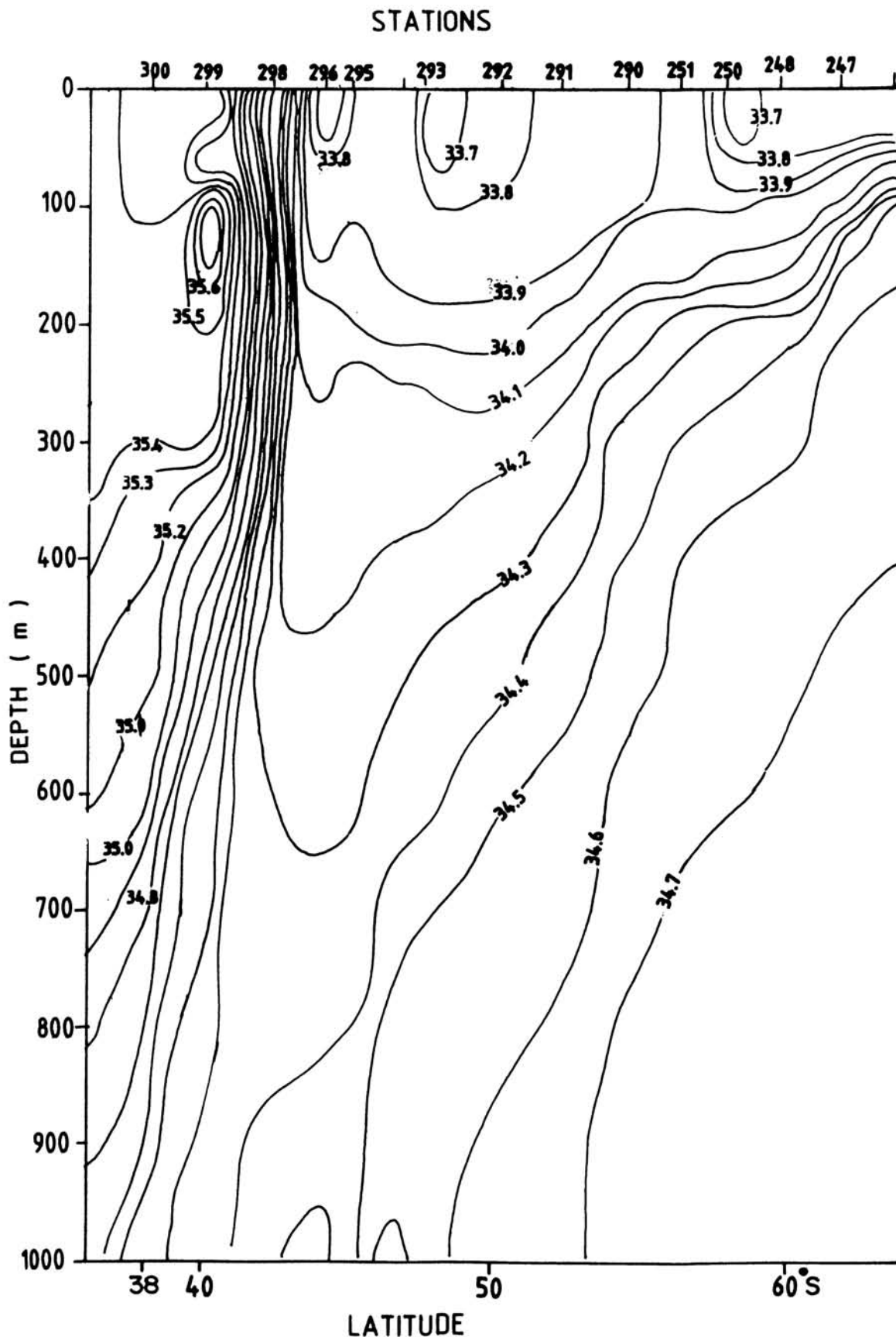


FIG.32.6 VERTICAL SECTION OF SALINITY ( ‰- Parts per mille )  
APPROXIMATELY ALONG 55° E

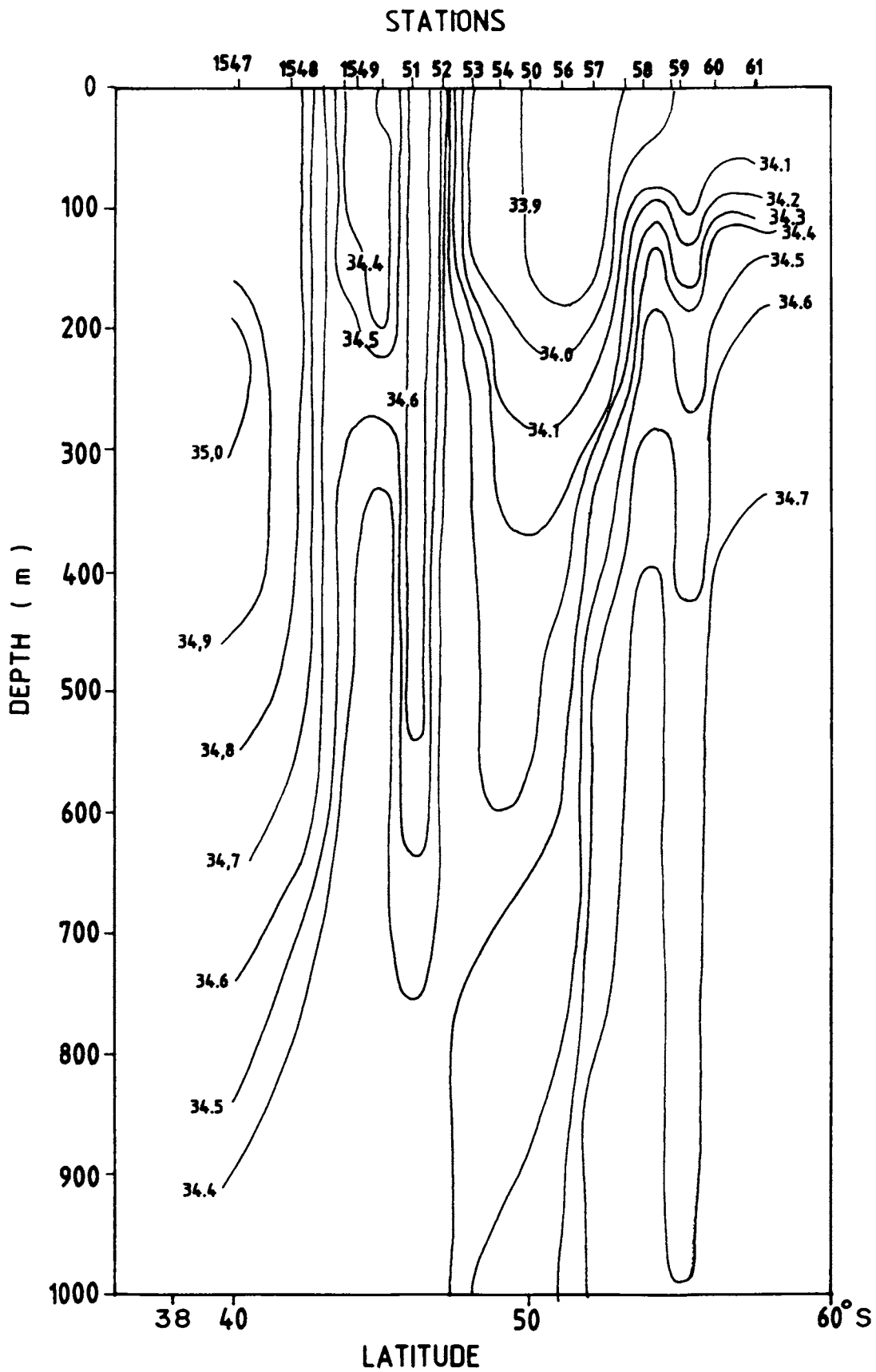


FIG.3.2.7 VERTICAL SECTION OF SALINITY ( ‰ - Parts per mille )  
ALONG 85°E



the Indian Ocean sector of the Southern Ocean. The Sub Tropical Front (STF) is not well developed in the section. Along this section the surface salinity observed at 40°S is 34.8‰ while at 55°E it is about 35.3‰.

### 3.2.8 Along 95°E

The section (Fig.3.2.8) along 95°E covered during post winter period shows pockets of low salinity water in the Antarctic zone. The subsurface halocline in the Antarctic zone is weak along this section. The melting of ice near Antarctica coast (Station 1373) is reflected in the reduction of salinity to less than 33.9‰. As in the previous section, along this section also, the low salinity core is shifted towards south (~49°S). Across SAF there is no surface salinity gradient. STF is very weak and it manifests as a double front on either side of 41°S.

### 3.2.9 Along 100°E

Fig. 3.2.9 represent the vertical distribution of salinity along 100°E between 38° and 60°S. This section shows a stronger homogeneous surface layer of salinity (~34.1‰) in the Antarctic Zone compared to previous section.

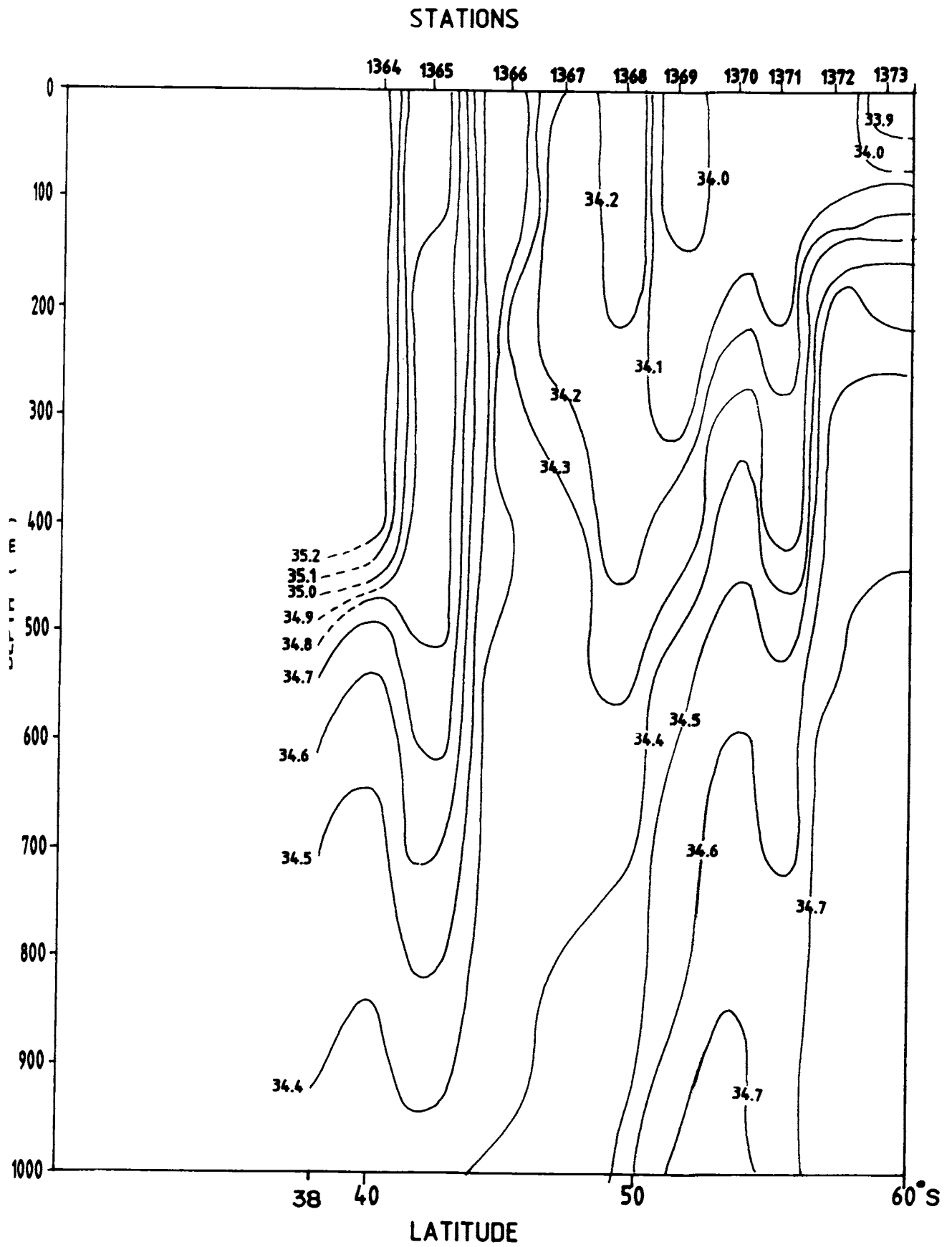


**FIG.3.2.8 VERTICAL SECTION OF SALINITY ( ‰- Parts per mille )  
ALONG 95°E**

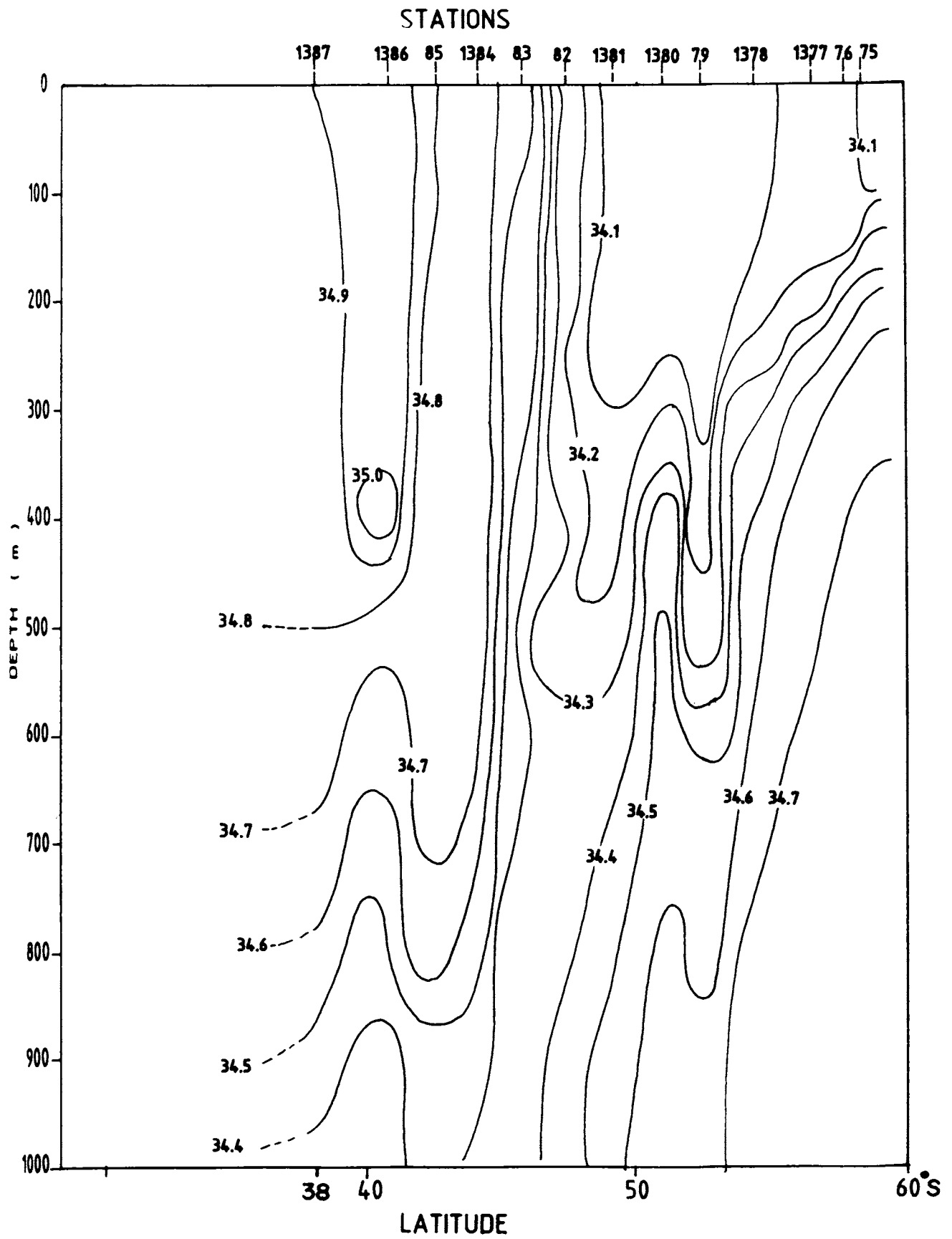


FIG.3.2.9 VERTICAL SECTION OF SALINITY ( ‰ - Parts per mille )  
ALONG 100°E

The core of the Antarctic Intermediate Water is shifted more towards north ( $46^{\circ}\text{S}$ ) reaching upto 1000 m depth. A haline front across SAF is depicted between stations 1381 and 1382. STF is very weak between stations 1386 and 1389.

### 3.2.10 Along $105^{\circ}\text{E}$

The section (Fig. 3.2.10) along  $105^{\circ}\text{E}$  covered during November shows a broader layer of uniform salinity ( $\sim 34\%$ ) in the Antarctic zone. This surface layer salinity is less than that at  $100^{\circ}\text{E}$ . This reduction in salinity is due to the melting of ice as the section corresponds to the beginning of summer. The halocline below Antarctic zone is further reduced with vertical salinity gradient of 0.4‰ per 150 m depth. The low salinity water associated with AIW sinks from  $50^{\circ}\text{S}$  near the surface and reaches 1000 m depth at  $47^{\circ}\text{S}$ . SAF manifests as a haline front between stations 1392 and 1396 extending upto 600 m depth. STF is very weak around station 1390.

### 3.2.11 Along $110^{\circ}\text{E}$

The section along  $110^{\circ}\text{E}$  (Fig.3.2.11) shows the distribution of salinity in the month of October. An isohaline layer is seen from  $50^{\circ}$  to  $60^{\circ}\text{S}$  extending to a

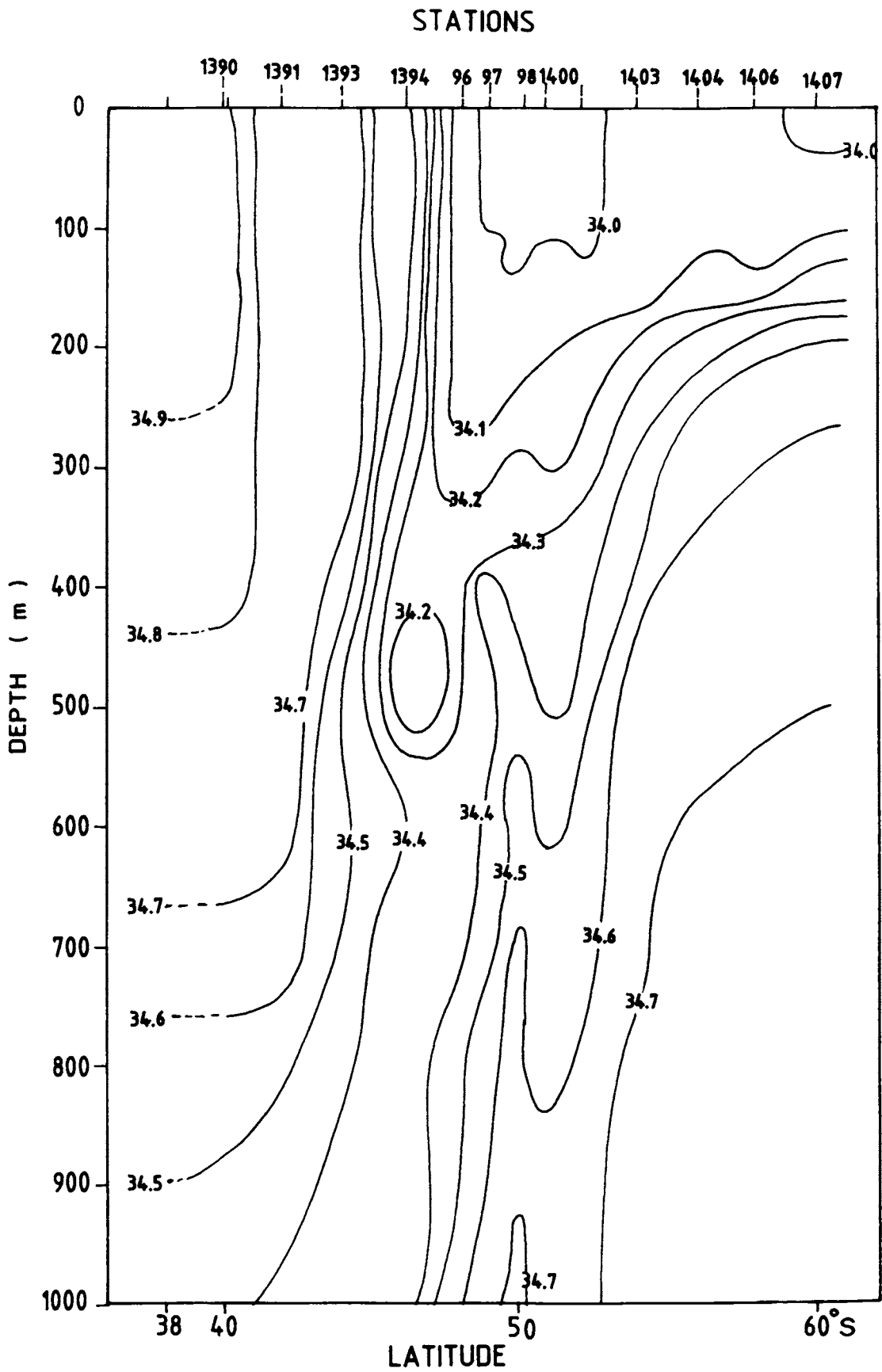


**FIG.3.2.10 VERTICAL SECTION OF SALINITY ( ‰ - Parts per mille )  
ALONG 105°E**

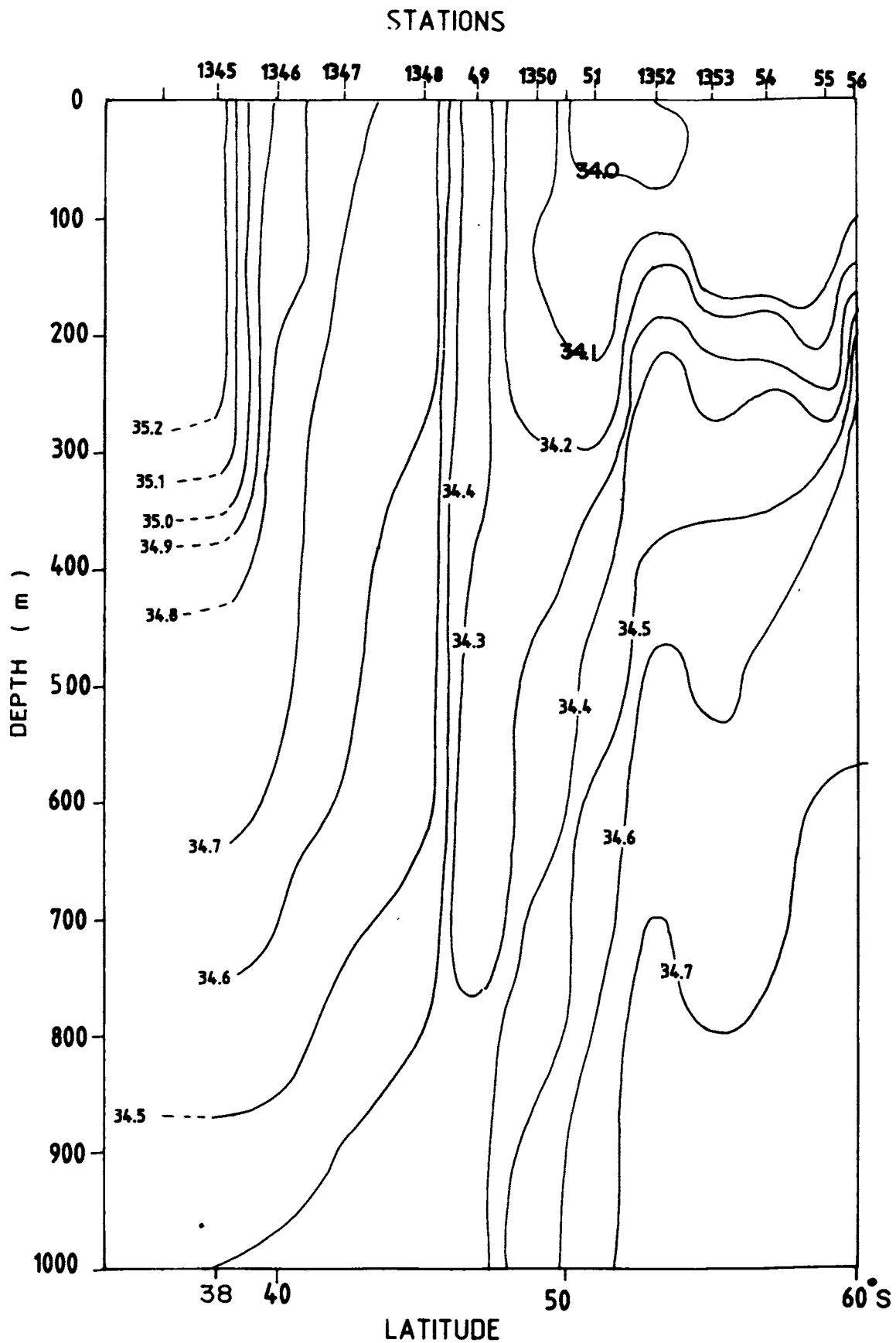


FIG.3.2.II VERTICAL SECTION OF SALINITY ( ‰- Parts per mille )  
ALONG 110°E

depth of 200 m. Halocline in the Antarctic Zone is considerably weak. The North Atlantic Deep Water rising around station 1352 is represented by the isohaline 34.7‰.

Along this section also Antarctic Intermediate Water sinks in a similar way as that seen in the preceding section. The SAF manifesting between stations 1349 and 1350 is weak. On comparison with the earlier section, STF along this section is found to be strong in the upper 400m only.

### 3.2.12 Along 115°E

Fig. 3.2.12 gives the salinity distribution along the section between the coasts of Australia and Antarctica during summer. When comparing the salinity values along 38°S latitude south of Australia and Africa, it is observed that salinity is reduced by 0.3‰ from west to east. In the Antarctic Zone the isohaline layer is extending upto a depth of 200 m. The Antarctic Intermediate Water (AIW) reaches to a depth greater than 900 m at 47°S. A haline front with a drop of about 0.6‰ associated with SAF is seen between stations 1263 and 1264

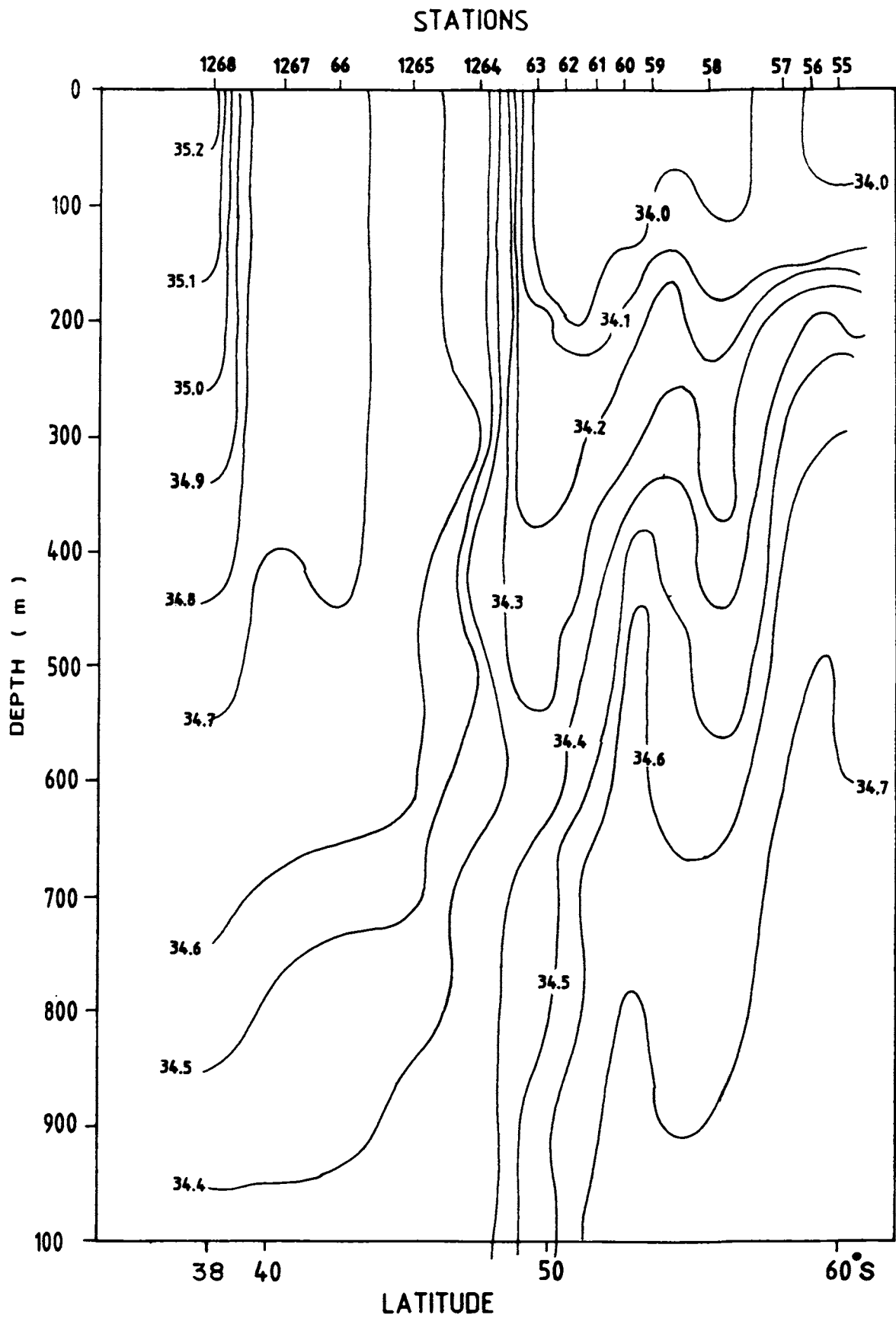


FIG3.2.12 VERTICAL SECTION OF SALINITY ( ‰- Parts per mille )  
ALONG 115°E



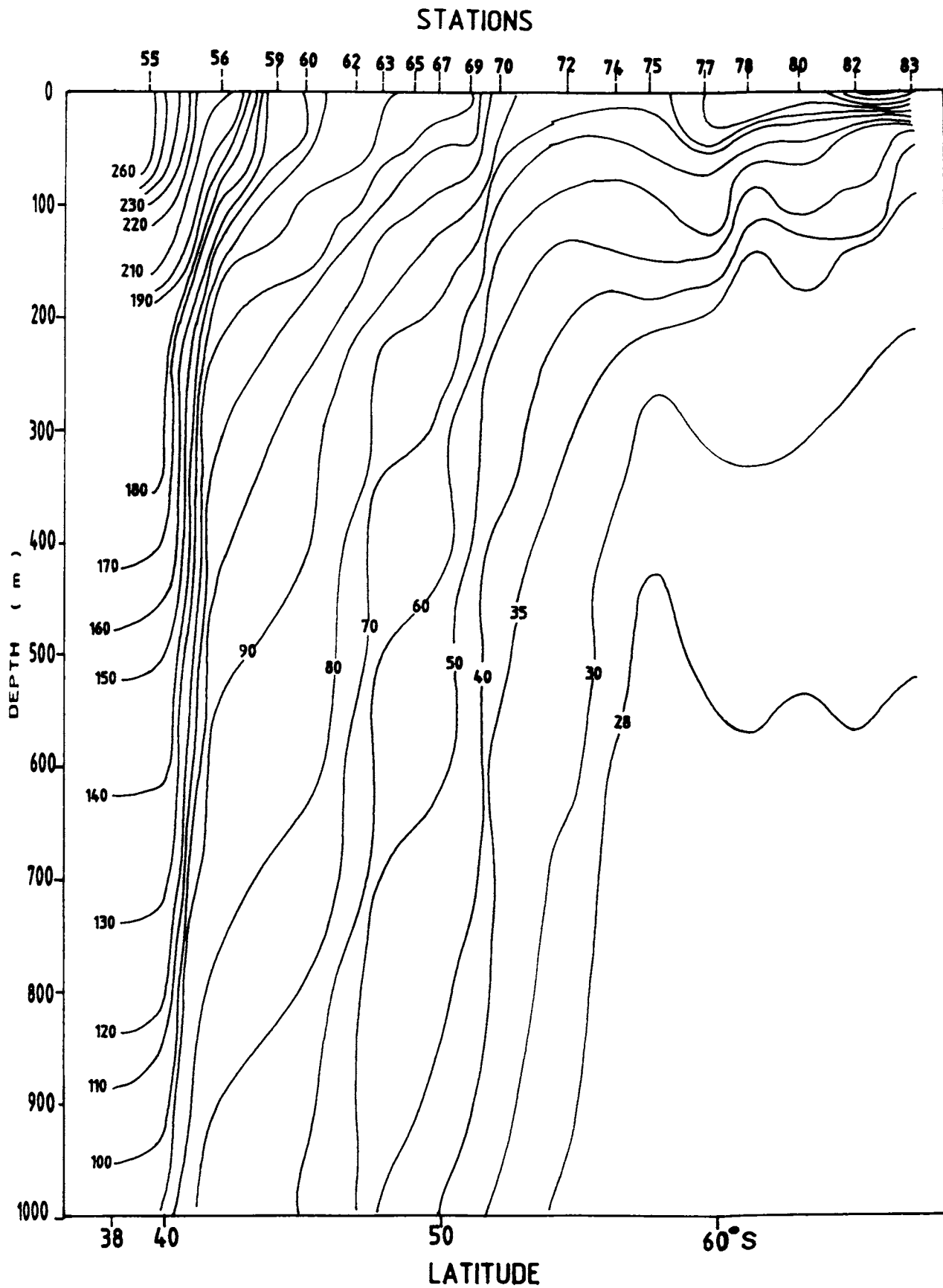
extending upto 600 m. STF is depicted around station 1268 in the upper 300 m.

### 3.3 Thermosteric anomaly

The thermosteric anomaly sections (Figs. 3.3.1, 3.3.2, 3.3.3, 3.3.4, 3.3.5, 3.3.6, 3.3.7, 3.3.8, 3.3.9, 3.3.10, 3.3.11 and 3.3.12) exhibit more clearly the dynamic nature of Antarctic waters. Since the thermosteric anomaly is a good approximation of density in the 0-1000m water column, the watermasses in the upper 1000 m responsible for the formation of the front can be differentiated. Thermosteric anomaly sections further serve the purpose to know whether a front is density or density compensated.

#### 3.3.1 Along 20°E

Fig. 3.3.1 shows the distribution of thermosteric anomaly along 20°E during summer. A strong pycnocline is seen in the Antarctic zone near the surface. Though there is no stronger gradient at APF, the vertical orientation of steric surfaces especially those between 40 and 70 cl/t shows the convergence. In the Antarctic Zone a uniform



3.3.1. VERTICAL SECTION OF THERMOSTERIC ANOMALY ( cl/t-Centi litre per ton )  
ALONG 20°E

denser layer ( $\sim 30$  cl/t) of Deep Water is seen below 400 m. From the stronger horizontal steric gradient around  $40^{\circ}\text{S}$ , the STF can be identified. It extends upto 1000 m.

### 3.3.2 Along $30^{\circ}\text{E}$

The Pycnocline observed in the Antarctic zone is weak compared to the earlier section (along  $20^{\circ}\text{E}$ ). Eventhough the subsurface orientation of isolines 60-70 cl/t shows an Antarctic Convergence, the surface manifestation of APF is eroded by the eddies generated from north. The complex steric pattern due to the eddies as shown by the wavy nature of isanosteres results in strong current shears in the northern region of the section. The bifurcation of the strong gradient in thermosteric anomaly in the north shows two opposite regimes of currents - Agulas Current and ACC embedded with a warm water eddy.

### 3.3.3 Along $35^{\circ}\text{E}$

The section approximately along  $35^{\circ}\text{E}$  covered during December shows a strong pycnocline around 50 m depth confined to the southern part of Antarctic zone. The dome shaped structure of isanosteres around station 8 indicates the divergence in the flow pattern associated with rising

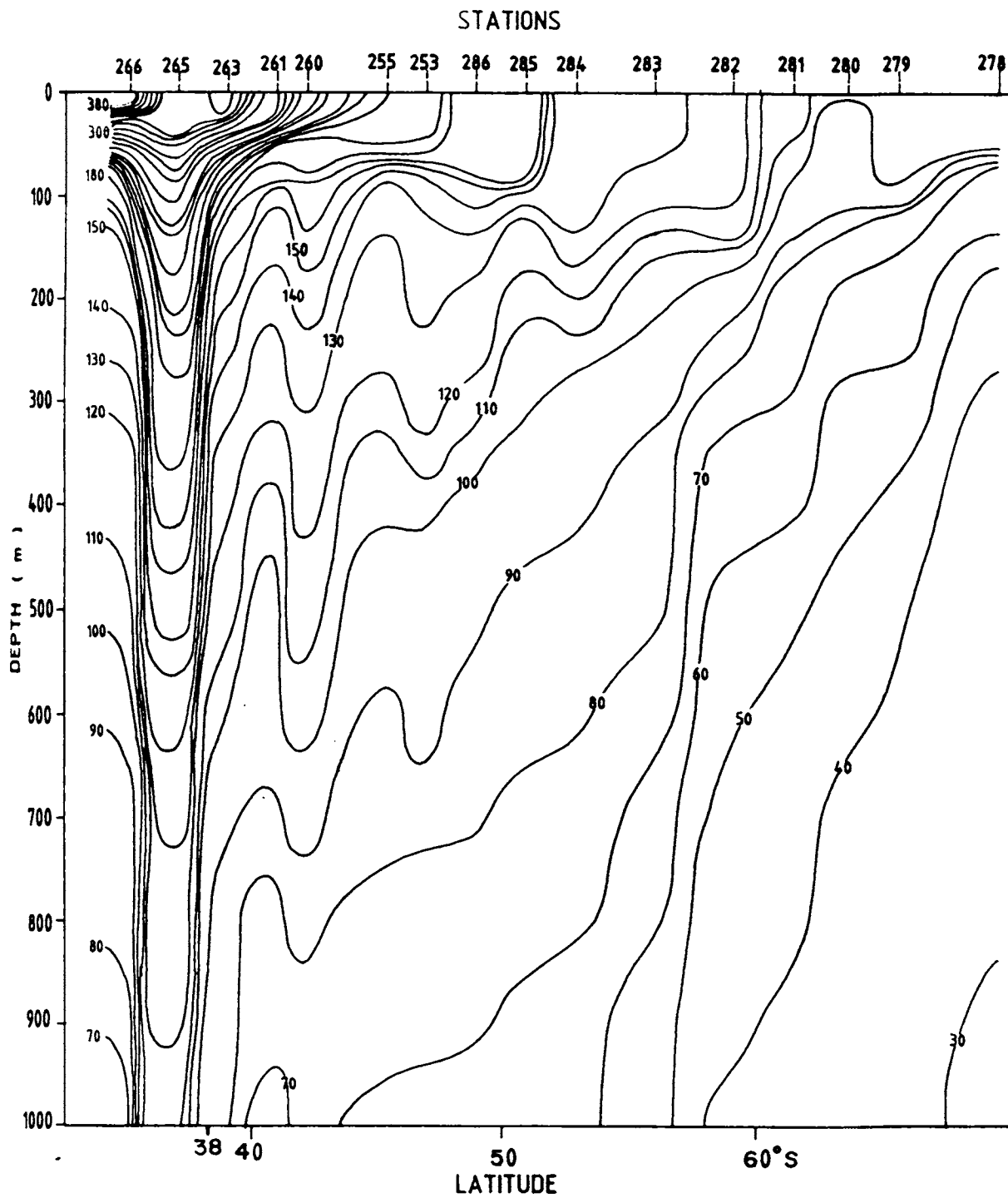


FIG.332 VERTICAL SECTION OF THERMOSTERIC ANOMALY ( cl/t-Centi litre per ton )  
APPROXIMATELY ALONG 30°E

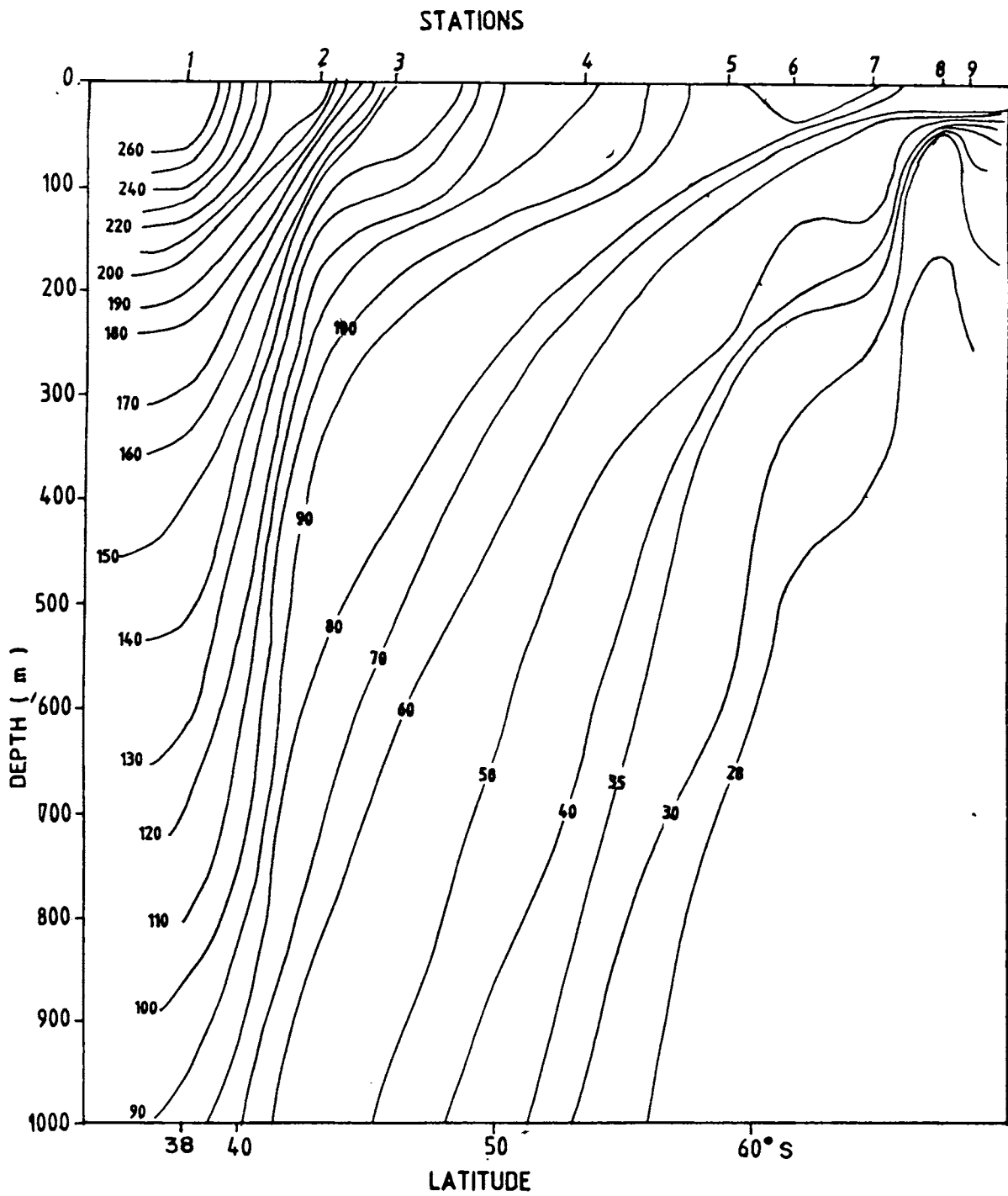


FIG.3.33 VERTICAL SECTION OF THERMOSTERIC ANOMALY (  $^{\circ}\text{C}/\text{t}$ -Centi litre per ton )  
ALONG  $35^{\circ}\text{E}$

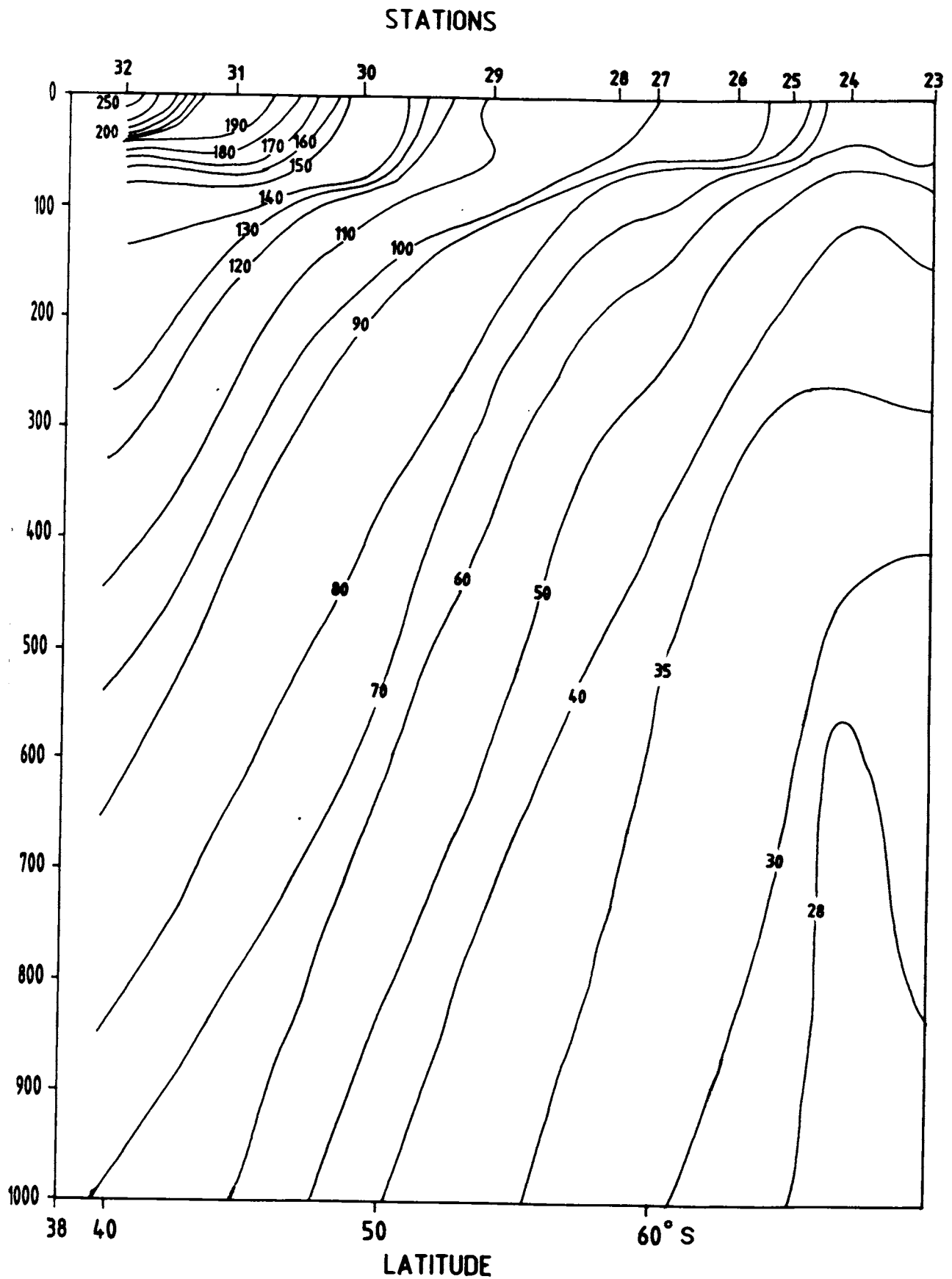
of Deep Water. The orientation of isanosteres further shows the diffused nature of Antarctic Circumpolar Current between  $40^{\circ}$  and  $60^{\circ}$  S as seen from their reduced slopes compared to earlier section. The stronger gradient between stations 10 and 11 represents the thermohaline front (STF).

#### **3.3.4 Along $40^{\circ}$ E**

The section along  $40^{\circ}$ E (Fig. 3.3.4) shows the absence of a strong pycnocline in the Antarctic zone. The flow of Antarctic waters is shown by the more northward extent in the slope of isanosters. The Sub-Tropical Front between stations 31 and 32 as inferred from both temperature and salinity gradients (Figs.3.1.4 and 3.2.4) is not seen with corresponding stronger density gradient.

#### **3.3.5 Along $45^{\circ}$ E**

Fig. 3.3.5 represents the thermosteric anomaly distribution along  $45^{\circ}$ E during March. The near surface pycnocline in the Antarctic zone is stronger than that in previous section. Below the Antarctic zone a water of relatively uniform density is encountered. APF is located between stations 38 and 39 in the upper 1000 m from the



3.4 VERTICAL SECTION OF THERMOSTERIC ANOMALY ( cl/t-Centi litre per ton ) ALONG 40° E

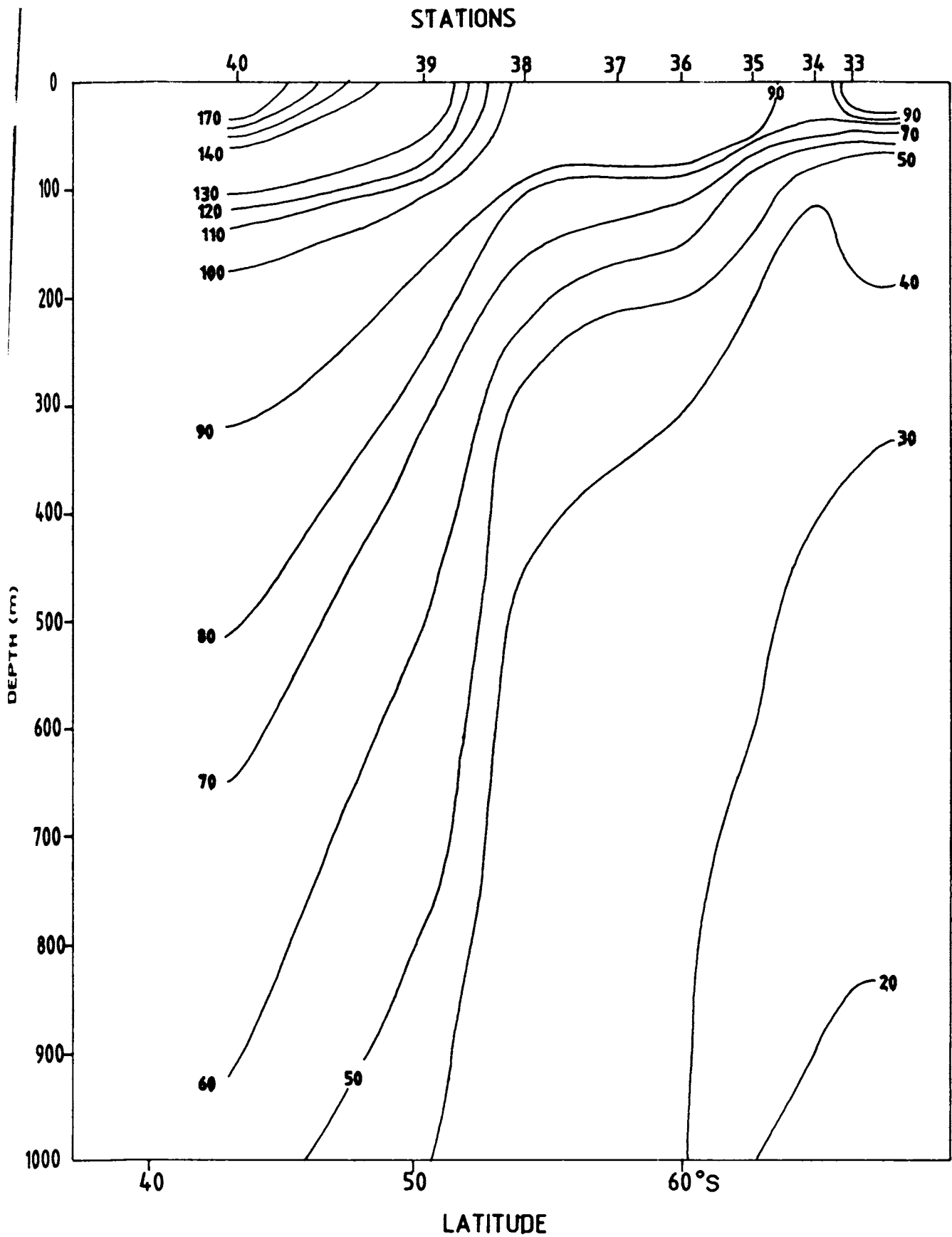


FIG.3.35 VERTICAL SECTION OF THERMOSTERIC ANOMALY ( cl/t-Centi litre per ton ) ALONG 45° E



orientation of steric surfaces between 40 and 70 cl/t. Further in the northern portion, no stronger steric gradient is seen suggesting the presence of a single front at 45°E.

### 3.3.6 Along 55°E

Fig. 3.3.6 presents the thermosteric anomaly approximately along 55°E. The Pycnocline in the Antarctic zone becomes weak in contrast to that at 45°E. The slopes of isanosteres show a broader interaction between Subantarctic and Subtropical waters. An anticlockwise flow around station 293 in the upper 100 m depth water column is envisaged due to penetration of eddy into the area. A very strong gradient of 110 cl/t per 3° latitudinal distance is shown across STF (between stations 296 and 299) near the surface.

### 3.3.7 Along 85°E

The vertical section of thermosteric anomaly (Fig.3.3.7) along 85°E exhibits intensification in the flow pattern of ACC compared to the western sections. The vertical orientation of isanosteres between 40 and 60 cl/t shows the Antarctic Convergence whereas those between 90

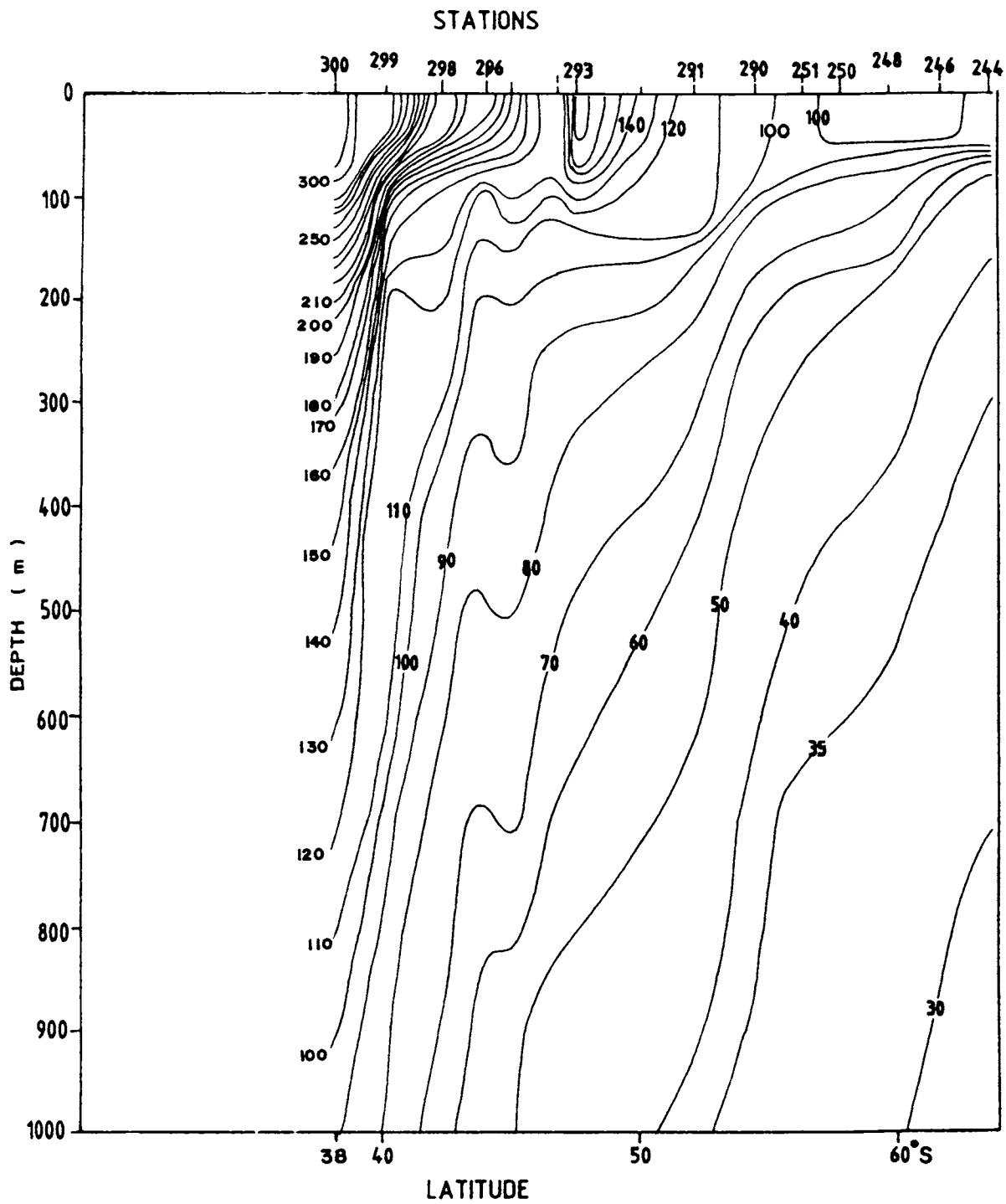


FIG.3.3.6 VERTICAL SECTION OF THERMOSTERIC ANOMALY ( ct/t-Centi litre )  
APPROXIMATELY ALONG 55°E

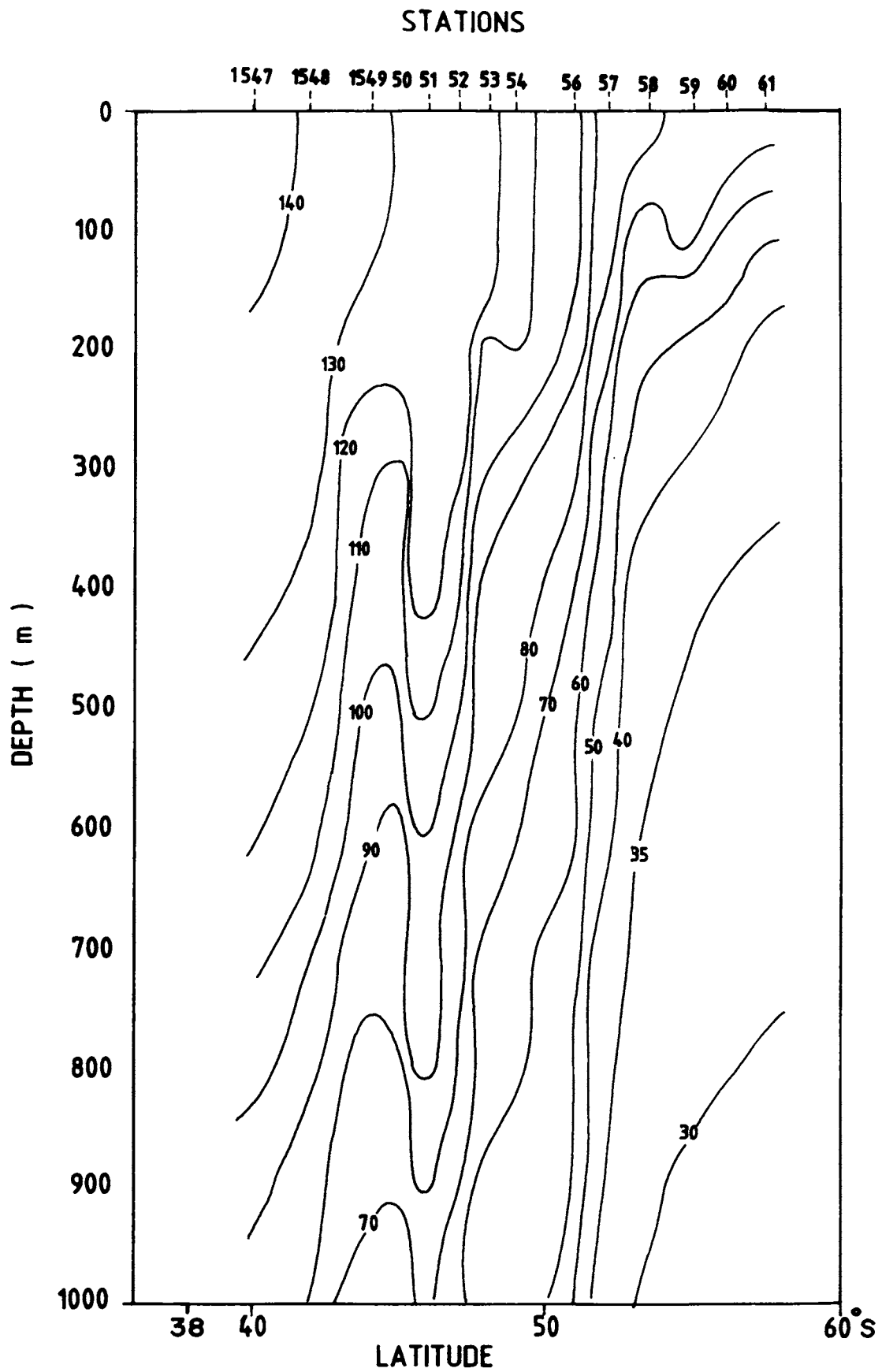


FIG.3.3.7 VERTICAL SECTION OF THERMOSTERIC ANOMALY (  $\text{cl/t}$ -Centi litre per ton ) ALONG  $85^\circ\text{E}$

and 120 cl/t indicate Sub-Antarctic Convergence. The orientation of isanosteres shows that zonal axis of ACC is in between 46° and 52°S. Horizontal shears in the flow pattern are expected in the subantarctic region facilitating more interaction between STF and SAF. Compared to the western sections, lower steric values are encountered in the northern portion of the section mainly due to lower temperatures during winter.

### 3.3.8 Along 95°E

Fig. 3.3.8 shows the thermosteric anomaly section along 95°E during post winter season. As in the section at 85°E, there is no strong pycnocline in the Antarctic zone. Between stations 1371 and 1372 a convergence is seen extending to greater depths. The vertical orientation of isanosteres around station 1369 shows the presence of another convergence. The steep slope of isanosteres suggests the stronger intensity of ACC like at 85°E.

### 3.3.9 Along 100°E

The distribution of steric values along 100°E (Fig. 3.3.9) shows that the pycnocline in the Antarctic zone is completely eroded. The more vertical orientation of steric

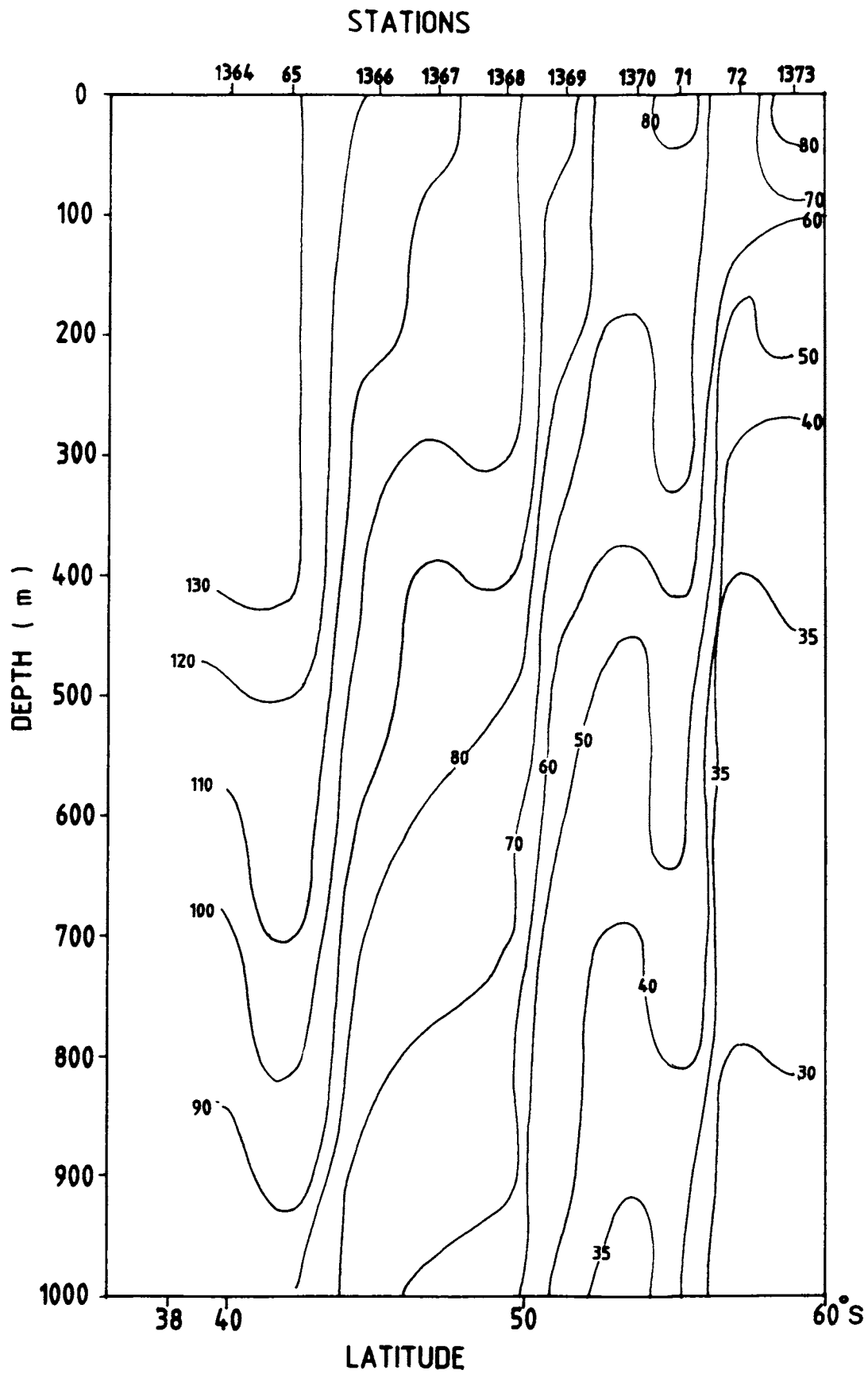


FIG.3.3.8 VERTICAL SECTION OF THERMOSTERIC ANOMALY ( cl/t-Centi litre per ton ) ALONG 95°E

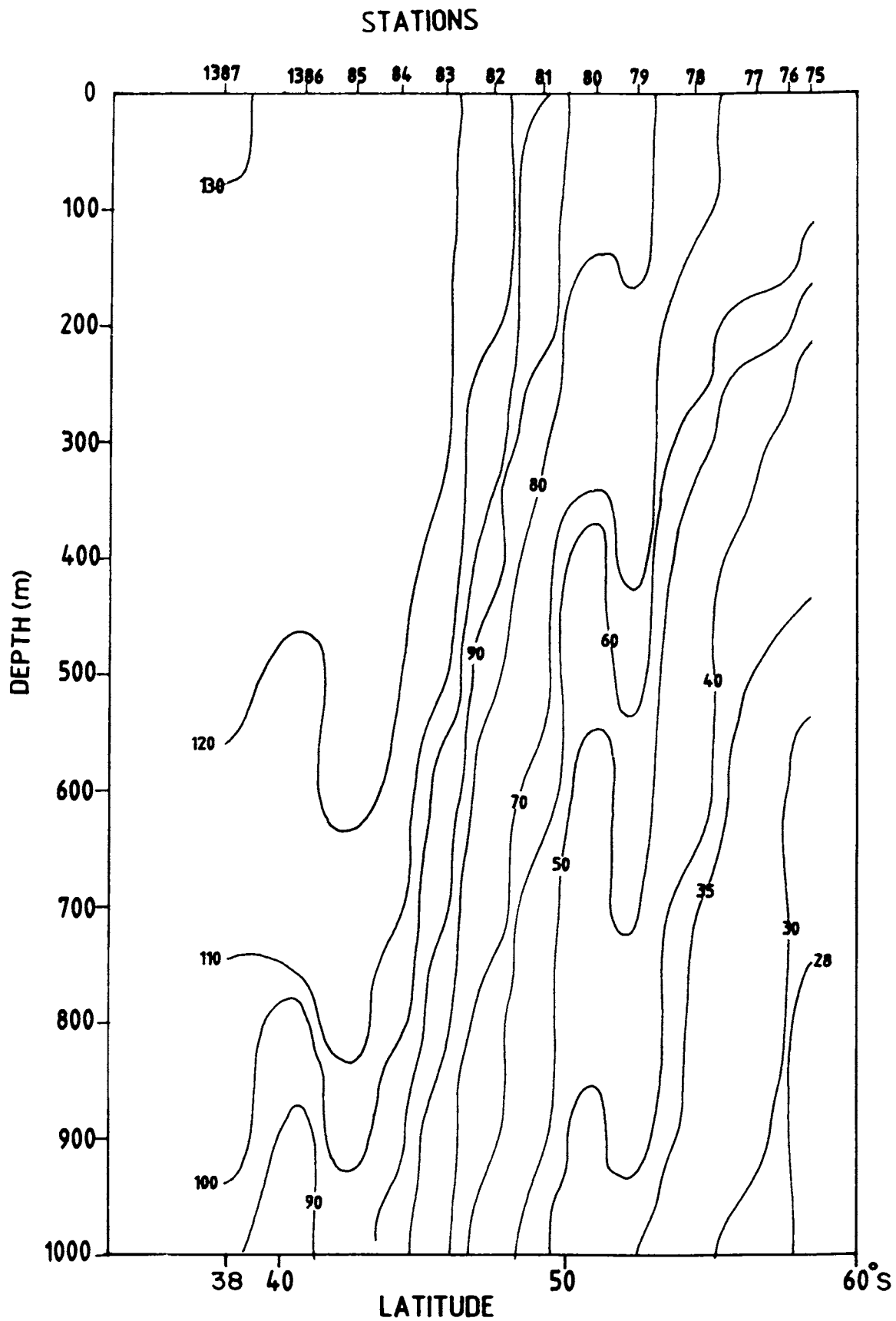


FIG.3.3.9 VERTICAL SECTION OF THERMOSTERIC ANOMALY ( cl/t-centi litre per ton ) ALONG 100°E

surfaces around station 1378 shows the presence of Antarctic Convergence. The steeper slope of isanosteres indicate that ACC is narrow and strong in this region. The presence of SAF is depicted by the vertical orientation of 100-110  $\text{cl/t}$  steric surfaces around station 1382. The troughs and ridges between SAF and APF help the horizontal mixing to be more pronounced in the subantarctic region. A layer of uniform density is seen between stations 1383 and 1386 and extends upto 600 m depth suggesting the absence of STF or atleast its weak manifestation.

### 3.3.10 Along 105°E

The Sub-Antarctic front is depicted as the only strongest front with a density gradient more than 30  $\text{cl/t}$  per 2° latitude distance. As in the previous section, a layer of uniform density is seen between stations 1390 and 1394 upto a depth of 600 m suggesting the ambiguity of STF. The ACC is inferred to be more concentrated around SAF.

### 3.3.11 Along 110°E

The section covered during October shows a strong pycnocline around 250 m in the Antarctic zone (Fig.

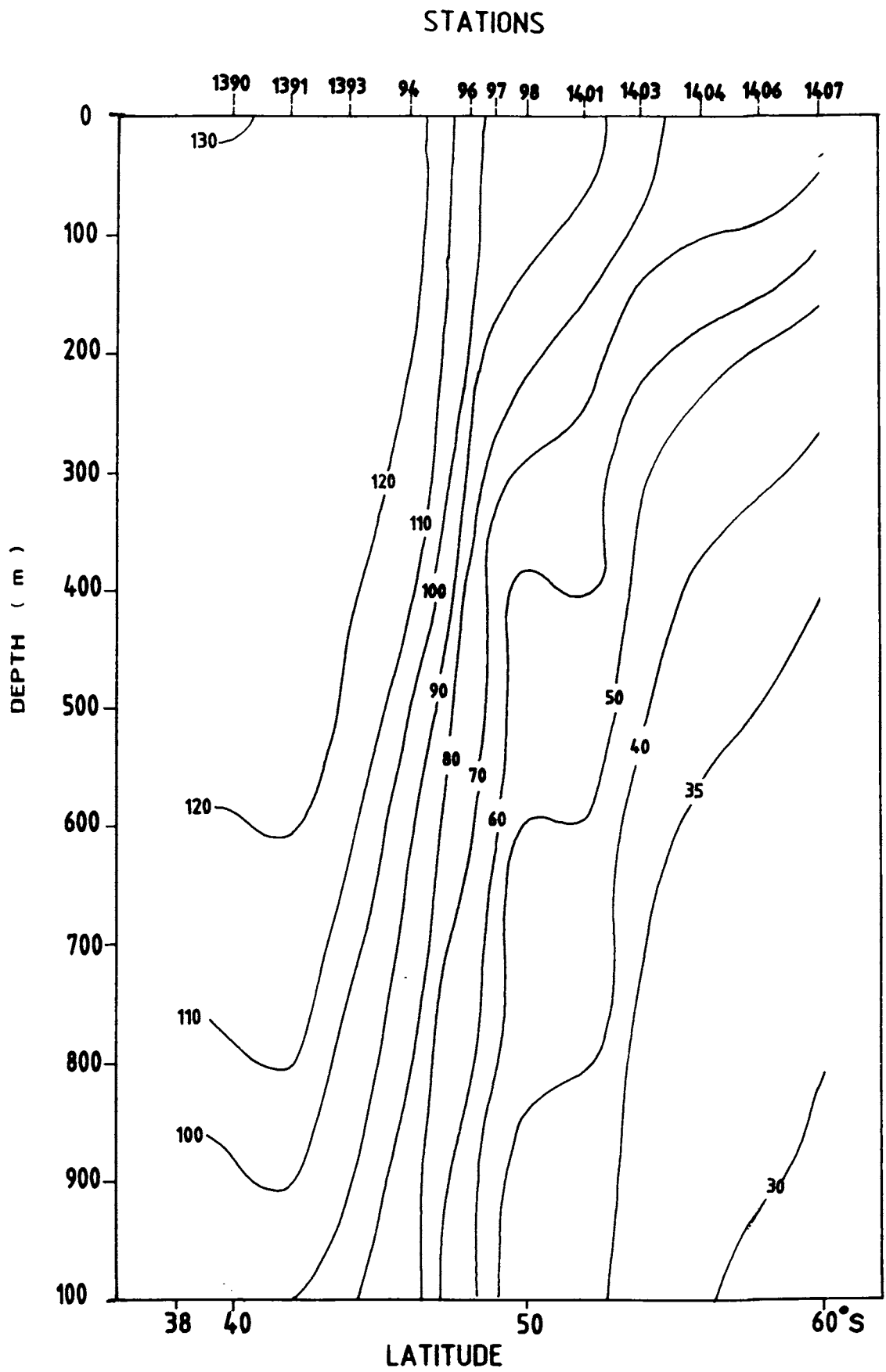


**FIG.33. VERTICAL SECTION OF THERMOSTERIC ANOMALY ( cl/t-Centi litre per ton ) ALONG 105°E**



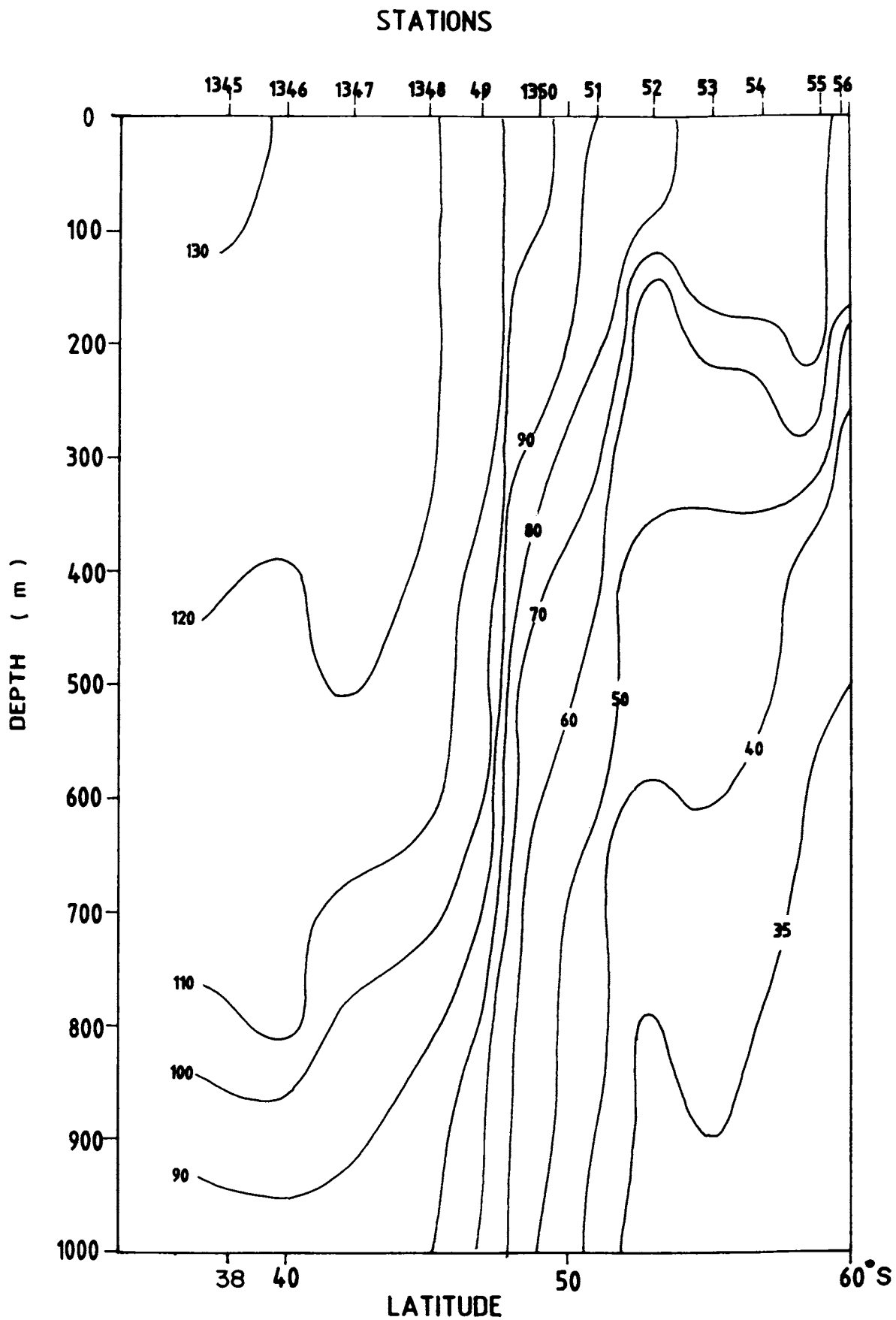


**FIG.3.3.II VERTICAL SECTION OF THERMOSTERIC ANOMALY ( cl/t-Centi litre per ton ) ALONG 110°E**

3.3.11). A strong gradient across SAF between stations 1349 and 1350 is manifested again as a single dominant front along this section. North of SAF a water of uniform density is seen doubting the existence of STF due to its density compensation.

### 3.3.12 Along 115°E

Fig. 3.3.12 shows the steric anomaly distribution between the coasts of Australia and Antarctica during summer. APF is suggested to exist between stations 1260 and 1261. However, SAF is seen between stations 1263 and 1264 as a single prominent front. The wavy like structure between SAF and APF indicates intense horizontal mixing within Subantarctic Zone. As in the previous section, the presence of surface density layer in the north does not suggest the existence of STF clearly. In the western most section STF is shown as the strongest front while in the eastern most section SAF is the strongest one.

## 3.4 Heat Content

The latitudinal distributions of heat content in the upper 500 m along the selected meridions are given in Figs. 3.4.1 to 3.4.12 showing different regimes of

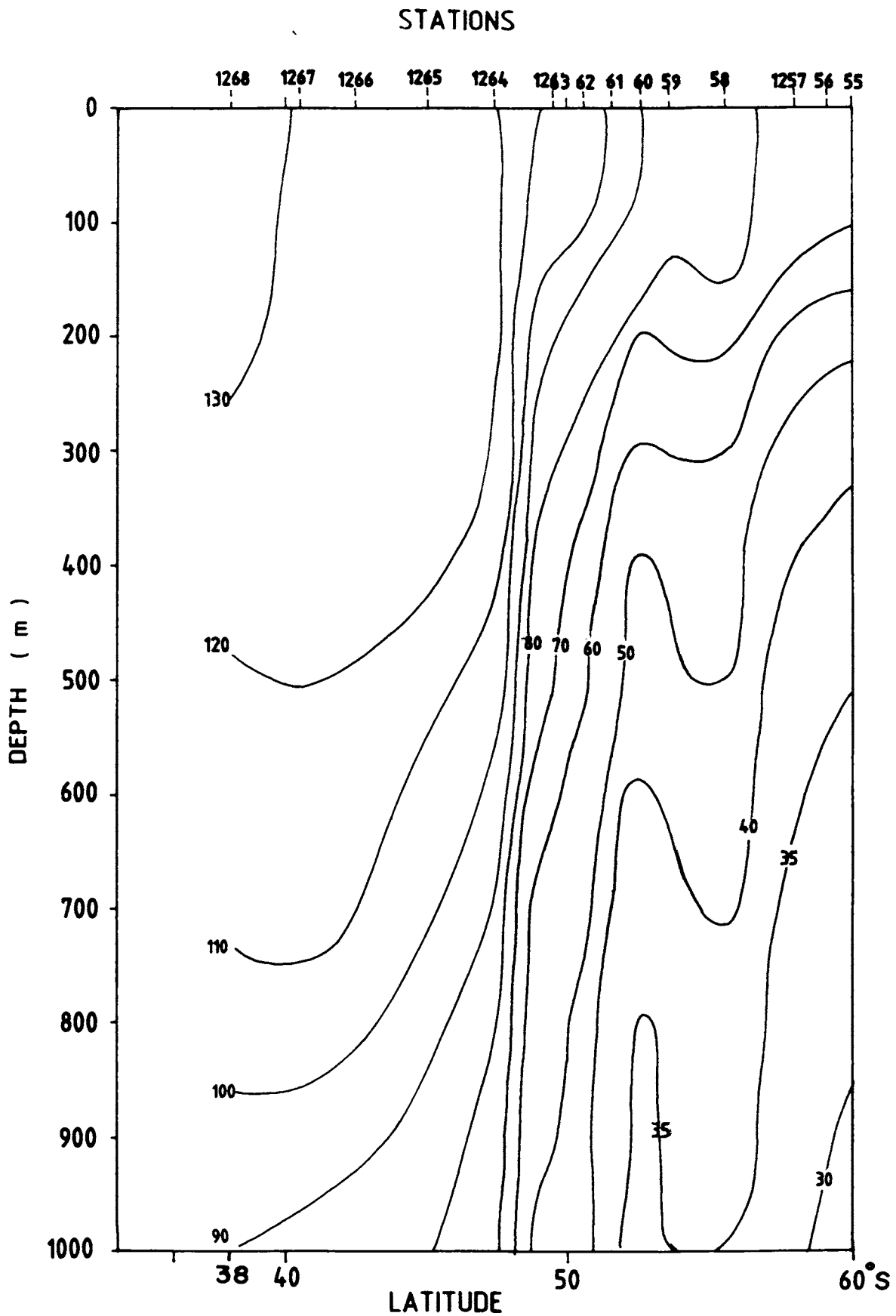


**FIG.3.3.12 VERTICAL SECTION OF THERMOSTERIC ANOMALY ( cl/t-Centi litre per ton ) ALONG 115°E**

watermasses and the sharp boundaries in between them. The meridional variations in the heat content facilitate the study of the poleward transport of heat.

A dramatic change in heat content of about  $27 \times 10^7$   $\text{J/m}^2$  is encountered across STF at  $20^\circ\text{E}$  (Fig.3.4.1). But the heat content distribution across STF at  $30^\circ\text{E}$  shows intermittent increase and decrease values by an order of  $6 \times 10^7$   $\text{J/m}^2$  (Fig. 3.4.2). These variations between  $42^\circ$  and  $44^\circ\text{S}$  are due to the effect of eddy turbulence. The variation of heat content along  $35^\circ\text{E}$  (Fig. 3.4.3) is similar to that at  $20^\circ\text{E}$ . The sharp change in the variation of heat content at  $44^\circ\text{S}$  gives clear identification of the southern end of STF. A fall of about  $13 \times 10^7$   $\text{J/m}^2$  in heat content is seen across STF along  $40^\circ\text{E}$  (Fig. 3.4.4). The heat content variability along  $45^\circ\text{E}$  (Fig.3.4.5) shows a change in meridional gradient around  $54^\circ\text{S}$  demarcating the subantarctic and Antarctic zones north and south of it. The abrupt change in heat content across STF at  $55^\circ\text{E}$  (Fig. 3.4.6) by more than  $22 \times 10^7$   $\text{J/m}^2$  indicates its regained strength. The decrease and increase in heat content from stations 293 to 296 is due to higher dynamic instability of STF enhancing mixing with subantarctic water.

The heat content variation along the section  $85^\circ\text{E}$

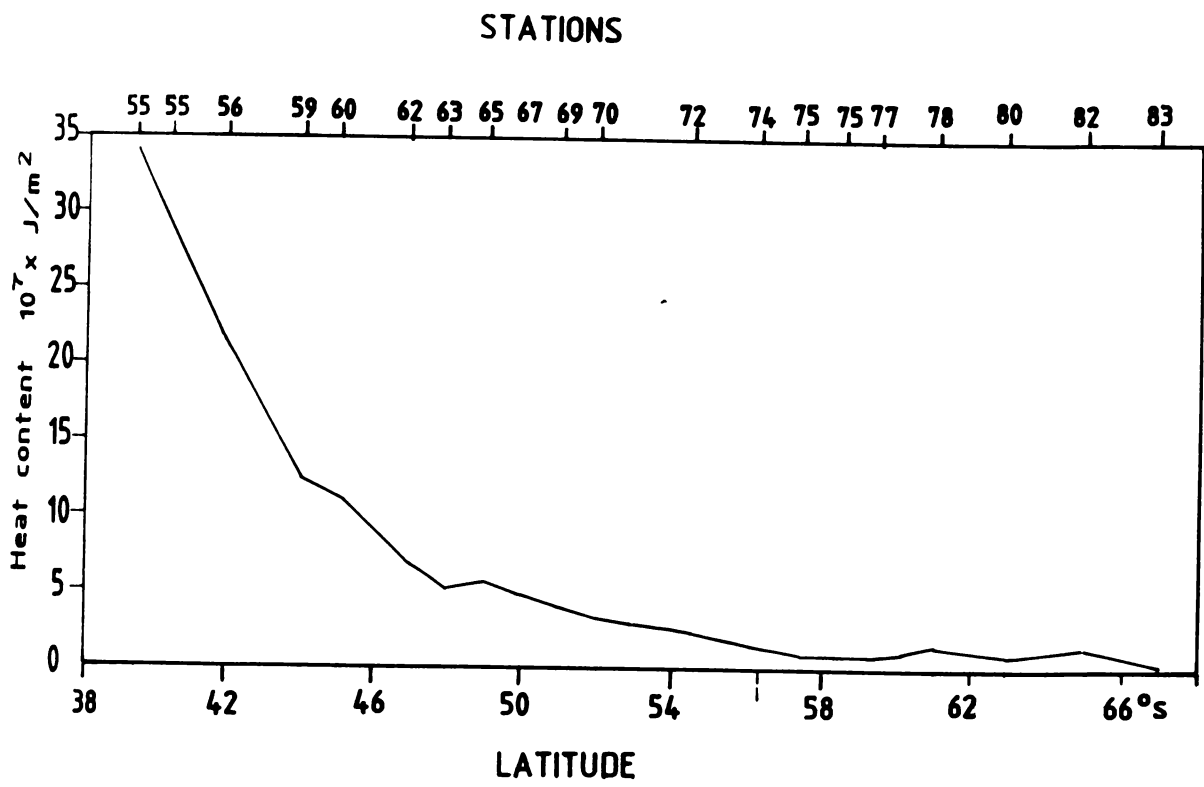


FIG.3.4.1 VARIATION OF HEAT CONTENT AT DIFFERENT FRONTS ALONG 20°E

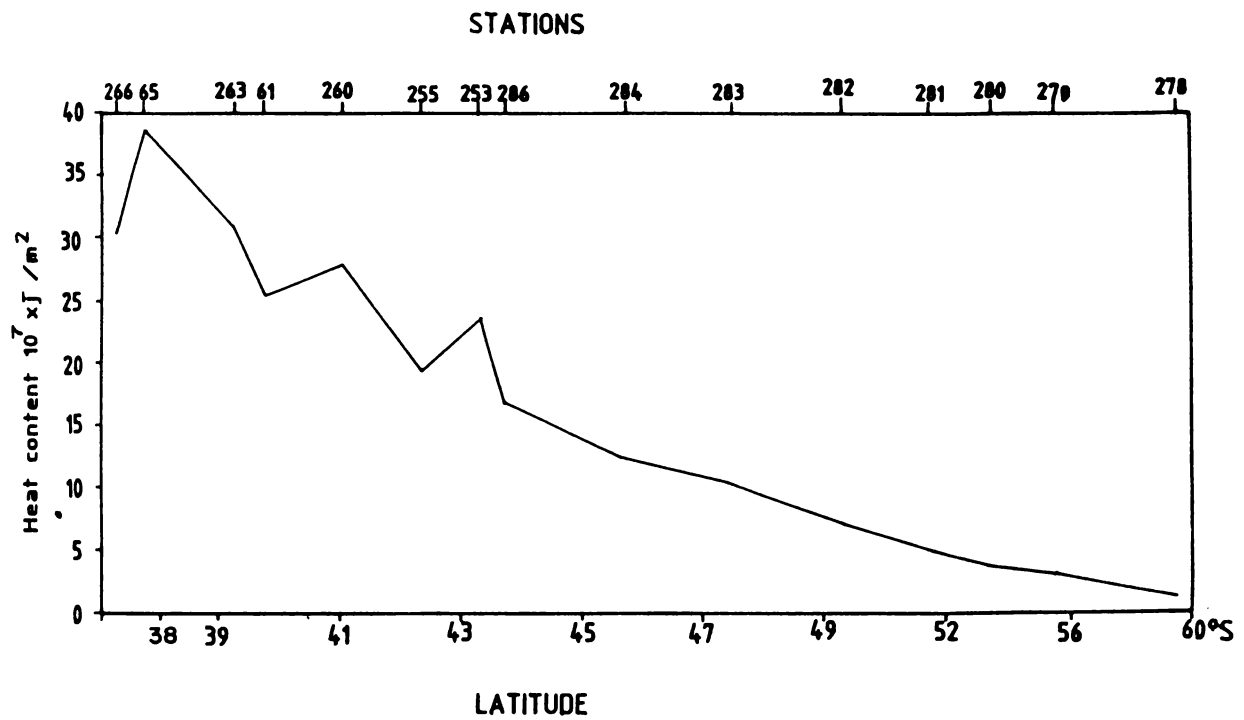


FIG. 34.2 VARIATION OF HEAT CONTENT AT DIFFERENT FRONTS ALONG 30°E

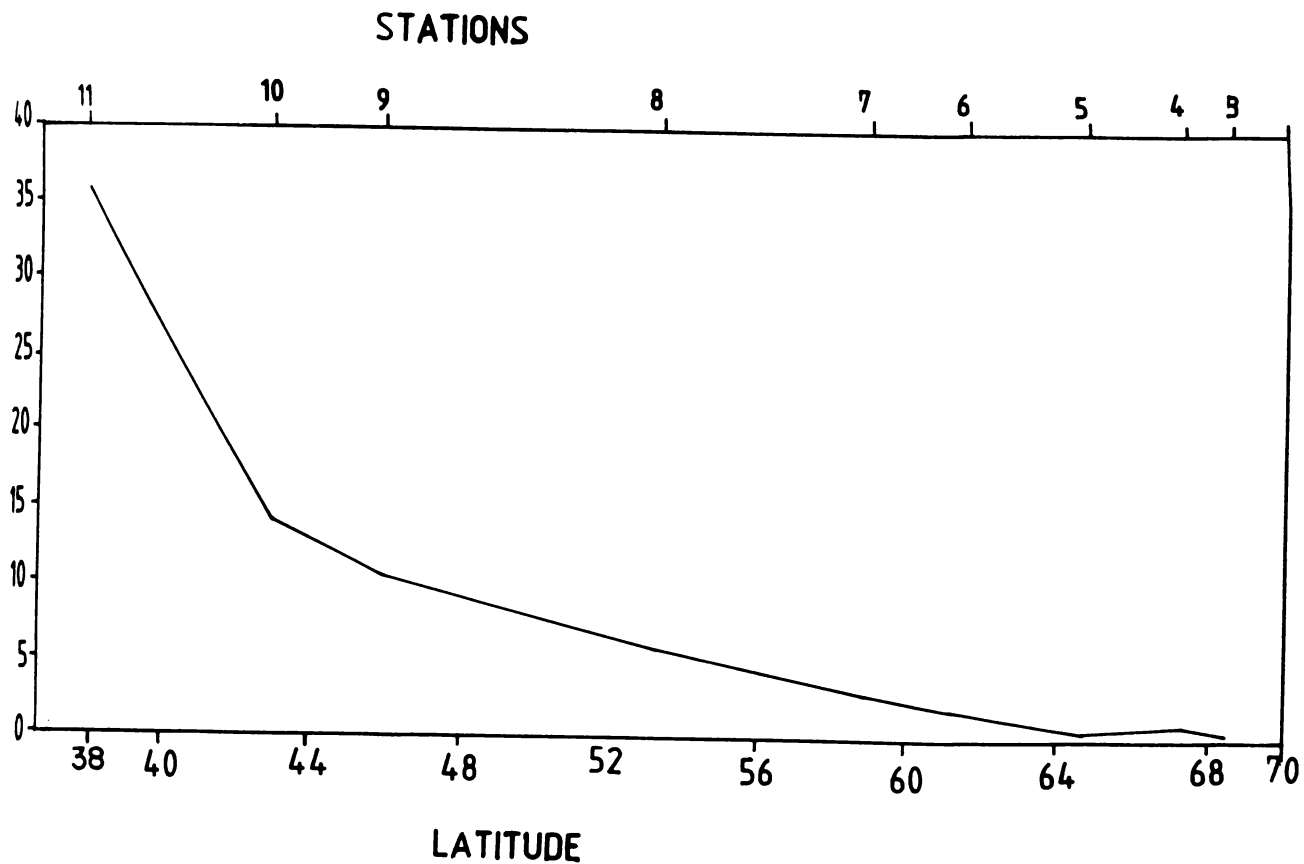


FIG.3.4.3 VARIATION OF HEAT CONTENT AT DIFFERENT FRONTS ALONG 35°E

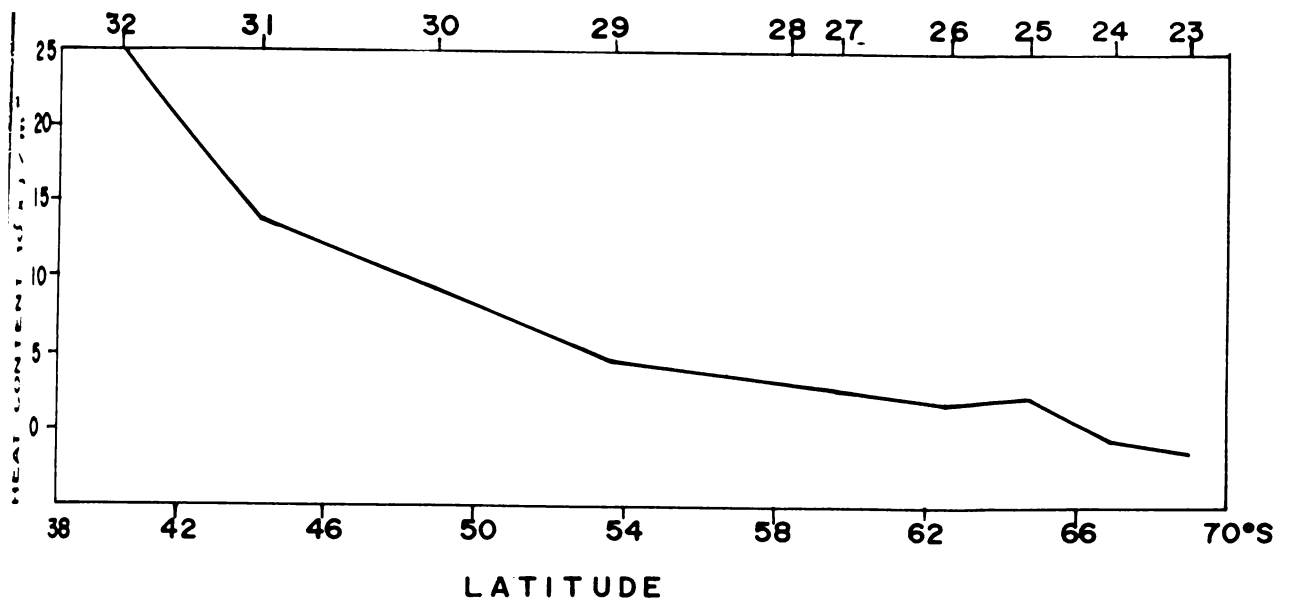


FIG.3.4.4 VARIATION OF HEAT CONTENT AT DIFFERENT FRONTS ALONG 40° E.



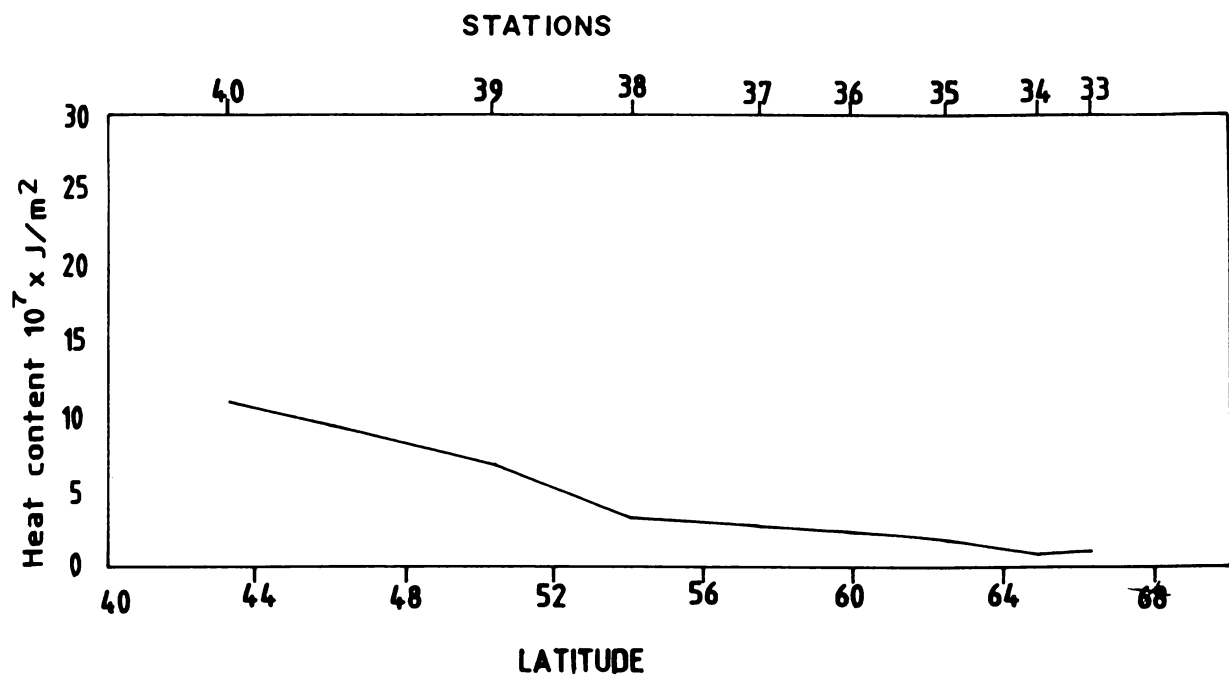


FIG.3.4.5 VARIATION OF HEAT CONTENT AT DIFFERENT FRONTS ALONG 45°E

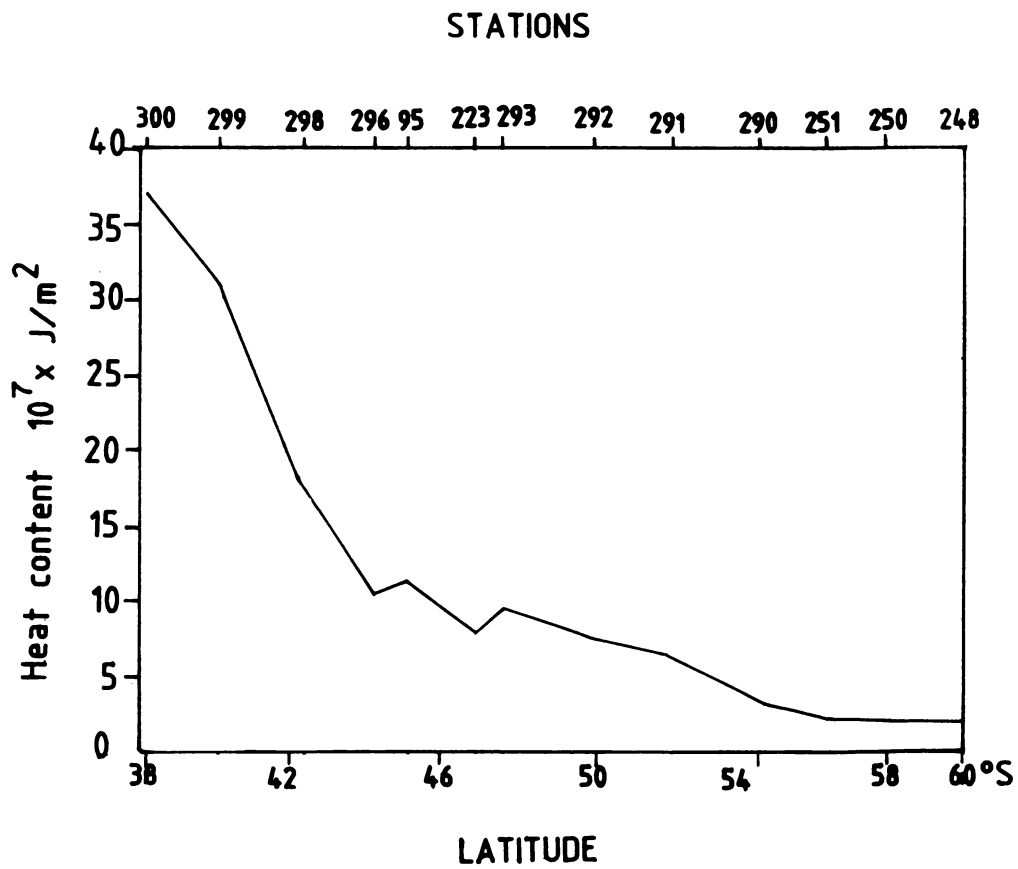


FIG.34.6 VARIATION OF HEAT CONTENT AT DIFFERENT FRONTS ALONG  $55^\circ\text{E}$

(during winter) is at a deviation from those along the earlier sections (Fig. 3.4.7). Here, the heat content drop is more at SAF by about  $7 \times 10^7 \text{ J/m}^2$  between stations 1552 and 1554 while across STF and APF the heat content variations are very less ( $5 \times 10^7 \text{ J/m}^2$ ). It is evident from the profile of heat content along  $95^\circ\text{E}$  (Fig. 3.4.8) that a prominent change in heat content occurs across SAF by about  $7 \times 10^7 \text{ J/m}^2$ . A sharp drop in heat content across SAF is seen uniformly along  $100^\circ$ ,  $105^\circ$ ,  $110^\circ$  and  $115^\circ\text{E}$  in the eastern study area (Figs. 3.4.9 to 3.4.12).

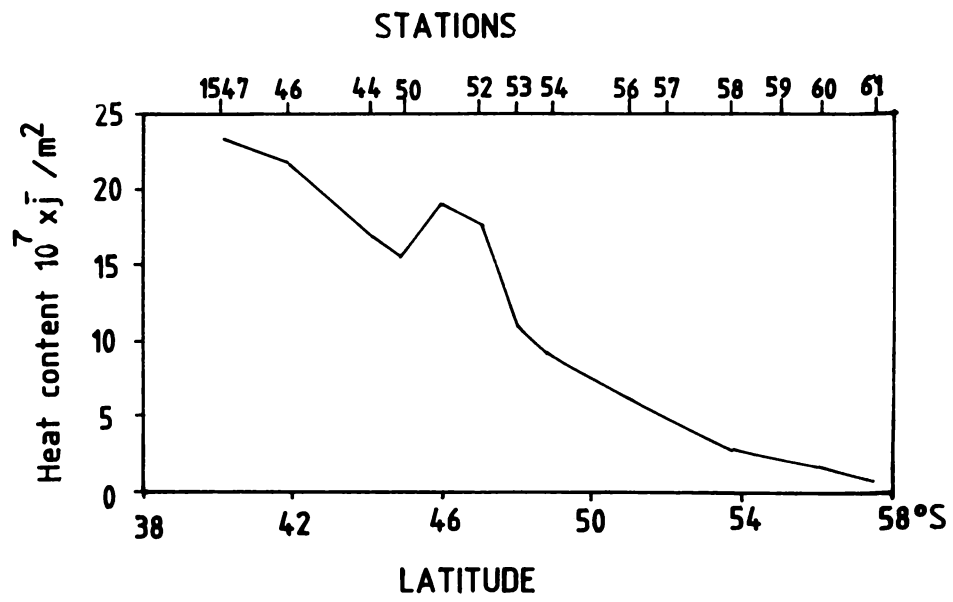


FIG.3.4.7 VARIATION OF HEAT CONTENT AT DIFFERENT FRONTS ALONG 85° E

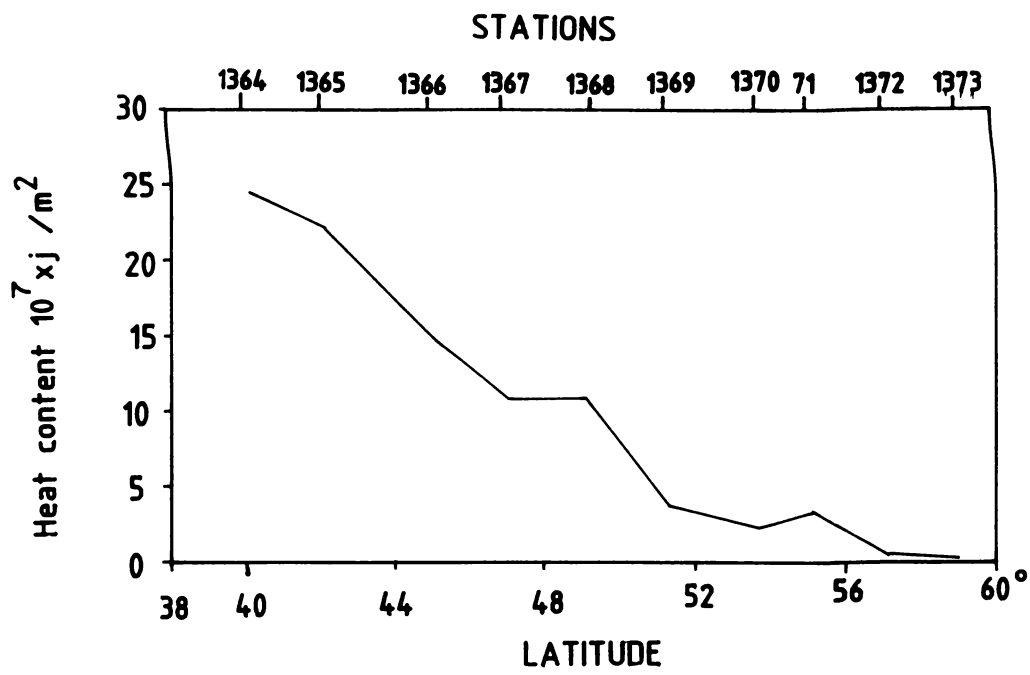


FIG.3.4.8 VARIATION OF HEAT CONTENT AT DIFFERENT FRONTS ALONG 95°E

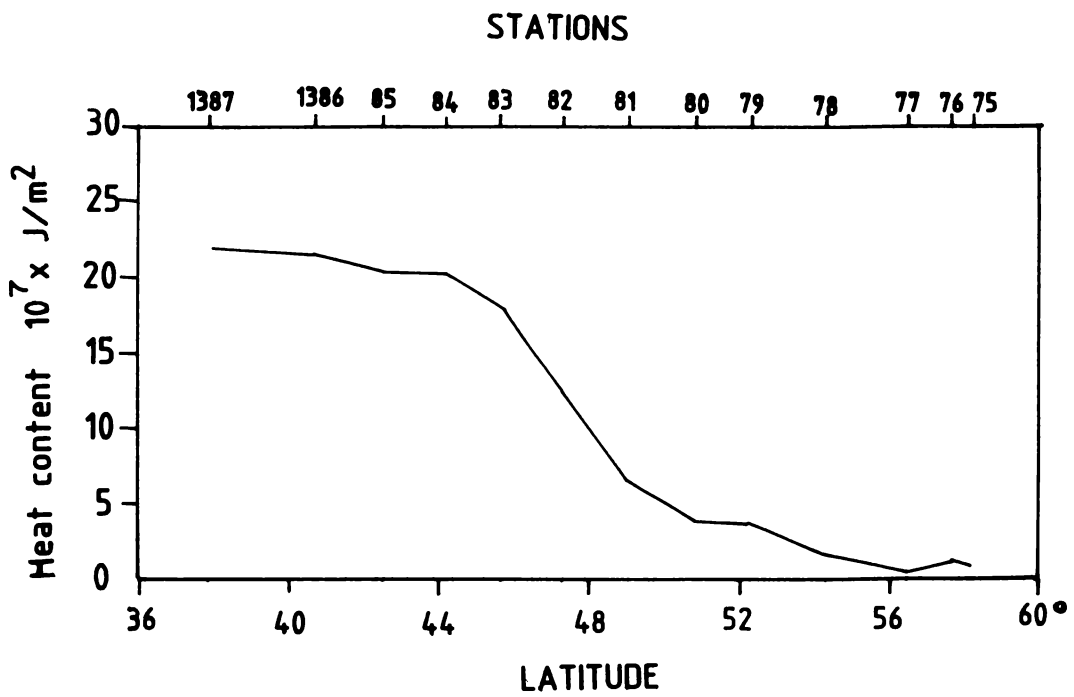


FIG.3.4.9 VARIATION OF HEAT CONTENT AT DIFFERENT FRONTS ALONG  $100^\circ\text{E}$

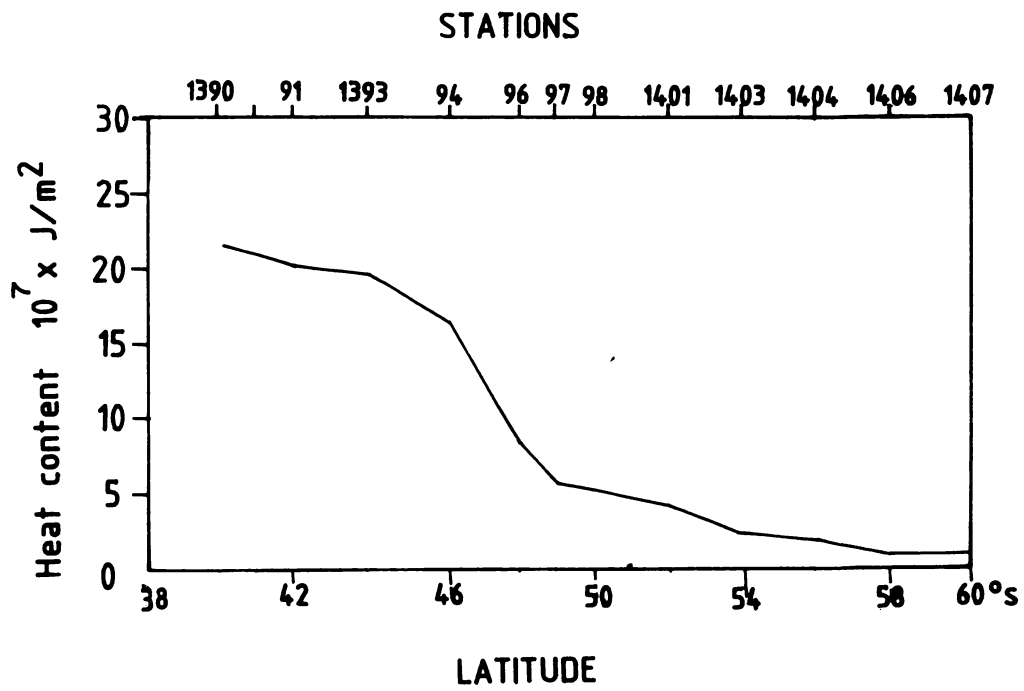


FIG.3.4. IO VARIATION OF HEAT CONTENT AT DIFFERENT FRONTS ALONG  $105^\circ\text{E}$

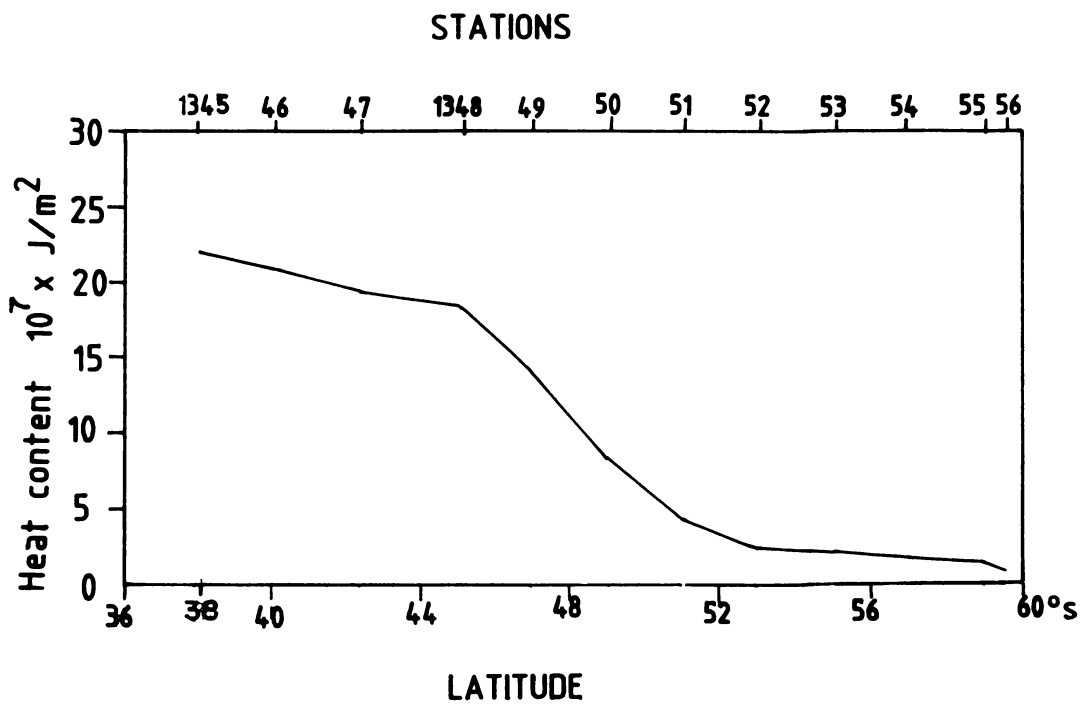


FIG.3.4.II VARIATION OF HEAT CONTENT AT DIFFERENT FRONTS ALONG 110°E



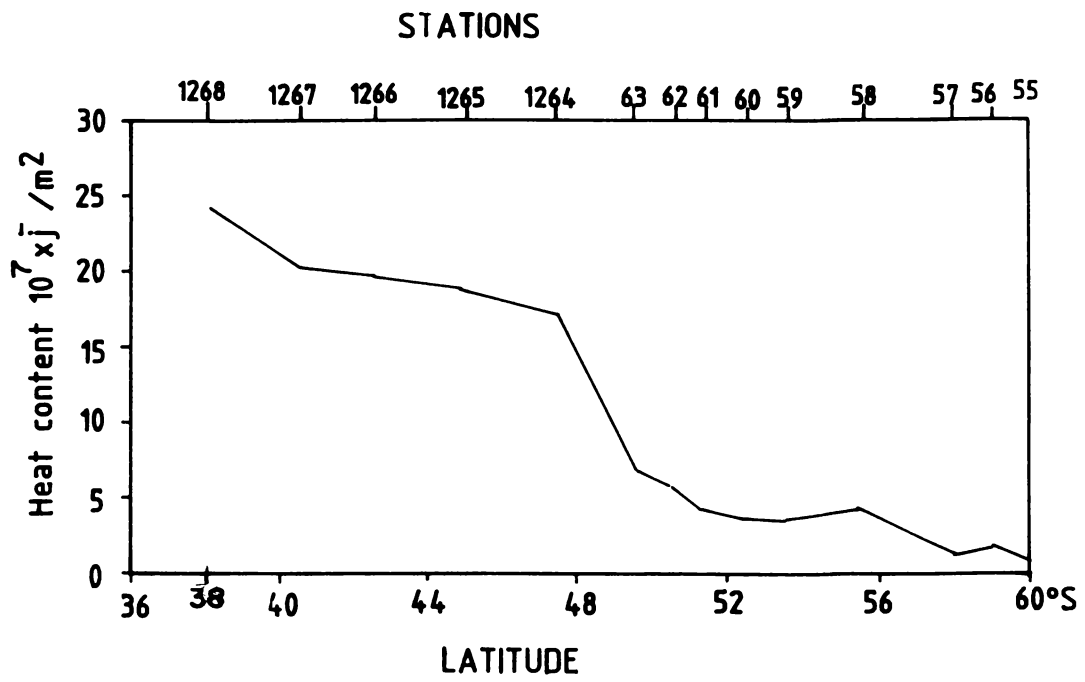


FIG.3.4.12 VARIATION OF HEAT CONTENT AT DIFFERENT FRONTS ALONG 115°E

# ***CHAPTER - IV***

## Zonal volume flux at frontal zones

Zonal volume flux in terms of Sverdrup (SV) units ( $1 \text{ SV} = 10^6 \text{ m}^3 \text{ S}^{-1}$ ) across 12 selected sections at various longitudes has been calculated. These meridional sections (Figs. 4.1 to 4.12) selected in western ( $20^\circ\text{--}85^\circ\text{E}$ ) and eastern ( $85^\circ\text{--}115^\circ\text{E}$ ) regions of the study area facilitate the study of regional variability in the volume flux. The general circulation of the Southern Ocean is dominated by zonal flow whose intensity changes at different meridians. The objective of the present study is to assess the role of the individual frontal zone in the distribution of volume transport through Temperature-Salinity-Volume (T-S-V) analysis and hence to identify the most important front as a flux donor to volume transport in the Southern Ocean. Since all the fronts are positioned in the eastward flowing ACC, it is expected that easterly volume fluxes would be dominant. The various solenoids bounded by isohalines and steric surfaces in the T-S-V diagram (Figs. 4.1 to 4.12), are marked with star symbol to represent the 50% of the total easterly flux at each longitude facilitating the identification of different modes (primary, secondary and tertiary) of transport. Both easterly and westerly fluxes across each selected longitude are estimated and presented in Figs. 4.1 to

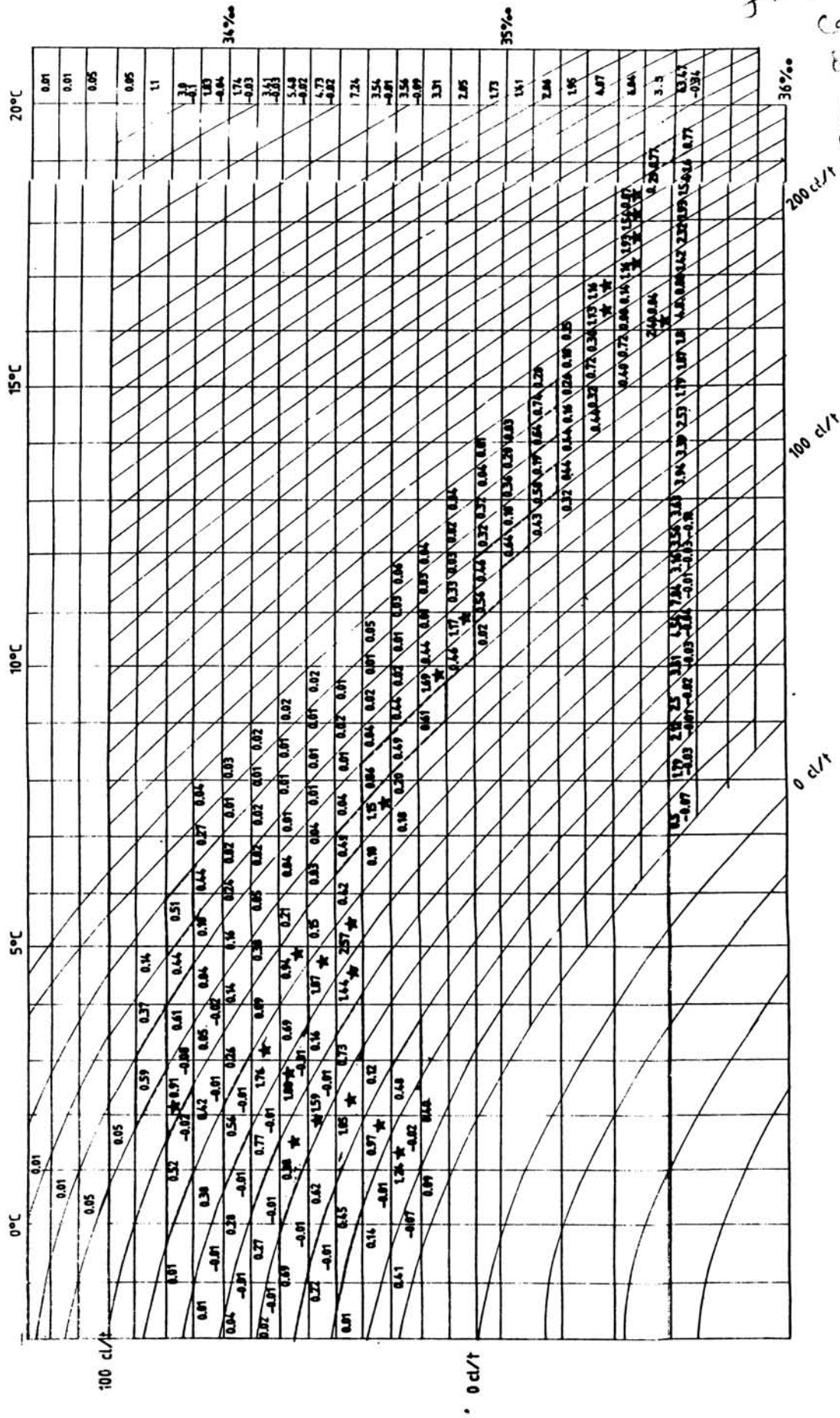
*Refer to the next (Page P. 29)*

4.12. In these T-S-V diagrams the volume flux is given through bimodal representation. Various solenoids form to indicate characteristic classes of thermohaline anomaly and salinity. Eastward (+ Ve) and westward (-Ve) volume fluxes are separately displayed for each characteristic classes with ranges of 10 cl/t in thermohaline anomaly and 0.1‰ in salinity.

The integrated fluxes between two consecutive steric surfaces are shown at the bottom while those between two consecutive isohalines are shown on the right side of the T-S-V diagrams. Further the fluxes displayed in the T-S-V diagram also give an idea on the temperature variation in addition to the thermohaline anomaly and salinity variations. Therefore by comparing the intervals of temperature with the corresponding T-S-V diagram the source of the flux can be identified. The following sections describe the volume flux at each longitude.

#### 4.1 Along 20°E

The eastward transport along 20°E is estimated to be around 63 SV whereas the westward flow is negligible. The bivariate distribution of flux along 20°E (Fig.4.1) covers 157 solenoidal classes within the salinity range of 33.3



*Handwritten notes:*  
 2.20  
 2.21  
 2.22  
 2.23  
 2.24

FIG. 4.1. ZONAL FLUX ALONG 20° E

35.6 ‰ and thermosteric anomaly range of 20-260 cl/t. The temperature characteristics of the flux within these classes vary between -2° and 20°C.

The primary mode within the first 50% has a diversity and spreads into 12 classes with a total transport of 17.2 SV in the range of 30-110 cl/t; 33.8-34.7‰ and 0-6°C. The secondary mode of easterly flux is observed in the range of 180-250 cl/t; 35.3-35.6‰ and 16°-19°C with a transport of 10.19 SV. The tertiary mode has a volume flux of 4.01 SV and is found between 100 and 140 cl/t surfaces with a salinity range of 34.5 - 34.9‰ and temperature range of 7-11°C. Thus the properties of these modes indicate that the maximum eastward flux (primary mode) is confined to the cold region. The secondary and tertiary modes of eastward flux are found at higher steric levels and hence are from warmer regions. These secondary and tertiary modes within high salinity further suggest that they are associated with STF.

Out of the primary mode of eastward transport of 17.2 SV nearly 50% (8.23 SV) is considered to be contributed by APF (salinity range 33.9 - 34.6‰ ; temperature range 1-4°C). The westerly flux seen in the range of 33.8-34.7‰ and 30-110 cl/t suggests that flux is

associated with East Wind Drift nearer to the Antarctic continent. Further examination of T-S-V diagram reveals that there is no westerly flow (-ve flux) at higher steric surfaces.

#### 4.2 Flux along 30°E

An increase in both eastward and westward transports is noticed across 30°E whose latitudinal extent is almost same as that of the previous one (Fig. 4.2). This increase in transport is due to the confluence of currents especially within STF region where its dynamic nature is high on account of the interaction with Agulhas Plateau. The eastward transport is 70.24 SV while the westward transport is 33.09 SV along this section. The westward flux at higher salinity range shows the effect of Agulhas Current at STF.

The bivariate distribution of total flux at 30°E comprises 258 solenoidal classes of salinity and thermosteric anomaly. The total flux is in the temperature range of -2-24°C and salinity range of 33.7-35.6%. Fig. 4.2 further shows that 50% of the total eastward flux represents mostly in a single mode in contrast to the multimode transport at 20°E. It has 32 solenoidal classes

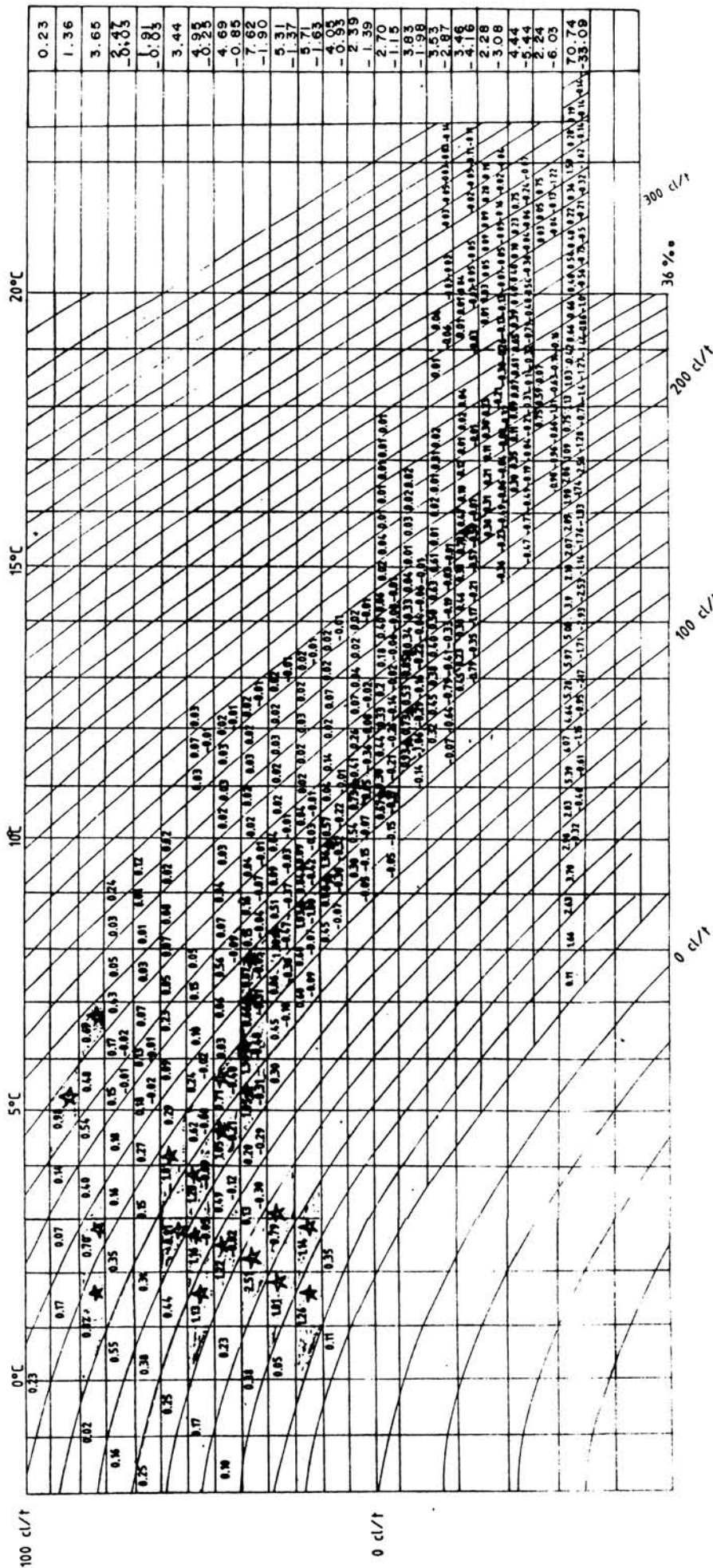


FIG. 4.2. ZONAL FLUX ALONG 30°E



between steric surfaces 30 and 200 cl/t, isohalines 33.7 and 35.3‰ and isotherms 1° and 16°C. In this single mode, the flux in the salinity range 34.6-34.8‰ and temperature range 0-1°C is due to the spreading of the Atlantic Deep Water and is about 1.26 SV. The significant contribution from APF in the 50% flux is 12.51 SV and that from STF is 7.34 SV. The characteristics of the single mode transport reveal that most of the fluxes is originated from high latitudes. The westward flux is dominant within the salinity range of 35 - 35.6‰, suggesting the remarkable influence of Agulhas Current at STF.

Although the larger number of total solonidal classes indicates heterogeneity in the overall flux characteristics, the less number of frequencies in the 50% of easterly flux limited in the Antarctic zone reveals that major flow is homogeneously characterised.

#### 4.3 Flux along 35°E

The amount of eastward flux around 61 SV approximately along 35°E (Fig. 4.3) is nearer to that at 20°E. The total flux is distributed among a large number (278) of characteristic classes in the ranges of 33.7-35.7‰ and 20-280 cl/t. However the flow is seen to be

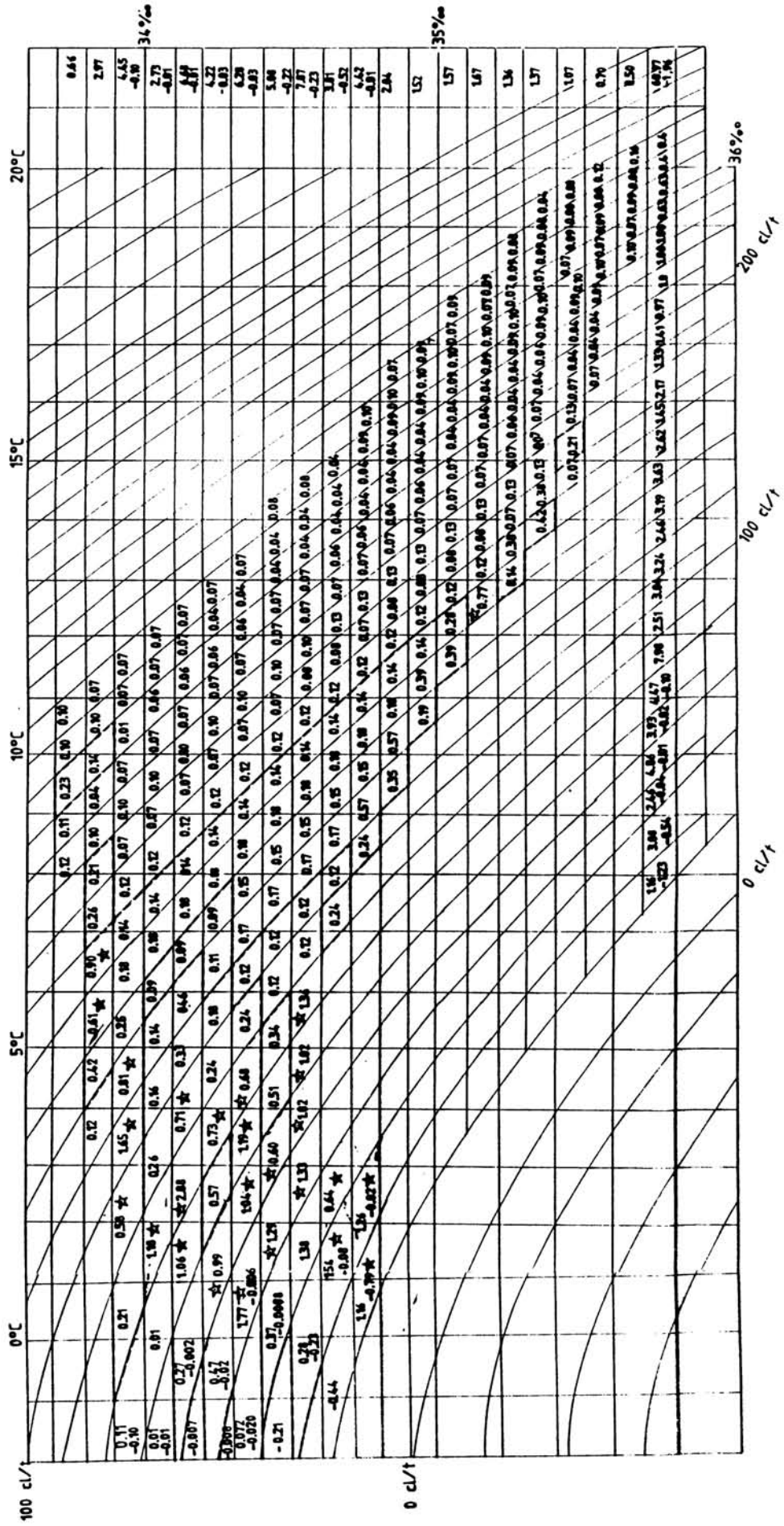


FIG. 4.3 ZONAL FLUX ALONG 35° E

predominant below 150 cl/t. The remarkable reduction in the westerly flux by one order from about 33 SV at 30°E to almost 2 SV at 35°E shows the minimal influence of Agulhas Current at STF. Like at the previous section, 50% of the total flux at 35°E is distributed predominantly in a single mode within the salinity range of 33.8-34.8‰ and temperature range of 0-7°C and spreads over 27 solenoidal classes.

Eventhough the hydrographic sections (Figs. 3.1.3 and 3.2.3) show a clear manifestation of both STF and APF, the dominant mode of flux confine more towards high latitudes than towards subtropical latitudes and as such Antarctic waters are extended more towards north. The single mode characteristics of flux further indicates that a major contribution of the mode is from APF in the salinity range of 33.8-34.6‰ and in the temperature range of 1-4°C. Out of 50% of the total eastward flux, about 19 SV lies between 50 and 120 cl/t is associated with APF whereas the flux associated with NADW is around 11 SV and that with STF is negligible.

#### 4.4 Flux along 40°E

A sharp decrease in the eastward flux is noted at

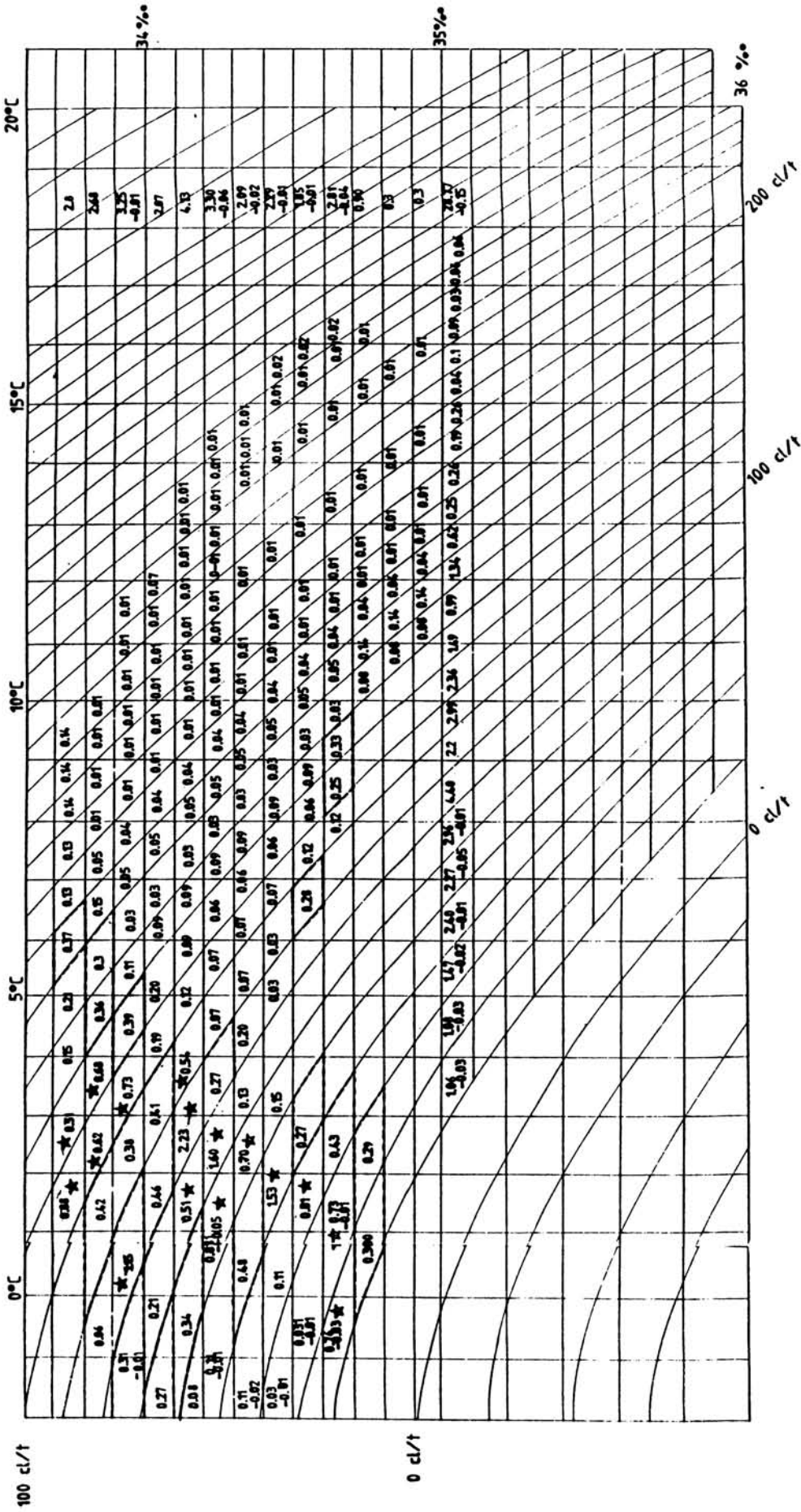


FIG. 4.4 ZONAL FLUX ALONG 40° E

40°E as compared to that at previous sections. The distribution of flux (Fig. 4.4) in 184 classes of salinity and thermosteric anomaly shows a dominant single mode in a similar way at 35°E, in spite of the considerable decrease in total flux (about 29 SV). The dominant mode in the 50% of easterly flux is distributed in less number (16) of solenoidal classes, lying in the salinity range of 33.7-34.7‰ and temperature range of -1-4°C and this again indicates that the major association of flux is with higher latitudes.

Though the distribution of hydrographic properties (Figs. 3.2.4 and 3.3.4) shows strong horizontal gradients in salinity and temperature across STF, the density gradient is found to be less compared to that at 35°E on account of counterbalancing of the gradients. This results in the lowering of the eastward flux to about 29 SV. The T-S-v diagram for 40°E longitude shows further reduction in the westward flux which is seen almost negligible.

#### 4.5 Flux along 45°E

This section has somewhat lower latitudinal extent from 43°-67°S as compared to the previous sections. Fig. 4.5 gives the distribution of zonal flux at 45°E. The

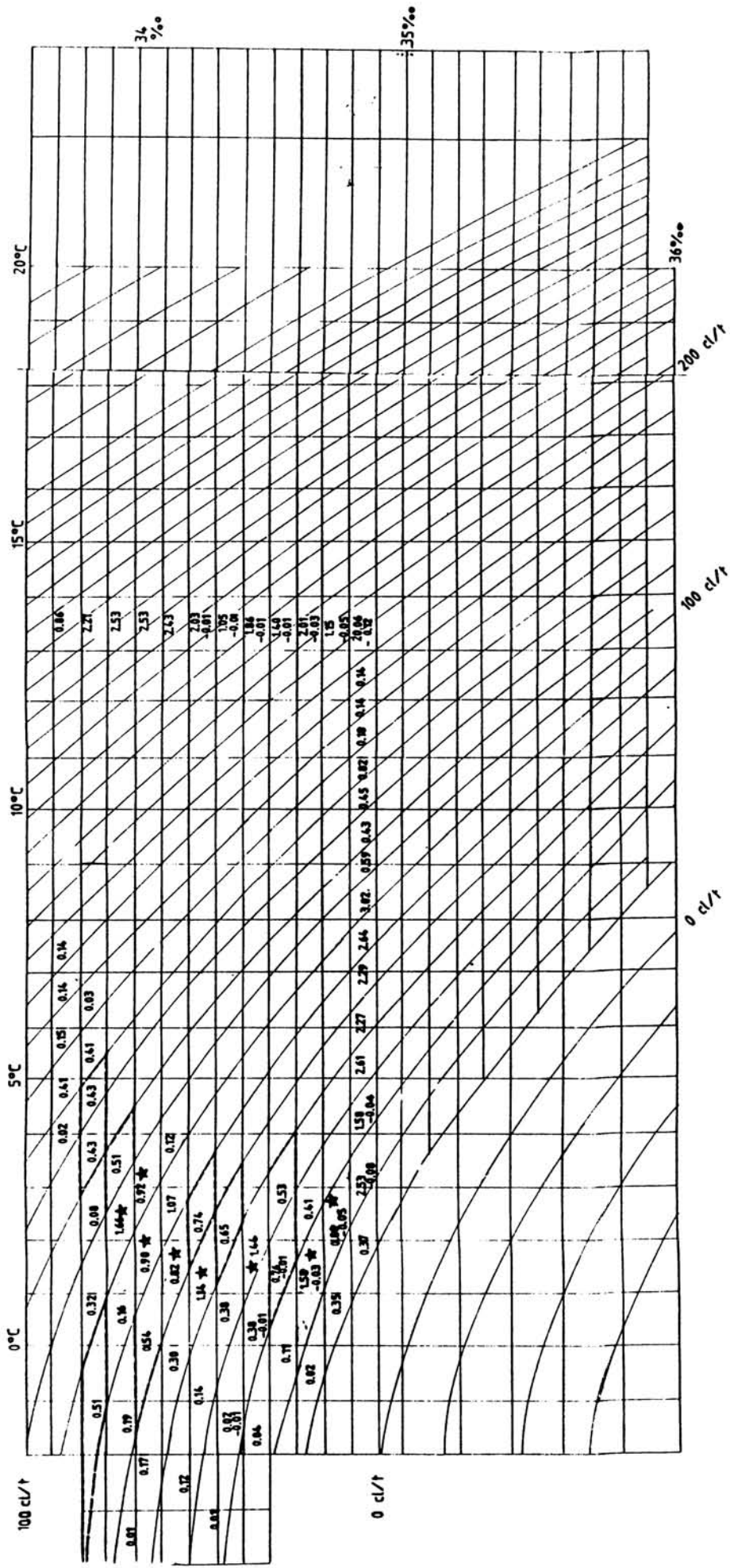


FIG. 4.5. ZONAL FLUX ALONG 45° E

total eastward flux across the section is about 20 SV. The reduction of the eastward flux from 40°E to 45°E is mostly attributed to the decrease in the latitudinal extent. The bivariate distribution of zonal flux along 45°E depicts the homogeneous nature of the flow conspicuously (Fig. 4.5). The total flow is distributed in 44 solenoidal classes with a salinity range of 33.7-34.8‰ and a steric range of 20-170 cl/t. 50% of the total eastward flux is shown by a single mode predominantly in the salinity range of 33.9-34.8‰, temperature range of 0-4°C and the steric level range of 30-100 cl/t. About 7.95 SV of the first 50% of eastward flux is contributed from APF.

#### 4.6 Flux along 55°E

The distribution of volume flux (transport) approximately along 55°E is shown in Fig. 4.6. The total flux across the section is around 55 SV, which is nearer to the order of fluxes at the far western sections along 20°E, 30°E and 35°E.

The bivariate distribution of the flux across 55°E indicates that flux is distributed in 313 classes within a salinity range of 33.6-35.8‰, thermosteric anomaly range of 20-320 cl/t and temperature range of -2°-21°C. The

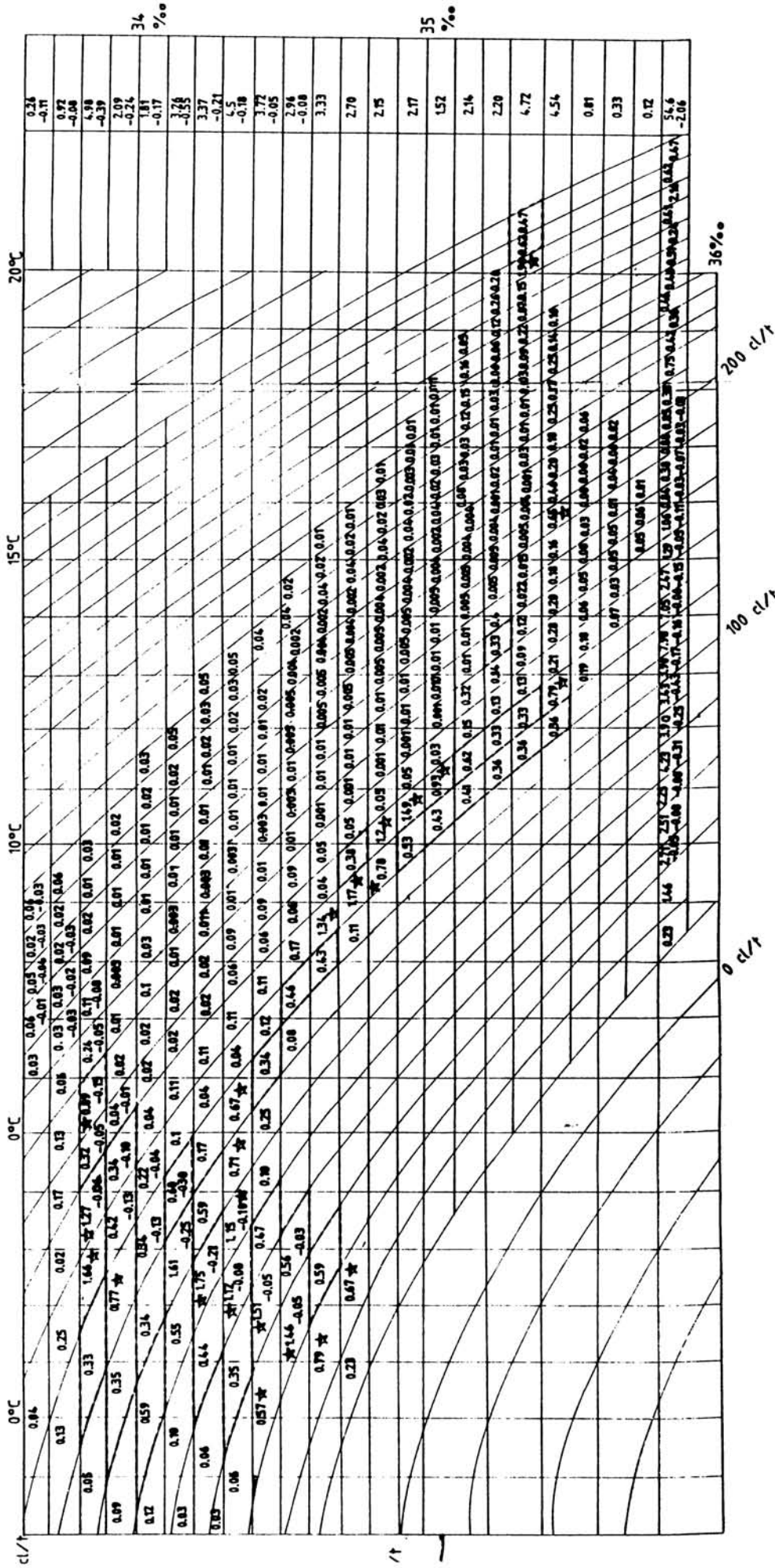


FIG. 4.6 ZONAL FLUX ALONG 55° E



sudden increase in the number of classes from 45° to 55°E is quite remarkable.

50% of the total eastward flux (55 SV) is distributed into different modes like in the western most section of 20°E. The primary mode is distributed in 14 classes in the steric level range of 30-140 cl/t, the salinity range of 33.8-34.8‰ and temperature range of 0-6°C, with a total flux of 14.99 SV. The secondary mode is depicted in six classes with a total volume transport of 8.35 SV in the salinity range of 34.6-35.5‰, temperature range of 8-16°C and steric level range of 110-190 cl/t. The tertiary mode is around 290 cl/t and at a temperature 20°C in the salinity range of 35.3‰-35.4 with a flux of 1.96 SV.

Out of the primary mode transport, more than 80% in the ranges of 33.8-34.5‰, 0-6°C and 40-120 cl/t is from APF. The secondary and tertiary modes are contributed from STF. The larger dynamic nature of STF especially near the surface causes the spreading of flux along different steric surfaces.

#### 4.7 Flux along 85°E

The seasonal change in the frontal zone and

associated mass transport at 85°E during winter are shown in Fig. 4.7. The zonal flux is estimated to be about 45 SV and distributed in 73 bivariate classes of salinity and thermosteric anomaly. The lesser number of bivariate classes at 85°E is very conspicuous one in contrast to the larger number at the previous sections. The watermass is quite cold ( $< 12^{\circ}\text{C}$ ) and less saline ( $< 35.1\%$ ) than that of western sections along which higher temperature and salinity are seen upto about  $22^{\circ}\text{C}$  and  $35.8\%$ . Eventhough the bivariate classes are less, the flow is heterogeneous as seen from the extension of the area marked by star symbol that represents 50% of eastward volume flux.

The primary mode within the 50% limit of the easterly flux is in between 120 and 140 cl/t and in the temperature range of  $7-10^{\circ}\text{C}$ . A part of the primary mode is the contribution from STF. The secondary mode between 80 and 110 cl/t in the salinity range of  $34.3 - 34.4\%$  and temperature range of  $4-7^{\circ}\text{C}$  occurs at SAF. A part of 50% flux in tertiary mode lies in the salinity range of  $33.8 - 33.9\%$  while the remaining part occurs between  $34.3$  and  $34.5\%$  in the lower temperature range of  $1^{\circ} - 3^{\circ}\text{C}$  corresponding to the spreading of Antarctic surface water and North Atlantic Deep Water (NADW).

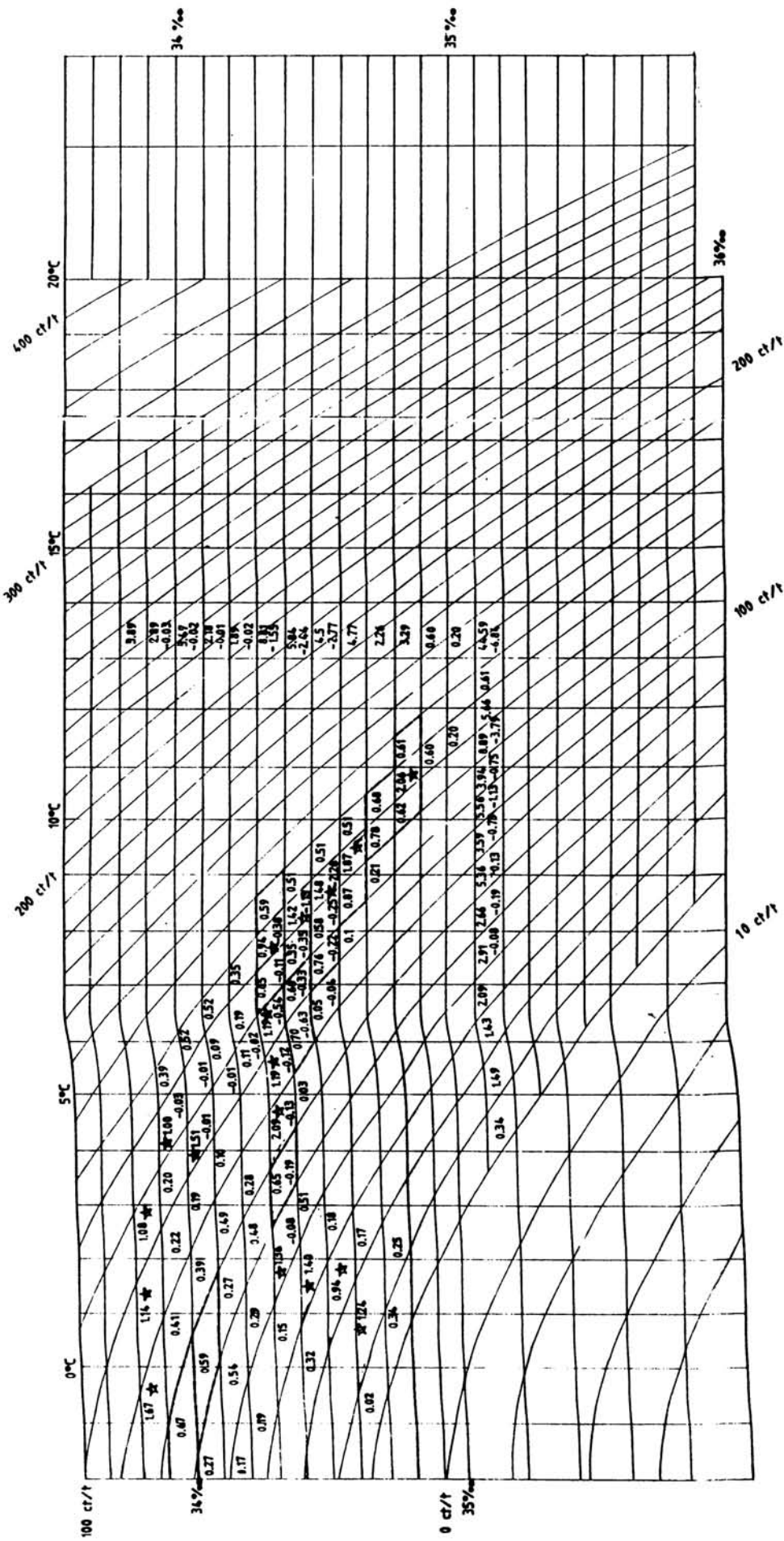


FIG. 4.7. ZONAL FLUX ALONG 85°E

The westerly flow is found increased from about 2 SV at 55°E to about 7 SV at 85°E and is predominant at higher steric levels. Between 120 and 130 cl/t surfaces the westward flow has a maximum volume transport of 3.79 SV. The complexity in the hydrographic structure and associated eddy around 43°S probably cause an increase in the westward flux due to bottom topography characterised with a mid oceanic ridge. Both maximum eastward (8.9 SV) and westward (3.8 SV) transports take place between 120 and 130 cl/t surfaces, suggesting stronger eddy activity in between STF and SAF.

#### 4.8 Flux along 95°E

The westerly volume transport is observed to be continuously higher (8 SV) at 95°E (Fig. 4.8). The eastward flux remains more or less same (around 42 SV). The zonal flux distribution in the T-S-V diagram along 95°E shows more homogeneous nature in comparison to that across 85°E. The primary mode in 50% of volume flux is represented in 10 solenoidal classes bounded by 30 and 100 cl/t surfaces. The eastward flux associated with the primary mode is 16 SV and is lying between 34-34.7‰ and -2° - 4°C ranges. The secondary mode constitute two solenoidal classes with a total eastward flux of 2.77 SV

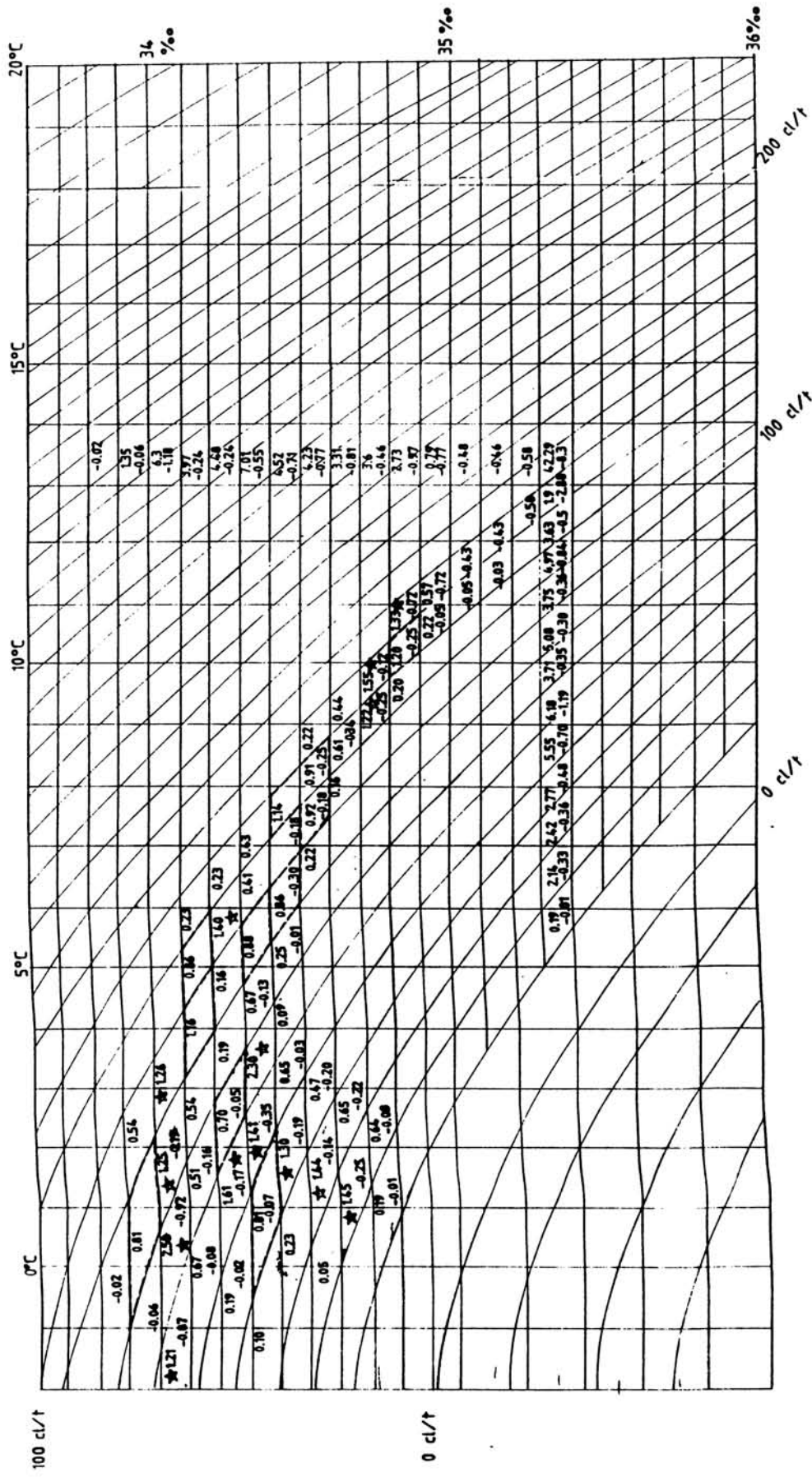


FIG. 4.8. ZONAL FLUX ALONG 95° E

in the steric level range of 110-130 cl/t; salinity range of 34.7- 34.8‰ and temperature range of 9- 11°C. The secondary mode represents contribution from STF. The tertiary mode is an isolated one in the ranges of 5-6°C, 34.2-34.3‰ and 100-110 cl/t with an associated flux of 1.4 SV from SAF.

The primary mode includes flux mainly from APF and it lies in salinity range of 34-34.7‰ and temperature range of 0-2°C. The scatter of this mode in the salinity range of 34.0-34.1‰ is due to continued presence of winter cold watermasses sinking around 60°S. More than 50% of the total eastward flux is from Antarctic zone. The westerly flows are widely distributed from lower to higher steric surfaces suggesting further intensification in the complex nature of the circulation in association with mid ocean ridge.

#### **4.9 Flux along 100°E**

The distribution of volume flux at 100°E is shown in Fig. 4.9. The estimated eastward transport is about 46 SV and the westward flux is 7 SV. Both the fluxes are more or less same as that across 95°E.

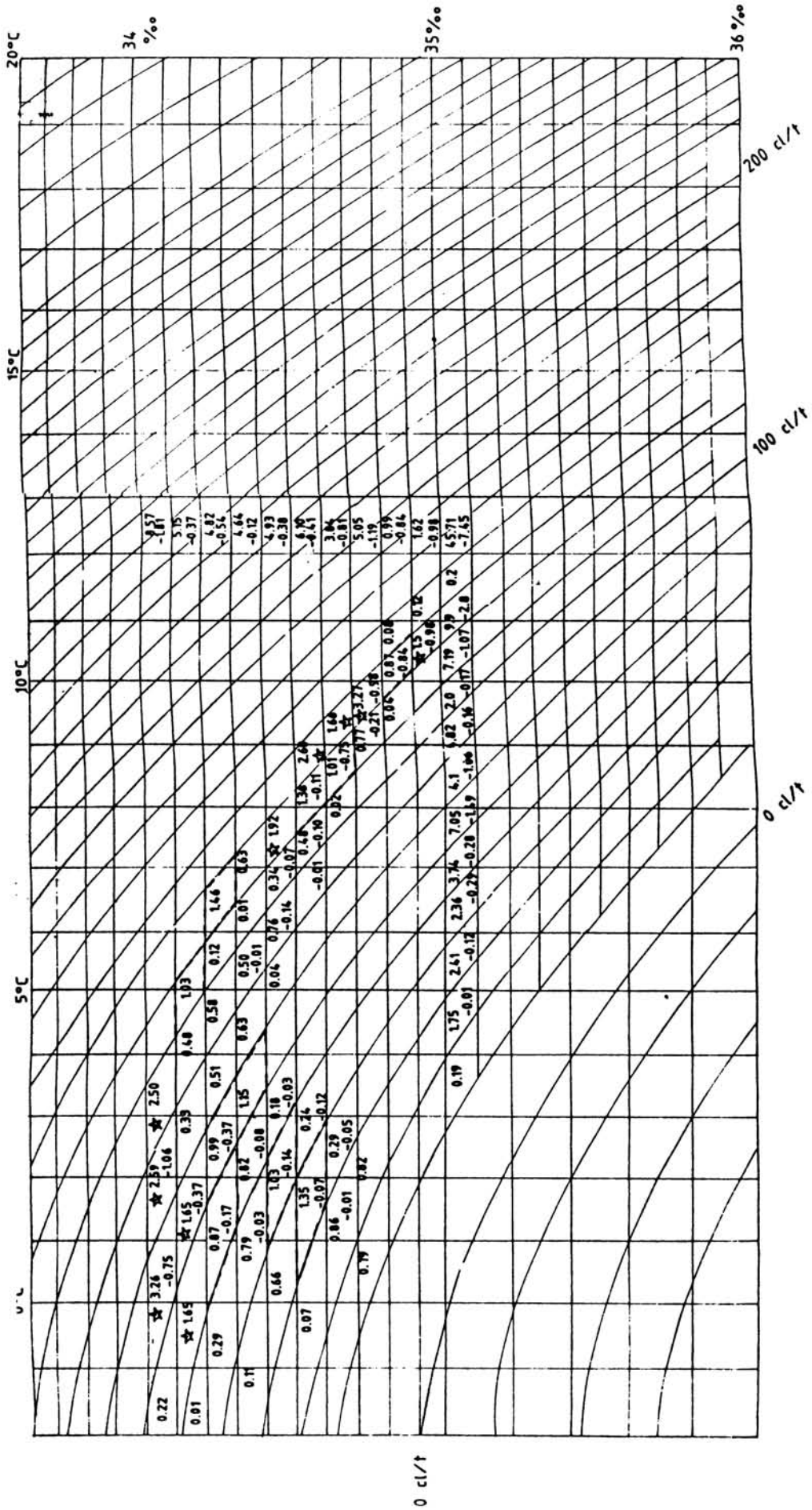


FIG. 4.9. ZONAL FLUX ALONG 100°E

The bivariate distribution of flux spans into 53 limited classes within the salinity range of 34-35‰. The limited number of classes indicate the narrowness of ACC in the eastern region. The primary mode is depicted in 5 solenoidal classes in the ranges of 60-100 cl/t, 34-34.2‰ and -2°-4°C. The total volume flux associated with the primary mode is 11.65 SV. Out of this, about 9.15 SV is from APF and the remaining 2.5 SV is from SAF. The secondary mode associated with STF and SAF is found between 110-130 cl/t in the salinity range 34.4-35.0‰ and temperature 7°-11°C.

The more or less same order of westerly flux (7.5 SV) at 100°E as compared to that at 95°E is distributed everywhere in the lower and higher steric surfaces, suggesting that the effect of mid ocean ridge is still prevailing.

#### **4.10 Flux along 105°E**

Fig. 4.10 shows the distribution of flux in the T-S-V diagram at 105°E. The total eastward flux is about 40 SV. The westward flux is found to be considerably reduced from 7.5 SV at 100°E to about 1 SV at 105°E. The bivariate distribution of flux is limited into 55 characteristic



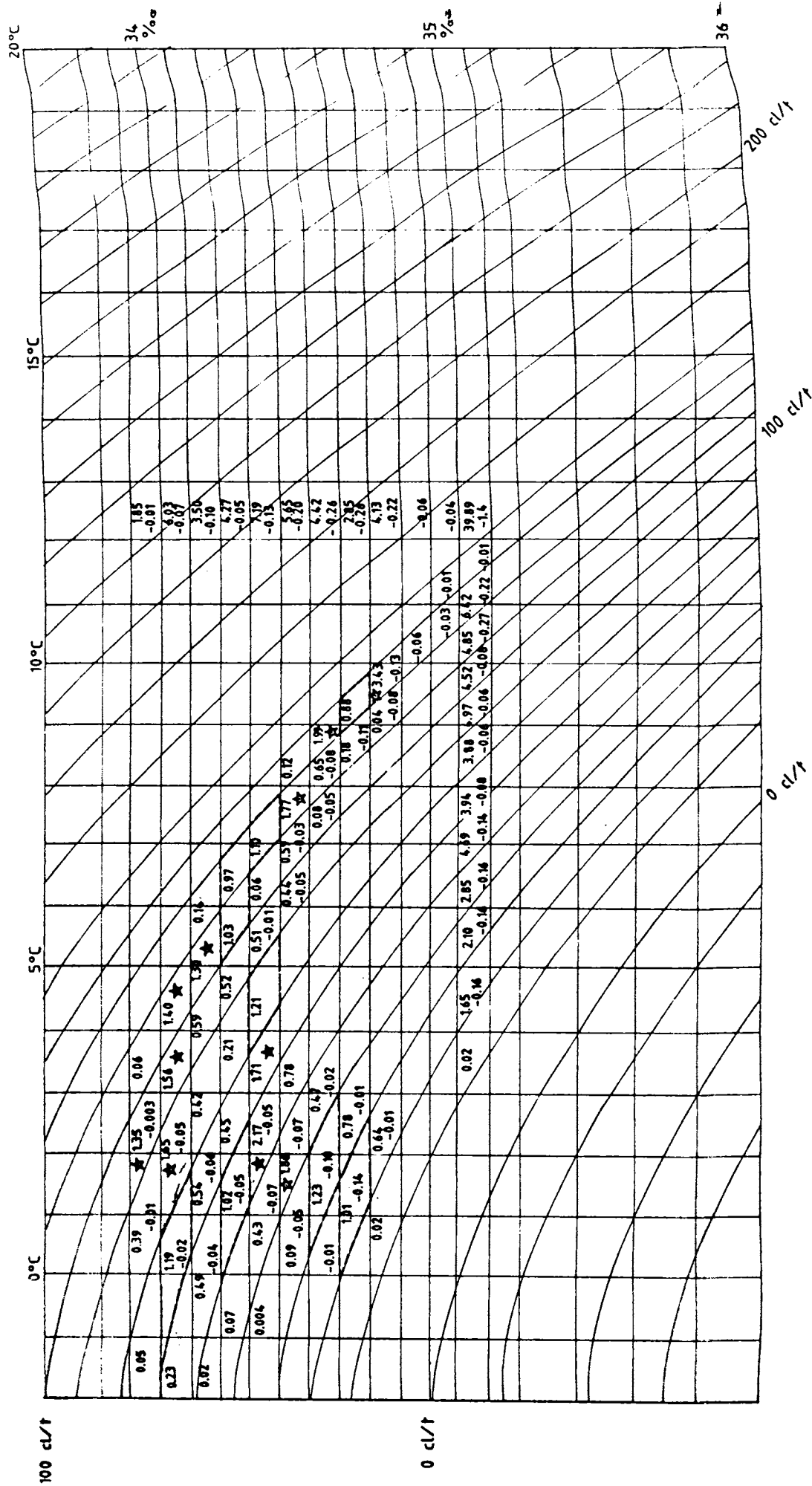


FIG. 4.10. ZONAL FLUX ALONG 105° E

classes within the steric surface range of 20-130 cl/t, salinity range of 33.9-35.0‰ and temperature range of -2-12°C. The primary mode is depicted in 5 solenoidal classes with a flux of 7.26 SV lying in the salinity range of 33.9-34.2‰ and temperature range of 1-5°C. The secondary mode is present in three classes in the salinity range of 34.4-34.8‰ and in temperature range of 7-10°C. It lies between 110-130 cl/t with a total eastward flux of 7.14 SV while the next mode (5.74 SV) is between 50 and 80 cl/t within the salinity and temperature ranges of 34.3-34.5‰ and 1-4°C respectively. A part of the primary and tertiary modes in temperature range of 1°-3°C and salinity range of 34‰-34.6‰ is the contribution (9.52 SV) from APF.

The flux of 7.24 SV which lies in the ranges of 3°-6°C, 34.1-34.2‰ and 7°-9°C, 34.4-34.6‰ comprises the contribution from SAF. The lower eastward flux (3.43 SV), lying between 120 and 130 cl/t surfaces, is contributed from STF and this in turn shows its weaker manifestation. The significant reduction in the westerly flux shows the decreased influence of mid oceanic ridge.

#### 4.11 Flux along 110°E

Fig. 4.11 shows the distribution of volume flux along

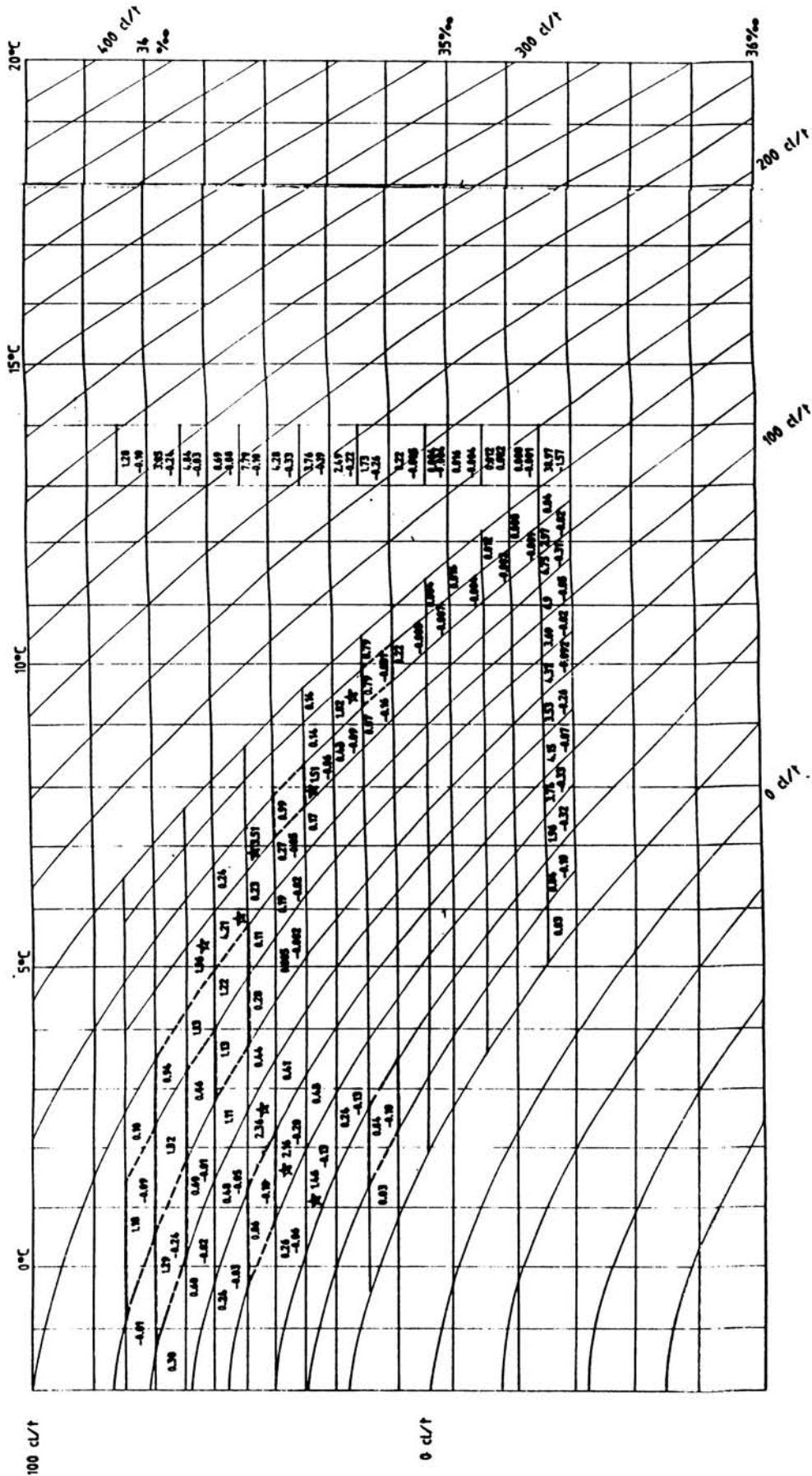


FIG. 4.11. ZONAL FLUX ALONG 110° E

110°E. The computed eastward flux is about 39 SV, almost equal to that across the previous section. This is represented in the T-S-V diagram comprising 56 solenoidal classes within the range of 20-140 cl/t; 33.9-35.3‰ and -2-13°C.

The primary mode distributed in 3 characteristic classes within the ranges of 100-120 cl/t, 34.1-34.4‰ and 5°-8°C is from SAF. The secondary mode is in the range of 40-70 cl/t and is depicted in 3 classes with a total eastward flux of 5.98 SV. It is in the temperature and salinity ranges of 1°-3°C and 34.3-34.6‰ respectively confirming the contribution from APF. The tertiary mode is shown in 2 solenoidal classes with a total eastward volume flux of 3.33 SV in the salinity range of 34.5-34.7‰ and temperature range of 8°-10°C. This mode at higher steric range of 110-130 cl/t indicates that the source of flux is STF.

#### 4.12 Flux along 115°E

The zonal transport across 115°E between Australia and Antarctica is shown in Fig. 4.12. The computed eastward transport is around 40 SV. The westward flux shows a slight increase of about 1.5 SV as compared to

that at the earlier section.

The bimodal distribution of flux along 115°E covers 60 solenoidal classes in the ranges of 33.9-35.2‰ and 20-140 cl/t. The distribution reveals that primary mode is spread over 6 solenoidal classes in between 100 and 130 cl/t steric surfaces. The total flux associated with the mode is 11.03 SV in the range of 34.3 and 34.8‰ and 6°-10°C. The secondary mode (5-SV) is represented in 3 classes between the steric surfaces of 50 and 70 cl/t in ranges of 34.3-34.5‰ and 0-3°C. The tertiary mode lies in the temperature range of 0°-4°C and salinity range of 33.9-34.1‰. In the primary mode, the flux of 6.76 SV in the ranges of 34.3-34.6‰ and 6°-9°C is the contribution from SAF. The remaining part (4.27 SV) of primary mode lying in the range of 34.6 - 34.8‰ and 9°-10°C is associated with STF. The distribution of flux reveals that the secondary mode and a part of tertiary mode are contributed from APF.

A closer examination of Fig. 4.12 reveals that the westerly flow prevailing in the lower steric level (below 100 cl/t) might be the result of the influx of waters due to Australian coastal current. The bivariate distribution confirms the heterogeneous nature of the flow

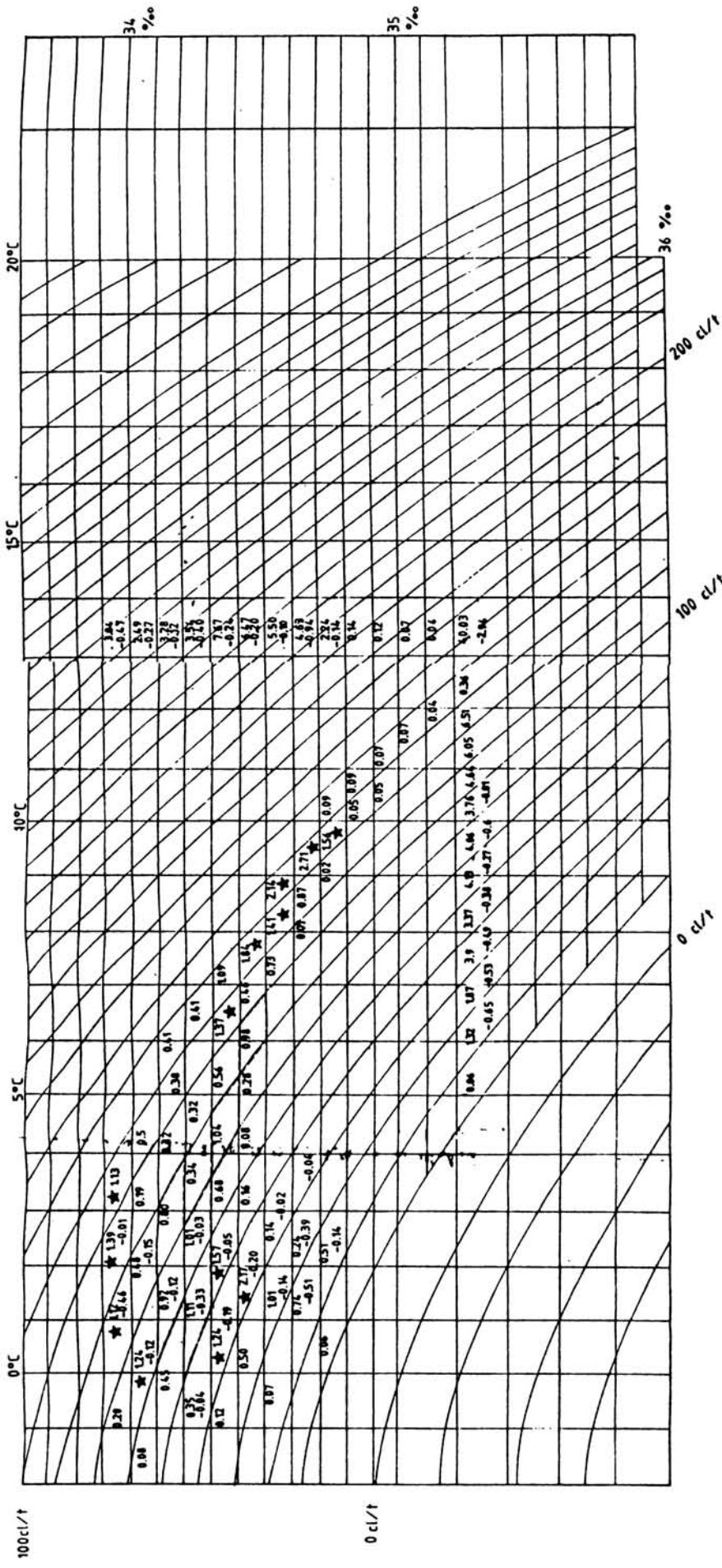


FIG. 4.12 ZONAL FLUX ALONG 115° E

compared to 110°E.

It is seen that flux in upper 1000 m is widely distributed in the west (156 classes across 20°E) while it is restricted to limited number of classes (60 classes across 115°E) in the east. This shows that ACC becomes narrow towards east. Also it is indicated that in both the regions of the study area, APF is significant as a flux donor to the easterly flow (Fig. 4.13). In the west the eastward flux is more or less same order across all the sections except at 40°E where it is decreased by nearly half. Such a drastic departure is not seen in the eastern region while the effect of mid oceanic ridge is clearly depicted in increasing the westward flux seen around 95°E.

Two boundary sections (one in the west along 20°E and another in the east along 115°E) extending from south of Africa and Australia continents have been considered in order to estimate the inter-oceanic exchange of waters between Atlantic, Indian and Pacific sectors of the Southern Ocean. As ACC extends upto a depth of 3000 m (Callahan, 1971; Reid and Nowlin, 1971 and Bryden and Pillsbury, 1977), the reference level to compute the flux has been extended accordingly upto 3000 m depth. The eastward fluxes across the western and eastern boundaries

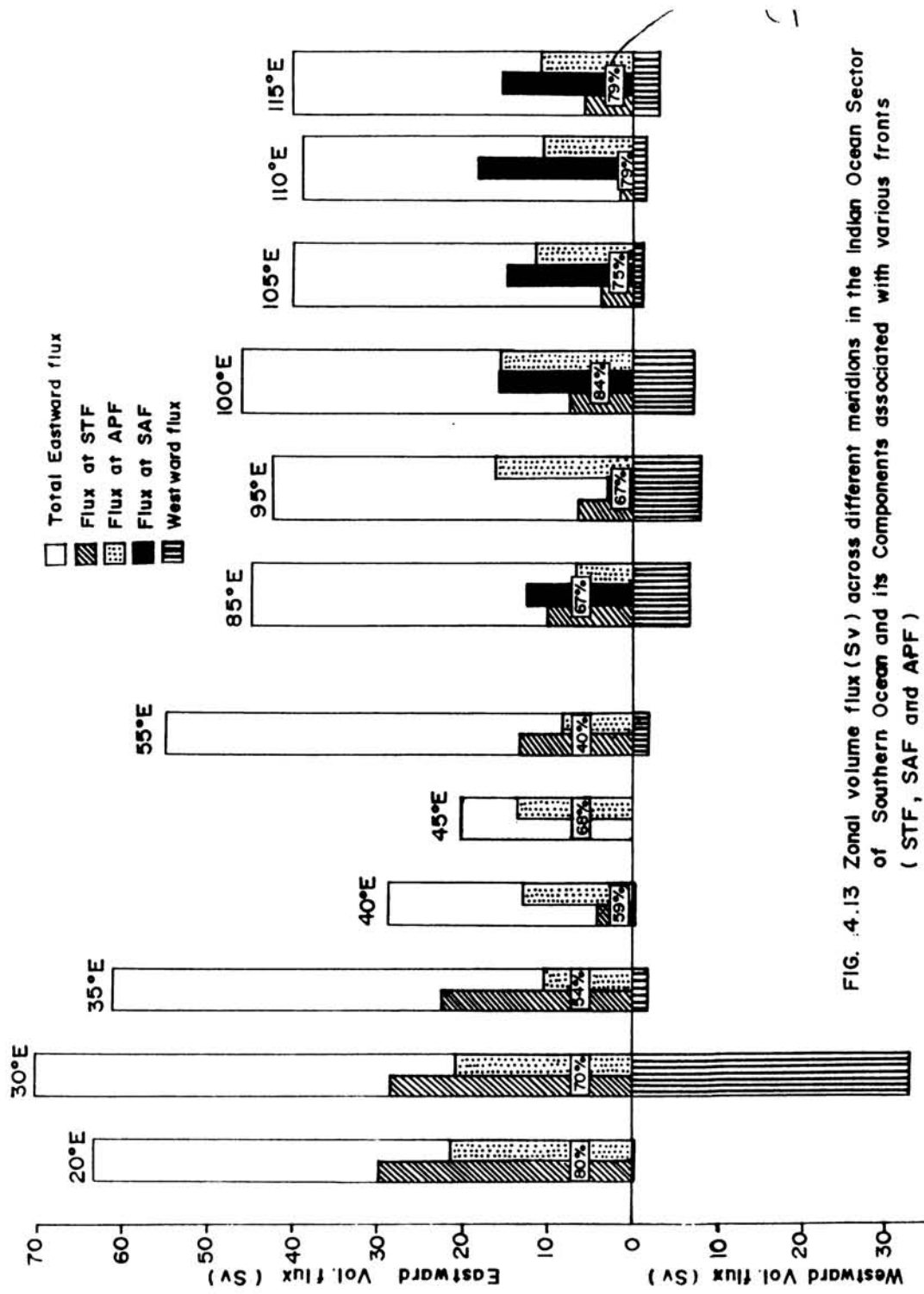


FIG. 4.13 Zonal volume flux (Sv) across different meridians in the Indian Ocean Sector of Southern Ocean and its Components associated with various fronts (STF, SAF and APF)



of the study area are 88.86 SV and 123.46 SV respectively while the corresponding westward fluxes are 17.24 SV and 27.20 SV giving rise to a net flux divergence of about 25 SV in the study area.

# ***CHAPTER - V***

## Fronts and Productivity

Frontal regions have been recognized as areas of higher productivity (Pomazonova, 1980; Ainley and Jacobs, 1981; Jaques and Minas, 1981 and Atkinson and Targett, 1983). Different hypotheses have been put up to study the mechanisms behind the relationship between fronts and productivity. Moreover the Southern Ocean, being a region characterized with well demarcated fronts, is an ideal area to test some of the proposed hypotheses on higher productivity. Fronts in the Indian Ocean sector of Southern Ocean are best fit for any investigations as they show considerable variation in their anatomy from western to eastern region as seen in Chapter III. It has been noted further that the primary production of the Southern Ocean as a whole is considerably low but for the presence of the fronts. Therefore the contribution of fronts in promoting the productivity needs to be well understood. Hence these fronts because of their unique spatial characteristics with their variation in intensity from west to east may be considered as areas for studying not only the interaction between physical and biological factors on promoting the open ocean biological productivity in general, but also the Southern Ocean

primary productivity in particular.

### 5.1 Classification of waters into different regimes

Among several methods in assessing the standing stock of phytoplankton to represent the primary productivity in the Southern Ocean, the chlorophyll. a (chl. a) concentration of surface waters has been considered for the present study. As major fronts in the Southern Ocean show strong distinction in their structure from western region to the eastern region, the study area has been divided into two areas - one west of 85°E and the other east of 85°E. The general characteristics of fronts in the respective regions are derived by averaging their properties in the corresponding areas. Additional data based on several crossings of ships of opportunity which include both surface and XBT observations have also been considered to obtain the general properties of different water regimes in the Indian Ocean sector of the Southern Ocean.

The data used in the eastern region have been obtained in the beginning of summer while in the western region the data represent the late summer condition. This selection of the data would facilitate the study of chl. a

concentration at each frontal zone with the advance of summer season. The latitude  $60^{\circ}\text{S}$  is taken as an arbitrary southern limit of the study area, since south of it the presence of pack ice together with icebergs affects the concentration of chl. a. The study area therefore covers from  $35^{\circ}$  to  $60^{\circ}\text{S}$ . The data points used for obtaining the average surface chlorophyll profiles in the western and eastern regions are 2220 and 2638 respectively taken from 12 Japanese Antarctic Research Expeditions (JARE) during 1967-1985.

The two convergences - STF and APF - with their circumpolar nature are well established in the Southern Ocean. In addition to these, SAF is also present in between STF and APF in the eastern region of the Indian Ocean sector of the Southern Ocean. Hence the waters in the western and eastern regions could be grouped into different regimes as follows. In the west, they are (1) subtropical waters between  $35^{\circ}\text{S}$  and northern boundary of STF (2) waters within STF zone (3) waters between STF and APF (4) waters within APF zone, and (5) waters between APF and  $60^{\circ}\text{S}$ . In the eastern region, waters between  $35^{\circ}$  and  $60^{\circ}\text{S}$  have been divided into seven regimes namely (1) subtropical waters between  $35^{\circ}\text{S}$  and northern boundary of STF (2) waters within STF zone (3) waters between STF and

SAF (4) waters within SAF zone (5) waters between SAF and APF (6) waters within APF zone and (7) waters between APF and 60°S. Tables 5.2.1 and 5.3.1 present the mean and standard deviations of various characteristics of different frontal zones for western and eastern regions respectively.

## **5.2 Fronts in the western region of the study area**

The surface and the corresponding subsurface positions of STF, SAF and APF have been plotted using the hydrographic data to obtain the north-south frontal slopes which in turn influence the congregation of phytoplankton.

### **5.2.1 Sub-Tropical Front (STF)**

About 28 crossings across STF are made use of to delineate its mean structure (Table 5.2.1). In the western region of the study area, STF lies between latitudes 40°29'S and 43°19' S with its mean axis at 41°59' S. The mean width of STF zone is around 310 km. There is considerable variation in its width (Standard deviation:  $\pm$  167 km). The mean gradients in temperature and salinity across STF are obtained as 0.04°C/km and 0.004‰/km respectively. The STF zone has a mean temperature of 14°C

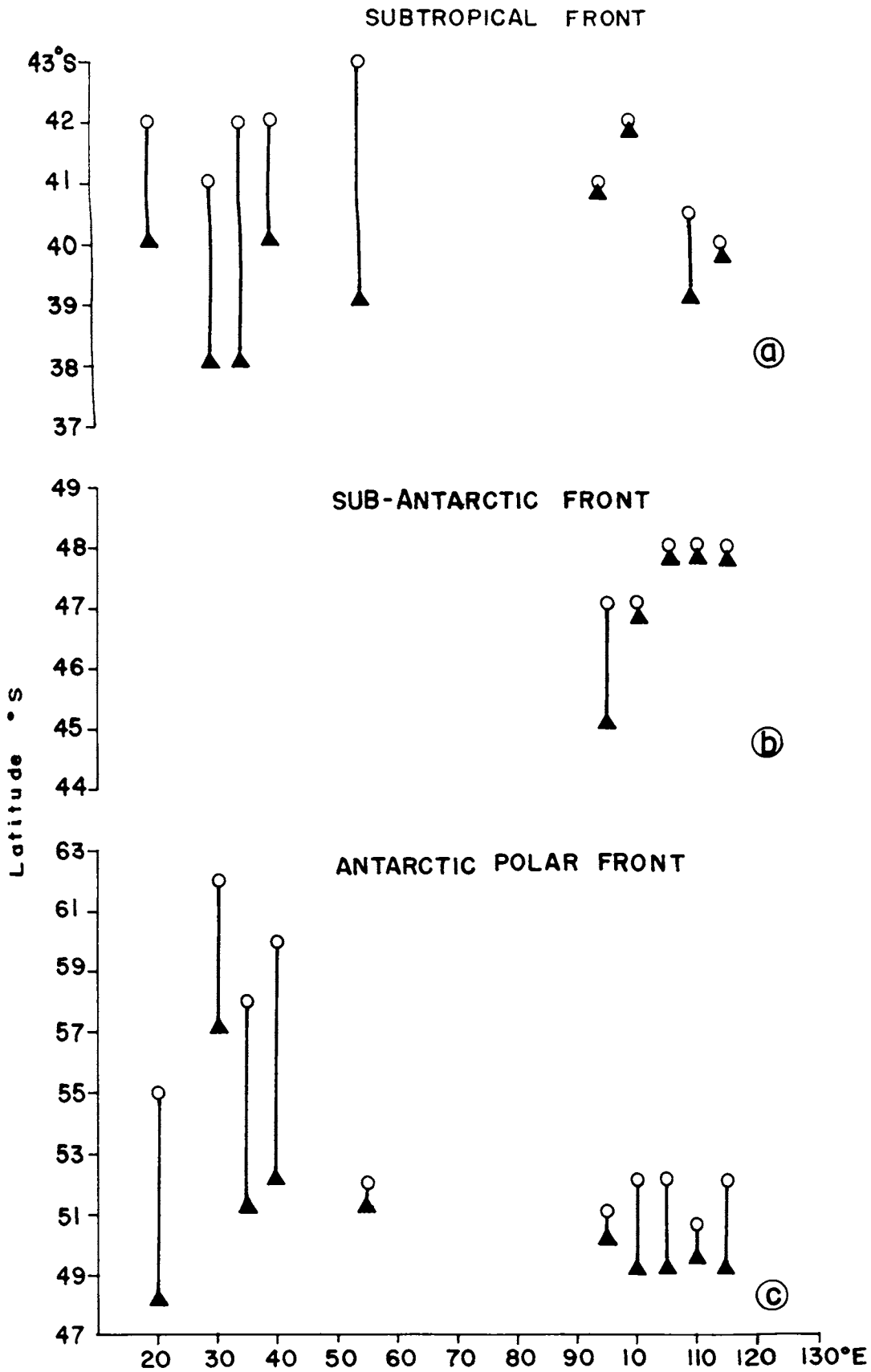


Fig.5.2.1 Latitudinal locations of Surface (○) and the Sub-Surface (▲) expressions of (a) Subtropical Front (b) Sub-Antarctic Front (c) Antarctic Polar Front. Three fronts along different longitudes





and a mean salinity of 34.60‰. The surface expression of STF is far south of the subsurface expression (Fig. 5.2.1a) indicating its northward downsloping. The average horizontal distance across which the slope maintains is around 3° latitude.

### 5.2.2 Antarctic Polar Front (APF)

The mean axis of APF in the western region of the Indian Ocean sector of the Southern Ocean is at 50°43'S (Table 5.2.1). The average width of the frontal zone is 276 km with a standard deviation of  $\pm$  169 km. The Antarctic Polar Front has a mean temperature of 4.4°C and its mean thermal gradient is 0.01°C/km which is four times less than that of STF. Further APF does not have considerable salinity gradient across it. The subsurface expression of APF is farther north than its surface expression indicating again northward downslope like in the case of STF. The average horizontal distance across which the front maintains its slope is about 5.5° latitude.

### 5.3 Fronts in the Eastern region of the study area

In the eastern Indian Ocean sector of the Southern

**Table 5.3.1 Fronts in the eastern region of the Indian Ocean sector of Southern Ocean**

		Latitudinal location		Temperature °C		Salinity ‰							
		From	To	From	To	From	To						
		Middle Width Km		Middle Range Grad- ient °C/km		Middle Range Grad- ient ‰/km							
STF Mean	37°31'	40°23'	38°57'	15.96	12.34	14.15	3.62	0.016	35.35	34.79	35.07	0.56	0.0039
Cro- ssings	1.48	1.88	1.36	1.58	1.44	1.28	1.58	0.100	0.39	0.37	0.37	0.19	0.0042
SAF Mean	46°31'	48°03'	47°09'	9.13	6.32	7.71	2.83	0.019					
Cro- ssings	1.77	1.24	1.34	1.50	1.50	1.42	0.96	0.009					
APF Mean	50°01'	52°10'	51°06'	4.95	3.05	4.01	1.89	0.010					
Cro- ssings	1.10	1.12	0.87	0.77	0.65	0.56	0.83	0.006					

Ocean, the presence of another front namely Sub-Antarctic Front (SAF) in between STF and APF is conspicuously present and it causes the major difference in the frontal morphology of the study area. The mean positions of the three major fronts with their corresponding gradients and the standard deviations are given in table 5.3.1

### 5.3.1 Sub-Tropical Front (STF)

The mean position of STF is found to be at  $38^{\circ}57'S$  with a standard deviation of  $\pm 1.4^{\circ}$  latitude. From 23 crossings, the average width of STF is found to be around 315 km but with a higher standard deviation of  $\pm 224$  km. Eventhough the width of STF is similar in the western and eastern regions of the study area, the standard deviation in its width is considerably high in the eastern region and this shows that STF in the east is more dynamically unstable. The range of temperature across STF in the east is about  $3.6^{\circ}C$  which is nearly half of that in the west. This results in the smaller gradient ( $0.02^{\circ} C/km$ ) in temperature as compared to  $0.04^{\circ}C/km$  of the western region.

The salinity gradient across STF is 0.004%. but the front has a mean salinity of 35.07%. which is higher than

that in the west. There is a lesser northward down slope as both surface and sub surface expressions are not much apart (Fig. 5.2.1a) while in the west, the slope was considerably high.

### 5.3.2 Sub-Antarctic Front (SAF)

Based on 27 observations across SAF, it is found to be at a mean location of  $47^{\circ}9'S$  with a standard deviation of  $\pm 1.34^{\circ}$  latitude (Table 5.3.1). Its mean width is around 189 km which is low in comparison with that of STF and the standard deviation in its width is also low ( $\sim 113$  km). The mean temperature of SAF is about  $8^{\circ}C$  and it has a slightly higher gradient ( $0.02^{\circ}C/km$ ) than STF. This frontal strength is also found to be stronger than APF whose intensity is  $0.01^{\circ}C/km$ , thus establishing SAF as the most prominent front in the east.

### 5.3.3 Antarctic Polar Front (APF)

The mean position of APF in the east based on 27 north south crossings is given as  $51^{\circ}6'S$  (Table 5.3.1). The width of APF is 237 km with a standard deviation of  $\pm 151$  km. The mean temperature of APF zone is  $4^{\circ}C$  with a range of  $1.9^{\circ}C$  and a thermal gradient of  $0.01^{\circ}C/km$ . In the

eastern region, the downward tilt of APF is more compared to corresponding tilts of STF and SAF but it is lesser than that of APF in the west (Fig. 5.2.1).

In general the downward tilting of fronts is considerably higher in the west than in the east suggesting the greater intermingling of surface and intermediate watermasses in the west.

#### **5.4 Meridional distribution of surface chlorophyll. a**

Before presenting the mean profiles of chlorophyll. a for different water regimes of the western and eastern regions, it is better to examine some individual meridional sections typically representing western and eastern regions. Two profiles are selected for this purpose-one between Africa and Antarctica (along 20°E) and the another between western Australia and Antarctica (along 110°E) - facilitating a study on the variability of physical properties and associated chlorophyll. a concentration.

##### **5.4.1 Along 20°E (between Africa and Antarctica)**

The surface distribution of chl. a along with surface temperature and salinity is shown in Fig. 5.4.1. The chl. a

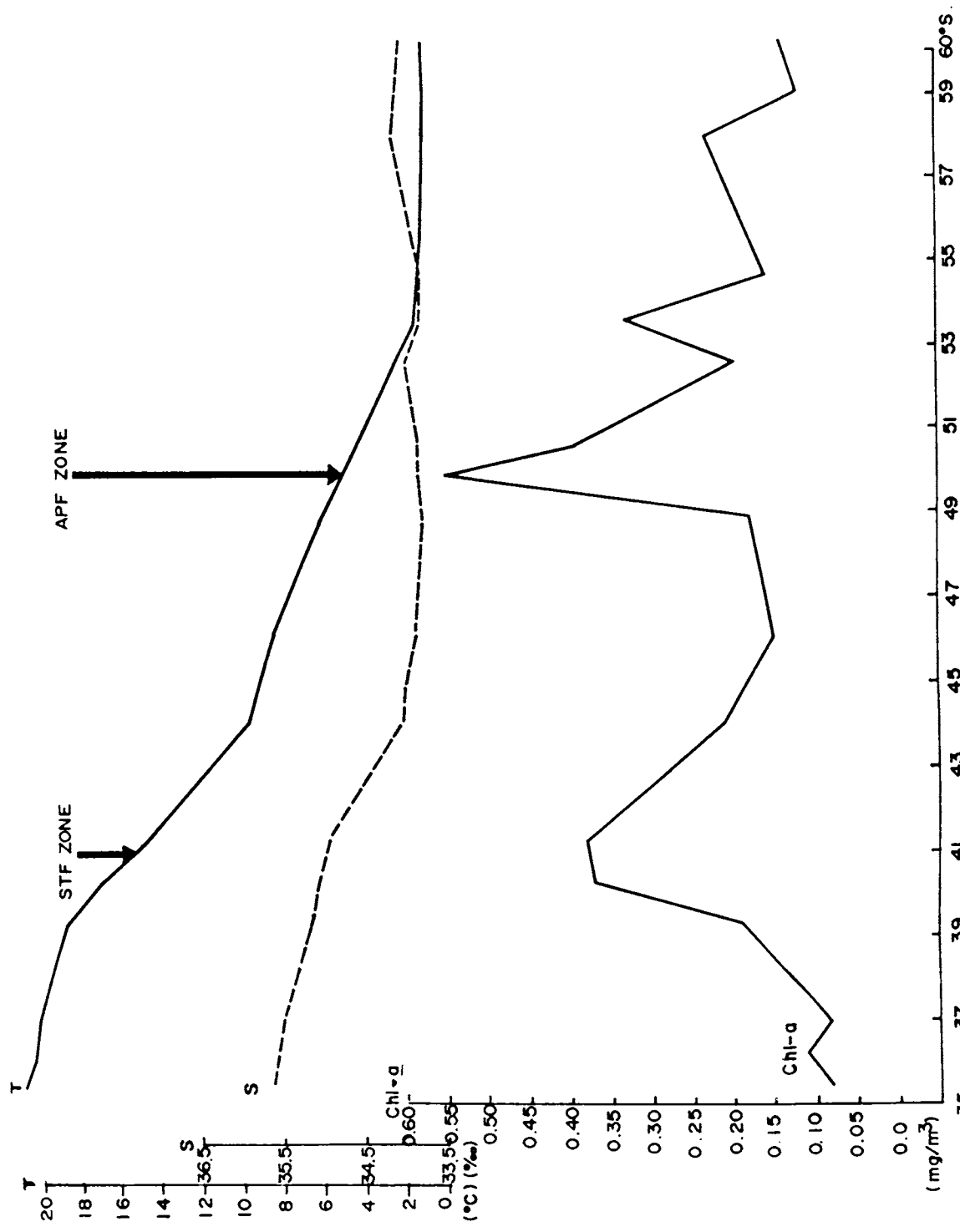


Fig. 5.4.1 The distribution of hydrographic properties and Chl-a along 20°E.

$\rho(\text{max}) \rightarrow S_1 \& S_2$       85  
 sinking should occur ← →,      upwelling and  
 why?

values range from 0.08 and 0.55  $\text{mg/m}^3$ . The striking feature of the chlorophyll. a distribution is the presence of two pronounced maxima around 41°S and 50°S. These two maxima represent STF and APF zones respectively as seen from the distributions of hydrographic properties. The first zone of chl. a maximum coinciding with STF is due to strengthening of the convergence associated with opposite zonal flows. After reaching to a lower value around 46°S, chlorophyll concentration again picks up at APF where it registers the highest value of about 0.55  $\text{mg/m}^3$ . Further south it shows a complicated structure characterised with the incidence of intermittent high and low values. The remarkable association of maximum chlorophyll. a values with the frontal zone is the most conspicuous feature of the meridional distribution.

#### **5.4.2 Along 110°E (Between the western Australia and Antarctica)**

Figure 5.4.2 shows surface chl. a, temperature and salinity distributions from north to south along 110°E. The association of maximum chlorophyll. a with the frontal zone is further confirmed as seen from the coincidence of chl. a concentration peaks with STF, SAF and APF. At STF, chl. a concentration is about 0.27  $\text{mg/m}^3$  while at SAF and

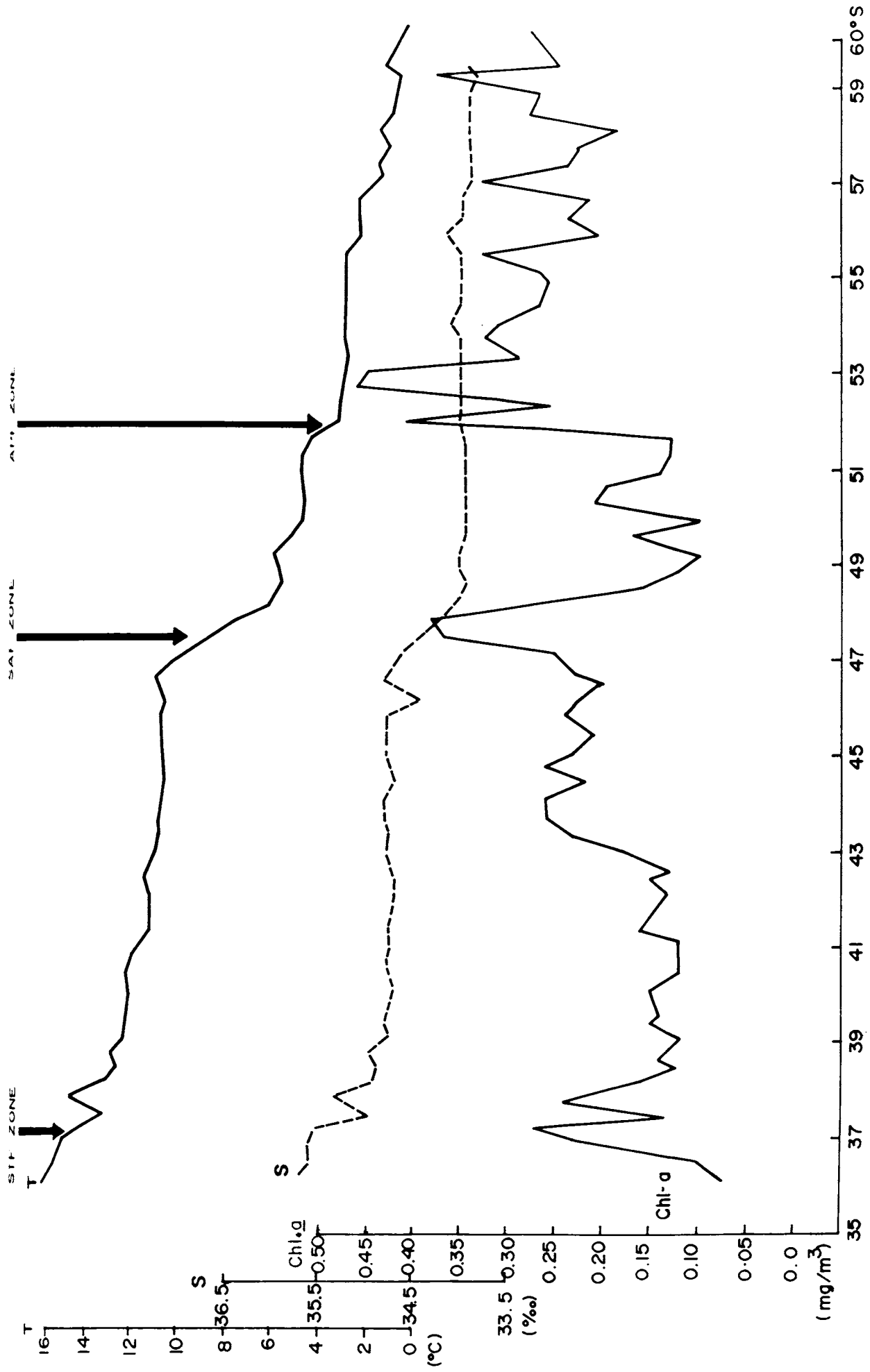


Fig. 5.4.2 The distribution of hydrographic properties and Chl-a along 110° E.



APF, it is 0.38 and 0.55 mg/m<sup>3</sup> respectively. Though SAF is stronger than APF, the intensity of chl. a peak at SAF is lower than that at APF. However, the general occurrence of higher chl. a south of APF suggests the importance of the Antarctic Waters as a productive regime.

### 5.5 Mean distributions of chl. a in different water regimes

The mean and standard deviation of surface chl. a as shown by a dot and dashed line for each zonal regime of the western and eastern regions of the study area are given in Figs. 5.5.1 and 5.5.2 respectively. The number of data points used for each regime are also indicated at the centre of dashed line in these figures.

#### 5.5.1 In the western region

The figure 5.5.1 basically shows the presence of two well defined maxima in chlorophyll. a values from sub tropical region to 60°S. It shows an increase of about 0.3 mg/m<sup>3</sup> in the mean surface chl. a values from subtropical water regime to the waters within STF zone where chl. a values greater than 0.5 mg/m<sup>3</sup> are encountered. There is a subsequent decrease in the sub Antarctic region

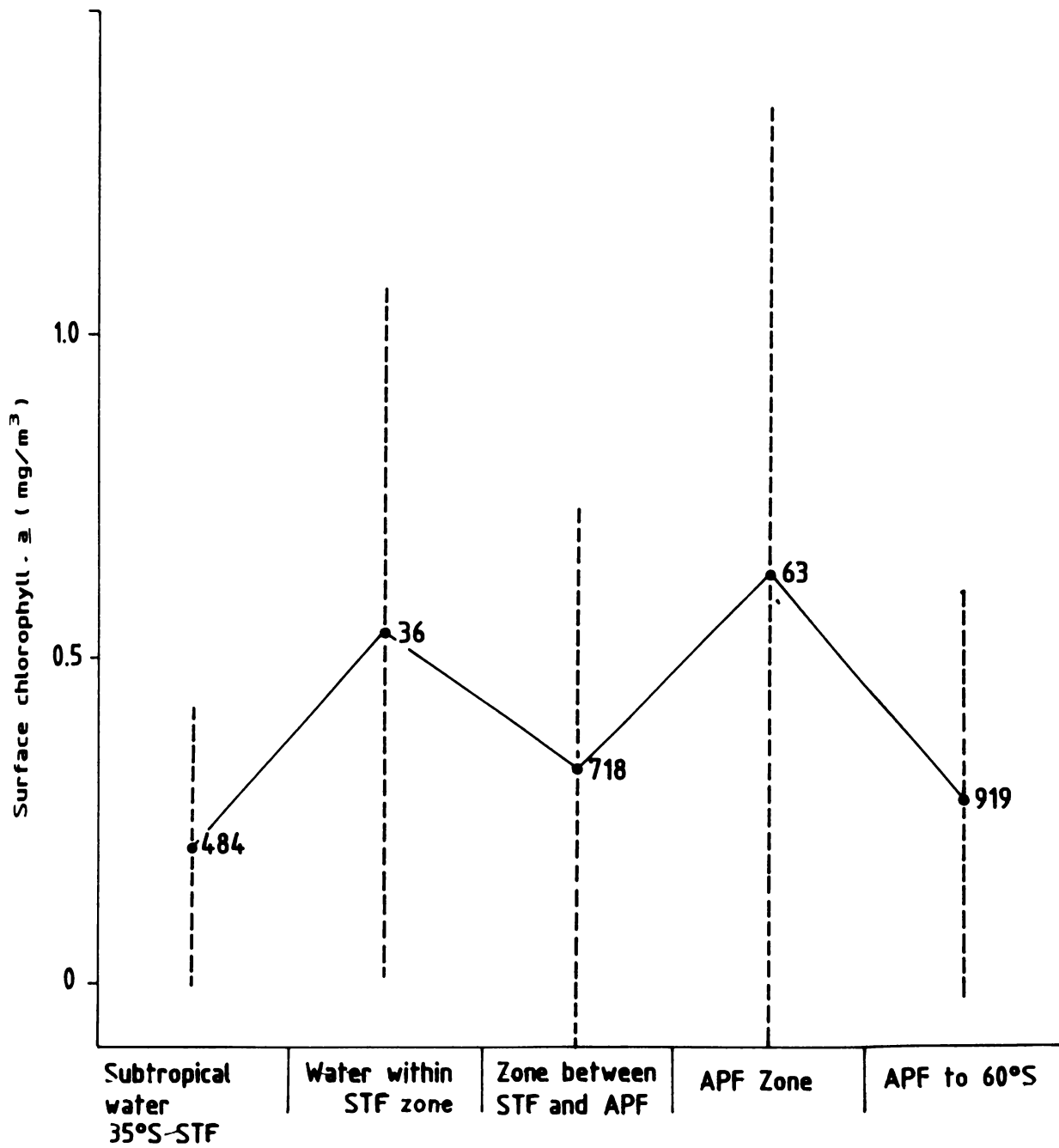


FIG. 5.5.1 Mean and standard deviation of surface chlorophyll $a$  in different water regimes in the Western region.

(between STF and APF). Further south again the chlorophyll concentration increases to greater than  $0.6 \text{ mg/m}^3$  at APF zone. Between APF and  $60^\circ\text{S}$  a sharp declination in the chl. a concentration is vivid. The incidence of higher standard deviations above the mean levels of chl. a at both APF ( $\pm 0.72$ ) and the STF zones ( $\pm 0.54$ ) reveal their complex dynamic nature.

### 5.5.2 In the Eastern Region

The latitudinal distribution of the chl. a distribution and its standard deviation for different water regimes in eastern region of the study area is shown in Fig. 5.5.2.

Like in the western region, in this region also the incidence of maximum values ( $> 0.90 \text{ mg/m}^3$ ) along with higher standard deviation ( $\pm 0.37$ ) takes place in the APF zone. Fig. 5.5.2 shows a gradual increase in the surface chl. a from about  $0.15 \text{ mg/m}^3$  in subtropical waters to a maximum value ( $> 0.6 \text{ mg/m}^3$ ) at SAF without presence of any intermediate maximum at STF like in the west. South of SAF, chl. a concentration decreases considerably and it shows a value  $0.53 \text{ mg/m}^3$ . From there it shows again a sharp ascent in the chl. a value to greater than  $0.9 \text{ mg/m}^3$

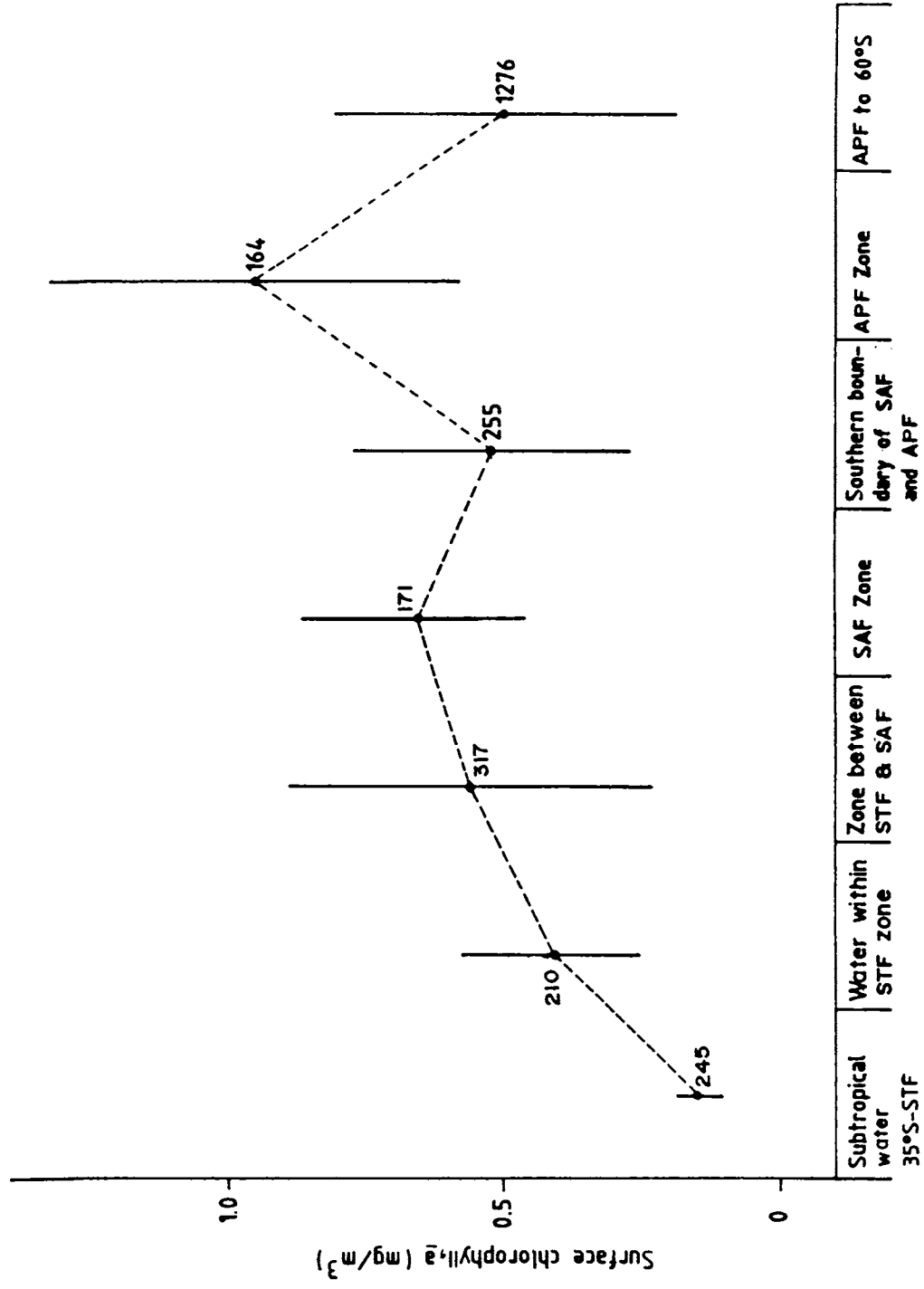


FIG. 5.5-2 Mean and standard deviation of surface chlorophyll a in different water regimes in the Eastern region.

at APF zone and then subsequent descent to  $0.5 \text{ mg/m}^3$  in the region between APF and  $60^\circ\text{S}$ .

In comparison with the western region (Fig. 5.5.1), a conspicuous feature seen is that all the waters except in the STF zone have more chl. a concentration in the eastern region. On the other hand, chl. a concentration has higher standard deviation throughout the western region where the data have been collected during late summer (March). During the early summer, icebergs and pack ice in Antarctic waters start melting and the blooms of phytoplankton that are present in this marginal ice waters obliterate in the APF zone of the eastern region and thus results in higher chl. a concentration.

# ***CHAPTER - VI***

## DISCUSSION

There is not much  
new/critical  
discussion.

It is mostly a  
summary/summary of  
various findings of  
of previous chapters.

### Fronts in the Indian Ocean Sector of Southern Ocean

A critical review of the available information on the Southern Ocean fronts has been presented in the introduction chapter of the thesis. In that the frontal characteristics of the two major oceans namely, the Atlantic and Pacific Oceans in contrast to the meagre information in the Indian Ocean have been brought to focus. In this Chapter, an attempt has been made to discuss the results of the present study on the fronts in the Indian Ocean sector of Southern Ocean with an objective of explaining the physical processes involved in their variation from the western to eastern regions of the sector and their importance as ~~a~~ biological productive areas. These fronts extending on a global scale are important to act as a source of circulation in the world ocean, especially through the formation of intermediate watermasses. A critical examination of volume transport across different meridions of the study area reveals that the fronts have significant variation owing to geographical rather than seasonal factors. The present study shows the importance of front as a flux donor to ACC. From the distribution pattern of hydrographic

Not  
X

properties along different longitudes in the study area, it is seen that Sub-Tropical Front (STF) and Antarctic Polar Front (APF) are the only two fronts in the west while a third front namely Sub-Antarctic Front (SAF) in addition to STF and APF is discernible in the east. Further the gradients of STF decreases from west to east. The effect of bottom topography is also seen in the study area in decelerating the eastward volume transport.

### **6.1 Sub-Tropical Front (STF)**

The mean position of STF in the western region is found to be at  $41^{\circ}59'S$  with a mean mid-temperature of  $14.2^{\circ}C$  and a standard deviation of  $\pm 2.5^{\circ}C$  based on 28 crossings (Table 5.2.1). These results closely agree with those presented by Lutjeharms and Valentine (1984) who obtained average picture of the STF on the basis of 17 crossings between Antarctica and south of Africa. STF in the west is an intense tumultuous front, making this area renowned for its extremely high variability (Lutjeharms and Baker 1980). At  $30^{\circ}E$ , the complex nature of STF is seen from the presence of ridges and troughs in the hydrographic properties (Fig. 3.1.2). The significant contribution of the Agulhas Current to STF is seen in the variation of volume flux at  $30^{\circ}E$  where a fairly large



amount of westerly flux (about 33 SV) encounters in comparison with that at 20°E. The southern edge of the Agulhas return current also called Agulhas convergence (Fukase, 1962) or Agulhas Front (Lutjeharms et al., 1981), coalesce with STF especially at 30°E, increasing the mean temperature and the frontal intensity as suggested by Lutjeharms and Valentine (1984).

The complex portrayal of STF at 30°E is of particular interest, since this feature has been found especially in this region. Earlier Nieman (1965) has indicated that the complex evolution of STF is more prominent in this region. These features probably are due to the presence of eddies spun out from the strong convergence region itself. The origin of these eddies has been observed in satellite infrared imageries of the region south of Africa (Lutjeharms, 1981a; Lutjeharms and Baker, 1980) and these eddies have further been observed to carry mesoscale turbulence towards southward (Lutjeharms 1981b).

STF in the east is found shifted north by about 3° latitude in comparison with STF in the west, though both regions are encountered with similar mean frontal widths and mid-temperatures. However, their standard deviation

are quite different from west to east. The standard deviation of width ( $\pm 224$  km) in the east is higher compared to that ( $\pm 167$  km) in the west. On the otherhand, the standard deviation in the mean mid-temperature is almost doubled ( $\pm 2.5^{\circ}\text{C}$ ) in the west in contrast to its lower deviation ( $\pm 1.3^{\circ}\text{C}$ ) in the east. The east-west variation in the standard deviation suggests that the strength of STF is not consistent throughout the study area. Occasionally, STF in the east is portrayed as a double front represented by two peaks in the thermal gradient around  $39^{\circ}$  and  $42^{\circ}\text{S}$  respectively. On the whole, STF is quite strong in the west with a mean thermal gradient of about  $0.04^{\circ}\text{C}/\text{km}$ , while in the east, its strength is reduced by about half. The results of Edwards and Emery (1982) also indicate a weak STF in the eastern Indian Ocean sector of the Southern Ocean. From the atlas of Wyrтки (1971), it is also inferred that the gradient of STF decreases from west to east. These studies hence suggest that manifestation of a weaker STF is the characteristic feature of the eastern region of the study area.

## 6.2 Sub-Antarctic Front (SAF)

The absence of SAF in the west and its clear

manifestation in the east are conspicuous features of the present study. The mean position of SAF in the east is 47°9'S with a standard deviation of  $\pm 1.3^\circ$  latitude. However, the studies of Lutjeharms (1985) have shown the presence of SAF far west of the present study area. The SAF is identified as the maximum gradient at surface in the temperature range of 3°-5°C. Earlier Sievers and Emery (1978) have considered similar criterion of identifying SAF in the Pacific Ocean sector of the Southern Ocean. The isotherms in the above temperature range merge with those of STF in the west with the result that a separate front (SAF) is not discernible between STF and APF.

Based on the physical and biological investigations carried out in the area including Marion, Crozet, Kerguelen and Heard Islands, Deacon (1983) has suggested that this region seems to be the one where more interaction and less gradation between Antarctic and Subantarctic waters occurs than in any other latitudes. His studies also indicate the effect of bottom topography on currents near the Kerguelen Island resulting in the closeness of STF and APF. It may be mentioned here that the region near the Prince Edward and Marion Islands is known for weakening of STF due to presence of several eddies (Lutjeharms and Valentine, 1988).

Irrespective of whether SAF is present independently or merges with STF in the west, the water characteristics south of STF shows subantarctic mode water in which a deeper near homogeneous layer (thermostad) in 400-600 m depth range below a seasonal thermocline is quite distinctive. The nomenclature "thermostad" has been given first by Seitz (1967) who defined it as a layer with a minimum vertical temperature gradient i.e. the antonym of thermocline.

### **6.3 Antarctic Polar Front (APF)**

The formation of a subsurface temperature minimum layer in the Antarctic waters is well illustrated throughout the study area (Figs. 3.1.1- 3.1.12). The distribution of hydrographic properties along various meridians confirms consistent presence of APF which is regarded as the northward extension of subsurface expression of 2°C isotherm situated in the temperature minimum layer. In the present study, APF is seen as the most prominent and stable front throughout the Indian Ocean sector of the Southern Ocean. The orientation of isanosteres (Figs. 3.3.1 to 3.3.12) becomes more vertical from west to east implying cumulative horizontal steric

gradients and high geostrophic velocity at APF. Gordon (1972) states that the core of zonal ACC closely follows the position of APF. The mean location of APF axis in the western region is at  $50^{\circ}43'S$ . In the eastern region it is shifted slightly southward and is found at  $51^{\circ}6'S$ . These mean positions of APF are comparable with those obtained by Lutjeharms and Valentine (1984) south of Africa. The corresponding width of APF in the west and east are about 275 and 237 kms. The east-west variation in the mean characteristics of APF lie within the accuracy limit of position fixing of APF and as such, it is difficult to say confidently about the intensification of APF in the east. The Scientific Committee on Antarctic Research (SCAR) report (Anonymous, 1981) indicates APF to a northward position (around  $47.5^{\circ}S$ ) at  $30^{\circ}E$  and southward (around  $50^{\circ}S$ ) at  $80^{\circ}E$ . But in the present study along  $30^{\circ}E$ , it is located at  $58^{\circ}S$ . This type of variation is expected due to eddy and meander formations over shorter periods (Joyce and Patterson, 1977). This view point is also supported by Sievers and Emery (1978).

The width of low salinity tongue (Fig. 3.2.2) due to sinking of surface waters in association with APF is high at  $30^{\circ}E$ . This is the only place amongst the various sections where the low salinity tongue ( $< 34.00 \times 10^3$ ) is

quite broader. The mean value of salinity minimum layer increases from west to east (Figs. 3.2.1 to 3.2.12). The most likely cause for the presence of such lower values in salinity minimum tongue in the west in the vicinity of APF may be due to flow of melted water from the Weddel-Sea pack ice across the Atlantic sector into the Indian Ocean sector during summer. This is inferred from the U.S. Navy Oceanographic Atlas (1957) which shows the extension of melted ice water tongue from 30°W to 30°E in the zone of Antarctic waters.

Section at 85°E covered in winter season gives a scope for understanding any seasonal variation in the characteristics of APF, since the rest of the sections are covered during summer. During summer the surface manifestation of APF gets eroded due to the melting of ice and subsequent heating of water, but in winter it is shown as an intense surface gradient in thermal structures (Fig. 3.2.7). The deepening of 1° to 1.5°C isotherms observed between 50 and 60°S in the upper 600 m depth indicates convective mixing and subsequent sinking of winter waters.

The average width of the subantarctic zone in the west is around 970 km, while in the east it is increased to around 1300 km. These values are found to be higher

amongst the different sectors of the Southern Ocean. South of Africa, the width observed by Lutjeharms (1985) is about 670 km. Further low values ( $\sim 300$  km) are encountered in the Drake Passage (Sievers and Emery, 1978). South of Australia also, on an average, the width of subantarctic zone is observed around 780 km (Edwards and Emery 1982).

Along sections  $35^\circ$  and  $40^\circ\text{E}$ , though APF is defined as subsurface expression of the northern limit of  $2^\circ\text{C}$  isotherm, the tongue of low salinity water (Antarctic Intermediate Water formed due to the mixing of Antarctic surface water with the northern waters) is seen extending upto  $42^\circ\text{S}$  and sinking in the temperature range of  $3^\circ\text{-}4^\circ\text{C}$ . This suggests that the denser waters at APF rather prefers to sink with a gentle downward slope between  $40^\circ$  and  $50^\circ\text{S}$  instead of moving vertically. Hence the width of a subantarctic region at subsurface depths is considered to be shorter than at surface where it is characterized with an average temperature of  $4^\circ\text{C}$ .

Another conspicuous feature observed in the vertical sections of temperature is the uniform presence of a well defined dicothermal layer (temperature minimum layer) in the upper 200 m column of the Antarctic zone wherein a

layer of cold water is sandwiched between warmer waters above and below. The dicothermal layer is formed due to heating of the surface water in summer. The dicothermal layer is further found to be less prominent in the eastern region probably due to the insufficient warming of the surface layer during the early summer.

In general, the Antarctic surface water is identified by its low salinity and low temperature in the surface layer. Below this, a warm high saline deep waters make an ascent towards the Antarctic divergence zone. This is in harmony with the results of the investigations carried out by Deacon (1982).

#### **6.4 Volume Transport**

The estimated volume transport exhibits both easterly and westerly flows in the Southern Ocean. The dominant eastward flow is the characteristic of ACC, while the westward flow is more localised relating to the bottom topography and the boundary processes of the study area.

The mean eastward flux in the entire area of study is 46 SV with a Standard deviation about  $\pm 14$  SV ( $\pm 30\%$ ). In addition to the contribution from the natural process



affecting the variability of fluxes, the higher standard deviation could be related partly to the inherent variations in the latitudinal extents which can explain about 50% of its value. Thus the deviations more than  $\pm 7$  SV can be attributed to the different processes of the Southern Ocean.

The estimated eastward flux at 20°E, south of Africa in the upper 1000 m, is about 63 SV. The computations of Jacobs and Georgi (1977) give rise to an eastward geostrophic transport of 129 SV between Cape Agulhas and Antarctica, with respect to a reference level of 3000 m. Georgie and Toole (1982) show similar order of volume transport ( $\sim 140$  SV) South of Africa. Hence the present study indicates that more than 50% of the total eastward flux with reference to 3000 m occurs generally within the upper 1000 m (across 20°E) wherein the strengths of the different front are well depicted. Out of the total flux along 20°E in the upper 1000 m, about 47% is contribution of STF and 39% is that of APF emphasising the importance of fronts in the Southern Ocean circulation.

The westward flux is maximum (33 SV) at 30°E amongst all the sections (Fig. 4.13). A secondary maximum ( $\sim 8$  SV) in westward flux is prominent at 95°E. The peak westward

flux at 30°E is resulted due to the Agulhas Current at higher steric surfaces in the northern part of the section. The westward flux which is almost negligible in the western region of the study area except at 30°E, is found to increase to around 8 SV between 85 to 100°E (Figs. 4.7, 4.8 and 4.9). This increase could be related to the effect of bottom topography characterized with mid ocean ridge. The ridge, a large scale topographic feature, causes meandering of the zonal flow especially north of the Sub-Antarctic Front. Earlier Callahan (1972) has also obtained a higher westerly volume flux of about 27 SV with reference to 3000 m near the Indian Antarctic ridge at 132°E.

A remarkable decrease by about 50% in the eastward flux is observed across 40°E. The eastward flux at 40°E is about 29 SV, though the length of section varies within  $\pm 15\%$  of mean latitudinal extent. Various studies of Gamberoni et al. (1978 and 1982) and Gamberoni (1979) have shown that the characteristics of frontal structure vary considerably around Crozet and Kerguelen Plateaus. Between 40°E and 50°E the effect of Crozet plateau is felt and the nature of the plateau with its stronger northward extension considerably deflects ACC much towards north than at other sections giving rise to lesser eastward flux

south of 40°S. Sarukhanyan (1985) also states that the eastward flowing ACC weakens to a larger extent in the region near Crozet plateau. Thus in this area, the estimated transport seems to represent only the diffused ACC with more meridional flux. In the eastern study area after passing Kerguelen plateau, the ACC swings back to its normal southward position with reinforcement in the flow field.

Eventhough the latitudinal extent of the section 45°E is much reduced, the sharp reduction in the eastward flux is related to the absence of STF across the section under consideration. The eastward transport at 55°E where topographic feature similar to that of Crozet plateau is not seen, is picked up again due to southward shift in STF. The eastward transport across 55°E is comparable to that at western boundary sections (20° and 30°E)

The volume transport along 85°E, which is the only section covered during winter, is around 45 SV in the upper 1000 m. SAF, a conspicuous feature in the eastern study area, contributes largest flux of about 13 SV (29%) at 85°E. On the otherhand, flux associated with STF considerably decreases to about 10 SV in contrast to that in the western study area. The two fronts SAF and APF

dominantly effect the total volume flux contributing more than 50%. The computed easterly flux is about 42 SV at 95°E and is not different much from that at 85°E. This shows that there is lesser influence of season on the flux. In the east the computed fluxes at 100°E, 105°E, 110°E and 115°E are about 46 SV, 40 SV, 39 SV and 40 SV respectively. This smaller spatial variations in the eastern study region lie within the confidence level of  $\pm 7.0$  SV and therefore are attributed to inherent changes in the latitudinal extents, but not due to natural processes.

Eventhough a number of studies have been made on the frontal characteristics, especially in the Atlantic and Pacific sectors of the Southern Ocean, a separate attempt to evaluate the contribution of each front on the zonal volume flux is made for the first time in the Indian Ocean sector. Among the three major fronts STF is important as a flux donor to ACC across 20°, 30°, 35° and 55°E sections, whereas APF is the main contributor in the remaining part of the western study area. The influence of APF is felt in the eastern study area. But in addition to this, a secondary front (SAF) is also found as a prominent contributor to ACC. The effect of STF on ACC is meagre at 40°E on account of topographical interaction with Prince Edward Island.

A slight increase in the westward flux ( $\sim 3.0$  SV) at the eastern most section ( $115^\circ\text{E}$ ) is possible due to the influence of mid oceanic ridge, south of Australia. Such a westerly flow noticed by Molinelli (1979) is described as a part of anticyclonic flow in the basin south of Australia. A slight increase in the westward flux ( $\sim 3$  SV) is therefore resulted due to the presence of eddy circulation especially over the ridge. Colton and Chase (1983) have noticed that the zonal flow over a zonally oriented Indian Antarctic ridge is intensified on the northern side of the ridge and is slowed down at its southern side. On such occasions of meridional shear in the zonal flow, development of clockwise eddies is possible.

Comparison of fluxes at  $20^\circ\text{E}$  and  $115^\circ\text{E}$  in the upper 1000 m, it is seen that in the Indian Ocean sector of the Southern Ocean, there is gain of volume by about 26 SV. The net transport in the Southern Ocean from the Atlantic Ocean sector to Indian Ocean sector is around 63 SV (Fig. 4.1), while the net flow from Indian Ocean sector to the Pacific Ocean sector is about 37 SV (Fig. 4.12). The lower net outflux into the Pacific Ocean south of Australia in the upper 1000 m is attributed to the weaker fronts (STF

and APF) occurring there. The flux estimations are further extended to 3000 m in order to study the overall effects of the fronts on zonal volume flux. The eastward fluxes along 20°E and 115°E are found to be around 89 SV and 123 SV and the corresponding westward fluxes are 17 SV and 27 SV in the upper 3000 m. Hence the net eastward flux from Atlantic to Indian Ocean is around 71 SV and the net eastward flux from Indian Ocean sector to Pacific Ocean is 96 SV giving rise to a divergence of 25 SV in the layer 0-3000 m. A remarkable coincidence is seen between the order (25 SV) of net divergence in the Indian Ocean sector of Southern Ocean and that of the Agulhas current which contributes a westerly flux around 33 SV. The flux distributions with respect to the different steric surfaces indicate that maximum flux is in the lower steric levels characterised with APF in both the western and eastern regions. A comparison of characteristics of computed flux at various longitudes shows that complex nature of the pattern decreases from western to eastern region of the study area. The complexity in the western region reflects the effects of Agulhas current and bottom topography.

#### 6.5 Productivity at the frontal zones

The surface chlorophyll. a distribution combined with

hydrographic properties shows that frontal zones are of highly productive areas. The confluence characteristics of the fronts especially those of APF increase the concentration of phytoplankton which do not have mobility on their own. The higher concentration of chl. a at the frontal structure is due to the convergence of watermasses accumulating the surface organisms. The statistically significant correlation between chl. a concentration at the sea surface and potential primary production made Allanson et al. (1981) to state that this concentration of chl. a at the frontal zones <sup>is</sup> are true picture of enhanced productivity. The stronger association of chl. a with the fronts indicates that the frontal zones are very important places of primary production in the Southern Ocean. A comparison between the western and eastern regions (Figs. 5.5.1 and 5.5.2) shows that except in the STF zone of the east, high chl. a values are present in each frontal zone. In both the western and eastern study areas, a peak in the chl. a concentration is seen in the APF zone. Amongst all frontal regions in the eastern study area, the APF region is encountered with highest values ( $\sim 1.0 \text{ mg/m}^3$ ) of chlorophyll. a. The consistent relation between chl. a and APF is also noticed by Pomazanova (1980) and Jacques and Minas (1981). According to the studies of Hart (1942) and Hasle (1969) a peak in

phytoplankton density shifts more to the south as season advances during austral summer season.

The factors which control the productivity of a region other than stability of watermass are availability of light and nutrients in the upper layer of the water column. The primary production at polar region is higher than that in subtropical regions. However during winter, the very poor illumination due to limited sun hours and stronger reflection from ice results in the lower degree of photosynthesis. Thus the chlorophyll, a concentration in the Antarctic waters increases by about 50% as the summer season progresses. Mean chlorophyll values in the regime between APF and 60°S is around  $0.25 \text{ mg/m}^3$  in the beginning of summer (Fig. 5.4.2) while in late summer, the mean value is around  $0.5 \text{ mg/m}^3$  (Fig. 5.4.1). Further, when ice melts, the surface salinity decreases and this inturn gives rise to a higher stability in the water column. Thus a shallow mixed layer of summer effects photosynthesis to increase further. Hart (1934, 1942) finds continuous bursts of phytoplankton growth soon after mid-summer at the southern latitudes. Fogg and Hayes (1982) and Wietak et al. (1982) have considered hydrographic stratification to be of paramount importance for productivity.



*stability due to the front*

Thermal stability is mainly responsible for the peaks in surface chl. a in the Southern Ocean fronts. The surface and subsurface expression of these fronts (Fig. 5.2.1) hardly coincide, especially the fronts in the western study area indicate their inclined nature with depth. The maximum distance between the surface and subsurface expression of APF in the western region, for instance, is about 638 km. Similarly STF also has a maximum slope in the west. A sloping front of this kind causes higher degree of stability in the water column and hence retain<sup>entire</sup> phytoplakton within the euphotic zone. Thus relatively higher chlorophyll values ( $\sim 0.6 \text{ mg/m}^3$ ) occur in the STF zone of the western region compared to the lower values about  $0.4 \text{ mg/m}^3$  in the respective zone of eastern region. However the comparatively low chl. a values associated with APF in the western region, though its slope is high, can be attributed to the seasonal effect. Further at the STF in the western region, the high chl. a values as compared to those in the east may be due to the stronger gradient (Fig. 5.5.1) in the west. The meandering of STF in the western region is more than that in the eastern region. The southward meandering of the front causes a vertical motion especially at the northern side of the meandering front. The additional pumping of water from the subsurface at the frontal edge causes a large flux of nutrients into

the euphotic zone, increasing the phytoplankton production.

### 6.6 Heat content associated with the front

?  
 otherwise does develop?  
 The convergence of two watermasses at the frontal zone causes the development of mixed layer affecting the heat content of the upper ocean and hence the air-sea interaction processes. The degree of variation of heat content in the upper 500 m in the Southern Ocean (Figs. 3.4.1 to 3.4.12) is examined with respect to the frontal characteristics. The latitudinal distribution of heat content shows a resemblance to the latitudinal distribution of temperature. It shows relatively sharp gradients across frontal zones. In the western region of the study area the variation of heat content at STF is more pronounced while towards eastern region its variation is remarkable across SAF. In both the regions, heat content variation is almost same across APF. Maximum variability in heat content is about  $27 \times 10^7 \text{ J/m}^2$  seen across STF in the western region of the study area. The spawning of frontal eddies is responsible for the faster meridional heat transfer and the production of such eddies are very common at STF (Lutjeharms and Valentine, 1988) disturbing the normal variation of heat content by about

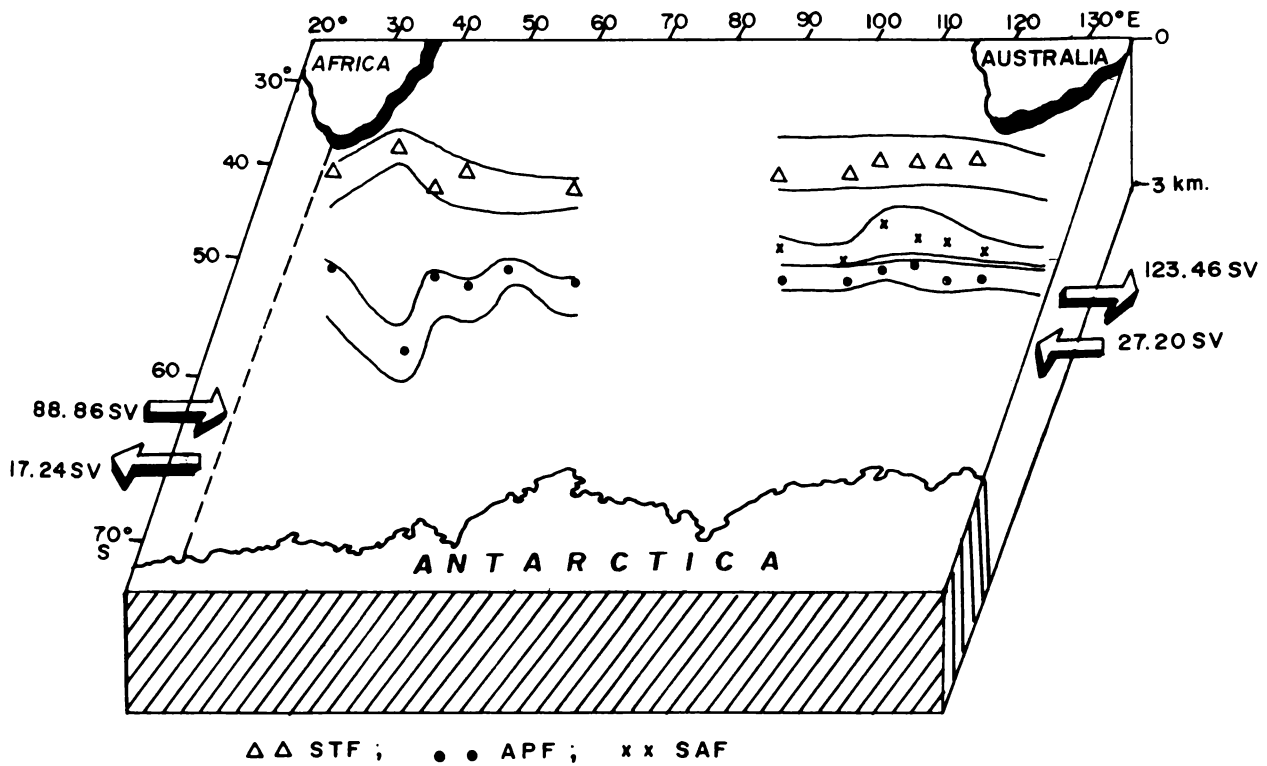


FIG. 6.1 Schematic diagram showing the dynamic nature of the fronts in the Study area

20% as seen at 30°E. Such changes in turn affect the meridional heat transfer and thereby global climate through air sea interaction process. The warm water pool with higher heat content enhances both the evaporative and sensible heat transfers from the ocean to atmosphere. This is in harmony with the finding of Menon et al. (1988) who have suggested an apparent relationship between the thermal regimes (STF and APF) in the Antarctic waters of the Indian Ocean sector of Southern Ocean and summer monsoon over India.

# ***CHAPTER - VII***

## Summary and Conclusion

Not many  
conclusions  
are given  
here

Realising the importance of oceanic fronts as biogeographical areas, efforts have been made increasingly during the past few years to study them. The knowledge of the nature and behaviour of these fronts is fundamental for a better understanding of the ocean ecosystem and their role in the changing global climate through air-sea interactive processes. The Southern Ocean is characterised by a number of conspicuous and persistent fronts. Though the investigations on fronts have been carried out much over the Atlantic and Pacific Sectors of the Southern Ocean, the corresponding frontal characteristics in the Indian Ocean sector, except the region below Africa and Australia, are least known.

This thesis is an outcome of the modest attempt of the author to enhance the knowledge of the major prominent fronts in the Indian Ocean sector of the Southern Ocean. The zonal volume transport in the upper 1000 m of the water column along with the mean and standard deviation of various frontal characteristics (position, width, gradients etc.) are presented in the thesis. The distribution of heat content of the water column and the hydrographic properties along 12 selected meridional

sections covering both western and eastern regions of the Indian Ocean sector of the Southern Ocean are depicted. The mean productivity, Chlorophyll a (Chl. a), in each water regime is also worked out from the data collected during several crossings of ships of opportunity.

The meridional distribution of hydrographic properties gives a qualitative identification of the fronts. The zonal volume flux which has been computed through bivariate classes of salinity and thermohaline anomaly helps to quantify the contributions of individual fronts on Antarctic Circumpolar Current.

The waters in the west have been divided into five regimes due to the presence of two fronts while in the east the Southern Ocean is divided into seven regimes by three fronts. The mean and standard deviation of surface chl. a in each frontal zone are estimated respectively for the western and eastern regions of the study area. The region around 40°E where topographic influence is felt due to Prince Edward Island shows weak STF.

On the whole twelve meridional sections - six in the western and six in the eastern region of the study area from 20° to 115°E are chosen to understand the

geographical variability of Southern Ocean fronts. All the sections except along 85°E have been covered during summer. The section along 85°E has been chosen in winter to facilitate a study on seasonal variations in the fronts, if any.

The volume flux computation has been extended upto 3000 m at 20°E south of Africa and at 115°E south of Australia to evaluate the zonal flux divergence of the study area.

The presentation of zonal flux in the T-S-V diagram divides the total flux into smaller fluxes, which are distributed into different classes of thermosteric anomaly and salinity. The vertical distribution charts of temperature, salinity and thermosteric anomaly have been examined together with T-S-V diagram to identify the frontal characteristics. By matching the charts of properties (temperature and salinity) with flux derivatives, the individual contributions of each front on the total zonal flux is derived.

The mean location of STF in the western region is 41°59'S. Its mean width is about 310 km along with a relatively small standard deviation of about  $\pm 167$  km,



representing the consistency in the strength of STF. In the eastern region STF is shifted towards the lower latitude and its mean position is  $38^{\circ}57'S$ . The mean width is about 315 km. The higher standard deviation of about 224 km in this region implies more dynamically unstable nature of STF.

SAF is a unique feature in the east and it has a gradient of  $0.02^{\circ}C/km$  which is the strongest of all the three permanent fronts in the east. Its mean location is  $47^{\circ}9'S$ . The position of APF in the western and eastern regions does not show much variation. The comparatively high standard deviation ( $\pm 169$  km) in APF zonal width in the west shows more dynamic nature of the front in this region. The absence of SAF and a clear gradation of Subantarctic mode water in the western region are due to the more northward movement of Antarctic waters. Hence the Sub antarctic zone is wider in the west than in the east.

The mean eastward flux in the upper 1000 m of the study area is estimated to be around 46 SV with a standard deviation of about  $\pm 14$  SV ( $\pm 30\%$ ). The variation in latitudinal extent of the sections affects the transport upto a maximum of about 7 SV i.e. 50% of standard deviation. Thus the variations above 7 SV could only be

considered due to the inherent features of hydrography.

Across  $20^{\circ}\text{E}$ , the eastward transport is about 63 SV in the upper 1000 m water column representing the inflow from the Atlantic Ocean while the westward transport into the Atlantic Ocean is quite negligible. However at  $30^{\circ}\text{E}$ , the eastward transport is around 70 SV, more or less same order as that at  $20^{\circ}\text{E}$  whereas the westward flow is found to be relatively high around 33 SV. This strong westerly flow is due to the Agulhas Current which carries subtropical waters to the Atlantic Ocean. Further at  $30^{\circ}\text{E}$ , the larger horizontal shear in the flow field due to the presence of west bound Agulhas Current north of STF and east bound ACC south of it generates eddy turbulence which is seen extending into Subantarctic regions.

The flux at  $40^{\circ}\text{E}$  is considerably reduced to about less than half of that at  $30^{\circ}\text{E}$ , indicating the effect of the northward shift in STF. This in turn makes ACC to spread to lower latitudes decreasing its intensity. Except along  $20^{\circ}\text{E}$  and  $55^{\circ}\text{E}$  all other sections in the western part of the study area shows a single dominant mode of transport due to the more northward extension of Antarctic waters. In the eastern region, the easterly flux is present with conspicuously less spatial variation

suggesting the narrowness of ACC. The secondary maximum (8 SV) in the westward flux seen around 95°E suggests the effect of Indian Antarctic mid-oceanic ridge on the zonal flow.

The net flux divergence is positive in the water column upto 3000 m. A net divergence of water upto 25 SV is obtained from the estimates of 88 SV and 123 SV of eastward flux and 17 SV and 27 SV of westward flux at 20°E and 115°E respectively. A remarkable coincidence exists between this order of net divergence in the Indian Ocean sector of Southern Ocean and that due to Agulhas Current emphasising the importance of the latter in the volume balance of the study area.

The primary mode in 50% volume transport in the western region is consistently confined to lower steric surface while in the eastern region such a consistency is not seen. This shows that in the western region of the study area ACC is well spread. However, zonal flux is found to be more uniform in the east than in the west. Further, the multistream nature of ACC is clearly depicted by the concentration of the flux at different fronts in the east.

In general two fronts STF (thermohaline front) and APF (thermal front) are present in the western region while in the east two thermohaline fronts (STF and SAF) and one thermal front (APF) are well pronounced. The area where the strongest front encounters is that associated with STF below South Africa, but in the east STF is weak. The frontal morphology based on the present study is schematically shown in Fig. 6.1. Among them the APF regime is characterized with higher productivity and especially in the east it is the region of maximum productivity.

Subtropical convergence, the northern boundary of Southern Ocean has largest degree of horizontal variability in the heat content promoting faster meridional transport of heat energy from subtropics to polar region. The higher dynamic nature of STF causes eddy shedding especially in the western region helping <sup>to make</sup> the poleward heat transfer more rapid.

Eventhough the present study infers that major fronts in the Indian Ocean sector of the Southern Ocean are considered as source regions for the intermediate depth circulation, the present degree of information on frontal characteristics and their regional variations, the mechanisms for higher productivity, their contribution to

ACC and air-sea interaction is still inadequate to arrive at definite conclusion. More data (during winter and summer) with greater spatial resolution are needed to study the zonal and seasonal variabilities in the frontal morphology. This additional information is useful for validation of numerical models developed to simulate the general circulation of the Indian Ocean sector of the Southern Ocean.

*Clarify the role of fronts on  $O_2$  exchange otherwise the sentence is incomplete. Belongs to Intro.*

The role of fronts on the Southern Ocean dynamics assumes greater importance in the recent times in the context of global warming on account of increased levels of carbon dioxide in the atmosphere. This in turn would cause melting of ice around Antarctic continent and thus further would affect the frontal characteristics. Therefore, it is essential to have a precise base line information on fronts in the Southern Ocean, especially in its least explored area of Indian Ocean sector in order to assess the effects of global warming.

The investigations on air-sea exchanges of momentum, heat and mass transfer at the fronts, which affect the meridional transport of heat, are needed to enrich the understanding of the changes in global climate. To achieve a better monsoon prediction and greater exploitation of

*who has developed? Give so Ref*

biological resources, an interdisciplinary work on the fronts in the Southern Ocean by the physical, chemical and biological oceanographers is inexplicable and this recommends a further research.

## REFERENCES

## REFERENCES

- Ainley, D.G. and Jacobs, S.S. (1981). Sea bird affinities for ocean and ice boundaries in the Antarctic. Deep Sea Res., 10A, 1173-1185.
- Allanson, B.K. Hart, R.C. and Lutjeharms, J.R.E. (1981). Observations on the nutrients, chlorophyll and primary productivity of the Southern Ocean south of Africa. South. Afr. Jour. of Ant. Res., 11, 3-14.
- Anonymous. (1970). Eltanin Report. Lamont Doherty Geological Observatory of Columbia University, Palisades, N.Y.
- Anonymous. (1971). Eltanin Report. Lamont Doherty Geological Observatory of Columbia University, Palisades, N.Y.
- Anonymous. (1981). Convention on the Conservation of Antarctic Marine living resources. SCAR Bulletin, 67, 383-404.
- Atkinson L.P. and Targett, T.E. (1983). Upwelling along the 60 m isobath from Cape Canaveral to Cape Hatteras and its relationship to fish distribution. Deep Sea Res., 2A, 221-226.
- Barcilon, V. (1966). On the influence of the peripheral Antarctic water discharge on the dynamics of the circumpolar current. J. Mar. Res., 24, 269-275.
- Barcilon, V. (1967). Further investigation of the influence of the peripheral Antarctic water. J. Mar. Res., 25, 1-9.
- ↘ Bang, N.D. (1973). Characteristics of an intense ocean frontal system in the upwelling regime west of Cape Town. Tellus., 25 : 256-265.
- Bathen, H.K. (1971). Heat storage and advection in the North Pacific Ocean. J. Geophys. Res., 76, 676-687.



- ☆ Bohncke, G. (1938). Temperature, Salzgehalt und Dichte an der Oberfläche des Atlantischen Ozeans. Zweite Lieferung. Wissenschaftliche Ergebnisse der Deutschen Atlantischen Expedition auf dem Forschungs und Vermessungsschiff (Meteor), 1925-7, 5, PP 187-250.
- ☆ Botnikov, V.N. (1963). Geographical position of the Antarctic Convergence Zone in the Antarctic Ocean. Inform. Bull. Sov. Antarctic Expedi. No.(41) (Eng. Ed.), 4 (4) ; 324-327.
- Brennecke, W. (1921). Die Oceanografischen Arbeiten der Deutschen Antarktischen Expedition, 1911-1912 Arch. Dt. See Wate, 33(1) : 1-216
- Bryden, H.L. and Pillsbury, R.D. (1977) Variability of deep flow in the Drake Passage from year long current measurements. J. Phys. Oceanogr., 7, 803-810.
- ☆ Burling, R.W. (1961). Hydrology of circumpolar waters south of New Zealand. New Zealand Dept. Sci. Ind. Res. Bull. 143, Memoir 10, 9-61.
- Callahan, J.E. (1971). Velocity structure and flux of the Antarctic Circumpolar Current South of Australia. J. Geophys. Res., 16 (24) 5859-5870.
- Callahan, J.E. (1972). The structure and circulation of deep water in the Antarctic. Deep Sea Res., 19, 563-575.
- Collins, C.A., Mooers, C.N.K., Stevenson, M.R. Smith, R.L. and J.G. Pattullo, (1968). Direct current measurements in the frontal zone of coastal upwelling region. J. Ocean. Soc. Jap. 24, 295-306.
- Colton, M.T., and Chase, R.P. (1983). Interaction of Antarctic circumpolar current with bottom topography : An investigation using satellite altimetry. J. Geophys. Res., 88, 1825-1843.
- Cresswell, G.R., Golding, T.J. and Boland F.M. (1978). A buoy and ship examination of the subtropical convergence south of western Australia. J. Phys. Oceanogr., 8, 315-320.

- Cromwell. and Reid. (1956). A study of oceanic fronts. Tellus, 8, 94-101.
- Deacon, G.E.R. (1933). A general account of the hydrology of the south Atlantic Ocean. Discovery Repts., 7, 171-238.
- Deacon, G.E.R. (1937(a)). Hydrology of the Southern Ocean Discovery Repts., 15, 1-124.
- Deacon, G.E.R. (1937(b)) Note on the dynamics of the Southern Ocean. Discovery Repts., 15, 125-152.
- Deacon, G.E.R., (1945). Water circulation and surface boundaries in the oceans. Discovery Repts., 15, 153-200.
- Deacon, G.E.R. (1964). The Southern Ocean. In : A review of British Scientific Achievement in Antarctica, Leds. R. Priestley, R.J. Adie and G de Q. Robin), Butterworths, London, 292-307.
- Deacon, G.E.R. (1976). The cyclonic circulation in the weddel sea. Deep.Sea.Res., 23, 125-126.
- Deacon, G.E.R., (1977). Comments on a counter clockwise circulation in the Pacific subantarctic sector of the Southern Ocean suggested by Mc Ginnis, Deep. Sea.Res., 24, 927-930.
- Deacon, G.E.R. (1979). The weddell Gyre., Deep.Sea.Res., 26, 981-995.
- Deacon, G.E.R. (1982). Physical and biological zonation in the Southern Ocean, Deep.Sea.Res., Part A, 29, 1-15
- Deacon, G.E.R., (1983). Kerguelen, Antarctic and sub anatrctic. Deep.Sea.Res., 30, 77-81.
- Deacon, G.E.R., (1984). The Antarctic circumpolar ocean. In: Studies in Polar Research, Cambridge University Press, 180 pp. → Edited by ?
- Defant, A. (1928). Die Systematische Enforschung des weltmeeres. z. ges. Erdk., Jubilaums Sonderband, 459-505.

- ☆ Drygalski, E.V. (1926). Ozean und Antarktis. Deut. Sudpol Exped., 7, 391-602.
- Edwards, R.J. and Emery, W.J. (1982). Australian Southern Ocean frontal structure during summer 1976-1977. Aust. Jour. of Mar and Fresh Water Res., 33, 3-22
- Emery, W.J. (1977). Antarctic Polar frontal zone from Australia to the Drake Passage. J. Phy. Oceanogr., 7, 811-822.
- Fandry, C. and Pillsbury, R.D. (1979). On the estimation of absolute geostrophic volume transport applied to the Antarctic Circumpolar Current. J. Phys. Oceanogr., 9, 499-555.
- ☆ Fofonoff, N.P. (1955). A theoretic study of zonally uniform flow. Ph.D. dissertation, Brown Univ., Providence, R.I. 46.
- Fogg, G.E. and Hayes, P.K. (1982). The relative importance of nutrients and hydrographic features for the growth of Antarctic plankton. Joint Oceanographic Assembly, Halifax, Abstracts, A 6.4, 60-61.
- Foster, L.A. (1972). Current measurements in the Drake Passage, M.S. Thesis, Dalhousie Univ., Halifax, N.S., Canada, 61 pp.
- Fukase, S. (1962). Oceanographic condition of surface water between the south end of Africa and Antarctica. Antarctic Record, 15, 53-110.
- ☆ Garner, D.M. (1958). The Antarctic Convergence South of New Zealand. N.Z.J. Geol. Geophys., 577-594.
- Garvine, R.W., and Munk, J.D. (1974). Frontal structure of a river plume. J. Geophys. Res., 79.
- Gamberoni, L., Geromi, L., Jeannin and Murail, J.F.. (1978), Hydrologie, Centre "National Pour Exploration des Oceans Resultats des Compagnes de la mer", 16, 35.

- Gamberoni, L. (1979). Quel hes elements Sur l' by drologie dis Oceans Indien Sudet Antarctique (Secteur Indien). Memories Museum National d' Histore Naturelle, Nouvelle Seriec, Sciences de la Terre 43, 21-31.
- Gamberoni, L., Geronimi, J., Jeannin. P.F. and Murail J.F. (1982). study of frontal zones in the Crozet Kerguelen region. Oceanologica Acta, 5, 290-299.
- Georgi, D.T. (1977). Temperature fine structure in the Southern Ocean. Ph.D. Thesis, Columbia Univ., New York, 343 pp.
- Georgi, D.T. (1978). Fine structure in the Antarctic polar front zone. Its characteristics and possible relationship to internal waves. J. Geophy. Res., 4579-4588.
- Georgi, D.T. (1981a). On the relationship between the large scale property variations and fine structure in the circumpolar Deep Water. J. Geophy. R., 86, 6556-6566.
- Georgi, D.T. and Toole, J.M. (1982). Antarctic Circumpolar Current and the oceanic heat and freshwater budgets. J. Mar. Res., 40, 183-197.
- Gibbs. (1970). Circulation in the Amazon River estuary and adjacent Atlantic Ocean. Jour. Mar. Res. 28, 113-123.
- Godfray, J.S. and Golding, J.J. (1981). The Sverdrup relation in the Indian Ocean and the effect of Pacific Indian Ocean through flow on Indian Ocean circulation and on the East Australian Current. J. Phys. Oceanogr., 11, 771-779.
- Gordon, A.L. (1966). Potential temperature, oxygen and circulation of bottom water in the Southern Ocean. Deep. Sea. Res. 13, 1125-1135.
- Gordon, A.L. (1967a). Structure of Antarctic waters between 20°W and 170°W. In Antarctic Map folio series, Folio 6, edited by V. Bushnell, Am. Geophys. Soc. New York.

- Gordon, A.L., and Goldberg, R.D. (1970). Circumpolar characteristics of Antarctic waters, Antarctic Map folio series, folio 13, edited by V. Bushnell, Amer. Geogr. Soc., New York 1970, 1-15.
- Gordon, A.L. (1970a). Antarctic Polar Front Zone. In: Antarctic Oceanology, I, Antarctic Res. Ser., 15, (ed. J.L. Reid), AGU Washington, D.C., 205-221.
- Gordon, A.L. (1971). Antarctic Polar front zone. Antarctic Res. Ser., 15, 205- 11.
- Gordon, A.L. (1971b). Recent physical oceanographic studies of Antarctic waters. In: Research in Antarctic, A.A.A.S. Publ. 93, (ed. L.O. Quam), Washington D.C., 609-629.
- Gordon, A.L. (1972). On the interaction of the circumpolar current and the Macquire Ridge In: Antarctic Oceanology, II, Antarctic Res. Ser., 19, (ed. D.E. Hayes) AGU, Washington, D.C., 71-78.
- Gordon, A.L. and Tcherina, P. (1972). Waters of the continental margin of Adelie Coast, Antarctica. In: Antarctic Oceanology II. The Australian New Zealand sector; (ed. D.E. Hayes), Ant. Res. Ser., 19, AGU Washington, D.C., 59-69.
- Gordon, A.L. and Molinelli, E.J. (1975). USNS Eltanin Southern Ocean Oceanographic Atlas, Cruises 4-55, June 1962 Nov. 1972. LDGO Centr. 2256, Palisades, N.Y.
- Gordon, A.L., Taylor, H.W. and Georgi, D.T., (1977a) Antarctic Oceanographic Zonation. In: Polar Oceans Conference, edited by M.J. Dunbar pp. 45-76, Arctic Institute of North America, Calagary, Alberta, Canada.
- Gordon, A.L. Georgi, D.T. and Taylor, H.W. (1977b). Antarctic Polar front zone in the Western Scotia Sea Summer, 1975, J. Phy. Oceanogr., 7(3), 309-328.
- Gordon, A.L. and Rodman, M.R. (1977). Southern Ocean temperature gradient near 2°C, Deep.Sea. Res. 24, 85-102.

- Gupta, R.S. and Qasim, S.Z. (1983). Chemical Oceanographic studies along a section from 32°S to Antarctica in the Southwestern Indian Ocean. In: Scientific Report of First Indian Expedition to Antarctica, Tech. Publ. No. 1, 69-77.
- Hart, T.J. (1934). On the phytoplankton of the Southwest Atlantic and the Bellingshausen Sea. Discovery Repts., 8, 1-268.
- Hart, T.J. (1942). Phytoplankton periodicity in Antarctic surface water. Discovery Rept., 21, 261-356.
- ☆ Hasle, G.R. (1969). An analysis of the phytoplankton of the Pacific Southern Ocean. Abundance, composition and distribution during the Brategg Expedition, 1947-1948. Hvalradets Skr : 52, 1-168.
- Hastenrath, S. (1982). On meridional heat transports in the world ocean. J. Phy. Ocea., 12, 922-927.
- Hidaka, K. and Tsuchia, M. (1953). On the Antarctic Circumpolar Current. J. Mar. Res., 12, 214-222.
- Holloway, G. (1986). Estimation of oceanic eddy transports from satellite altimetry. Nature, 323, 243-244.
- Horne, E.P.W. (1978). Interleaving at the subsurface front in the sloping water off Nova Scotia, Jour. Geo. Res., 83, 3659-3671
- ☆ Houtman, T.J. (1964). Surface temperature gradients at the Antarctic convergence. New Zealand Jour. of Geology and Geophysics, 7, 245-270.
- ☆ Houtman, T.J. (1967). Watermasses and fronts in the Southern Ocean South of New Zealand. Bull. New Zealand Dept Sci. Ind. Res. No. 174.
- ISOS Programme (1976). Ant. Jour. of United States., 3, 154-159
- ☆ Ivanov, YO A. (1959). Polozhenie i sezonnaya izmenchivost frontal 'n' Kh zon v Antarktike (Location and seasonal variations of frontal zones in the Antarctica). DOKl. ANSSSR, Vol. 129, 4.

- Ivanov, Yv. A. (1961). On frontal 'nykh Zonakh V Antarkticheskikh Vodakh (on frontal zones in Antarctic waters) Doklady Akademii Nauk SSSR, No. 3.
- Jacobs, S.S. and Georgi, D.J. (1977). Observations in the Southwest Indian/Antarctic Ocean. In A Voyage of Discovery. Ed. Angel, 43-84.
- Jacques, G. and Minas M. (1981). Production Primaire dans l'océan Indien de l'Antarctique en fin d'été. Oceanol. Acta., 4, 33-41.
- Joyce, T.M. and Patterson S.L. (1977). Cyclonic ring formation at the polar front in the Drake Passage. Nature., 265 (5590), 131-133.
- Joyce, T.M. Zenk, W. and Toole, J.M. (1978). The anatomy of the Antarctic polar front in the Drake Passage. J. Geophys. Res., 83, 6093-6113.
- Katz, E.J. (1969). Further study of a front in the Sargasso Sea. Tellus, 21, 259-269.
- Knauss, J.A. (1957). An observation of an oceanic front. Tellus, 9(2), 234-237.
- ☆ Koopman, G. (1953). Entstehung Und Verbreitung Von Divergenzen in der oberflächennahen Wasserbewegung der Antarktischen Gewässer. Deutsche hydrographische Zeitschrift, Ergänzungsheft 2, pp 38 + 2 plates.
- ☆ Kort, V.G. (1962). The Antarctic Ocean. Sci. Amer., 207, 113-128.
- ☆ Kort, V.G. (1967). Frontogenesis in the Southern Ocean. Information Bulletin, Soviet Antar. Exped. 65, 500-505.
- Lutjeharms, J.R.E. (1979). Interaction between the Agulhas Current and the subtropical convergence. CSIR. Res. Rep., 384.
- Lutjeharms, J.R.E. and Baker, D.J. (1980). A statistical analysis of the meso scale dynamics of the Southern Ocean. Deep Sea Res., 27, 145-159.

- Lutjeharms, J.R.E., Fromme, G.A.W. and Valentine, H.R. (1981). Oceanic frontal systems between Africa and Antarctica. EOS, Trans. Amer. Geophys. Union., 62, 942 p.
- Lutjeharms, J.R.E. (1981a). Features of the Southern Agulhas Current circulation from satellite remote sensing. Sou. Afr. Jour. of Science., 77, 231-236.
- Lutjeharms, J.R.E. (1981b). Spatial Scales and intensities of circulation in the ocean areas adjacent to South Africa. Deep.Sea.Res., 28, 1289-1302.
- Lutjeharms, J.R.E. and Emery, W.J. (1983). The detailed thermal structure of the upper ocean layers between Cape Town and Antarctica during the period Jan-Feb, 1978. S. Afr. Jour. Antar. Res., 13, 4-14.
- Lutjeharms, J.R.E. and Valentine, H.R. (1984). Southern Ocean thermal fronts South of Africa., Deep. Sea Res., 31, 1461-1475.
- Lutjeharms, J.R.E. (1985). Location of frontal system between Africa and Antarctica Some preliminary results., Deep. Sea. Res. 32, 1499-1509.
- Lutjeharms, J.R.E. and Walters, N.M. (1985). Ocean colour and thermal fronts South of Africa. In: L.V. Shannon (Editor), The South African Ocean Colour and upwelling Experiment, Sea Fisheries Research Institute, Cape Town.
- Lutjeharms, J.R.E. and Foldvik, A (1986). The thermal structure of the upper ocean layers between Africa and Antarctica during the period Dec. 1978-March 1979. S. Afr. Jour. Antar. Res., 16, 13-20.
- Lutjeharms, J.R.E., Fromme, G.A.W. and Valentine, H.R. (1986). Die termiese oseaanstruktuur Suid Van Afrika. Verslagoor sestien navorsingsvaarte. WNNR Navorsingsverslag, 390.
- Lutjeharms, J.R.E. and Valentine, H.R. (1988). Eddies at subtropical convergence South of Africa., J. Phys. Oceano., 18, 761-774.



- Mackintosh, N.A. (1946). The Antarctic convergence and the distribution of surface temperatures in Antarctic waters. Discovery Reports, 23, 177-212, Plates I-XIV
- McCartney, M.S. (1977). Subantarctic Mode Water. In: Voyage of Discovery, ed. M. Angel., 103-109.
- ☆ Meinardus, W. (1923). Meteorologische Ergebnisse der Deutschen Sudpolar Expedition 1901-1903 Deutsche Sudpolar Expedition III, Meteorologic.
- Menon, H.B., Ramesh Babu, V. and Sastry, J.S. (1988). Apparent Relationship between Thermal Regime in Antarctic Waters and Indian Summer Monsoon. I. Jour. Mar. Sc., 17, 87-90.
- ☆ Midttun, L. and Natvig, J. (1957). Pacific Antarctic Water. Sci. Res. Norweg "Bratigg" Exped. 1947-1948, 3, 1-130.
- Molinelli, E.J. (1978). Isohaline Thermoclines in the Southeast Pacific Ocean. J. Phys. Oceanogr., 8, 1139-1145.
- Molinelli, E.J. (1979). Isopycnal transport by the Antarctic circumpolar current and the Antarctic influence at intermediate water densities. Ph.D. Dissertation, Columbia Univ., New York, 216 p.
- Molinelli, E.J. (1981). The Antarctic influence on Antarctic intermediate water. J. Mar. Res., 39, 267-293.
- Montgomery, R.B. and Stroup, E.D. (1962). Equatorial waters and currents at 150°W in Jul Aug. 1952. Johns Hopkins Oceanogr. Studies, 1, 68 p.
- Mooers, C.N.K., Collins, C.A. and Smith, R.L. (1976). The dynamic structure of the frontal zone in the coastal upwelling region off Oregon. J. Phys. Oceanogr. 6, 3-21.
- ☆ Mosby, H. (1934). The waters of the Atlantic Antarctic Ocean Norwegian Antarctic Exped. 1927-1928. Sci. Results Vol. 1, 112-133.

- Munk, W.H., and Palmen, E. (1951). A note on the dynamics of the Antarctic circumpolar current. Tellus, 3, 53-55.
- Naqvi, S.W.A. (1986). Some oceanographic observations in the polynya and along a section in the Southwest Indian Antarctic Ocean. Scientific Report of Third Indian Expedition to Antarctica, Tech. Publ. No.3, 75- 85.
- Neumann, G. and Pierson, W.J. (1966). Principles of Physical Oceanography Prentice-Hall, Engle-wood Cliffs, N.J.
- Nieman, W.A. (1965). Sea temperatures between Cape Town and Antarctica. S. Afr.Geogr. J. 47: 41-44.
- Nowlin, W.D., Whitworth III, T. and Pillsbury, R.D. (1977). Structure and transport of the Antarctic circumpolar current at Drake Passage from short-term measurements. J. Phys. Oceanogr., 7, 788-802.
- Nowlin, W.D. Jr. and Clifford, M. (1982). The Kinematic and Thermohaline zonation in the Antarctic circumpolar current at Drake Passage. J. Mar. Res., 40, 481-507.
- Okubo, A. (1970). Horizontal dispersion of floatable particles in the vicinity of velocity singularities such as convergences. Deep. Sea. Res. 17, 445-454.
- Orlanski, I. (1969). The influence of bottom topography on the stability of jets in a baroclinic fluid. J. Atmos. Sci. 26, 1216- 239 .
- Orlanski, I and Cox, M.D. (1972). Baroclinic Instability in Ocean currents. Geophys. Fluid. Dynam. 4, pp: 297-332.
- Ostapoff, F. (1962a). On the fictionally induced transverse circulation of the Antarctic circumpolar current. Dt. hydrogr. z. 15, 103-113.
- Ostapoff, F. (1962b). The salinity distribution at 200 m and the Antarctic frontal zones. Dt. hydrogr. z., 15, 133-141.

- Pak, H. and Zaneveld, J.R.V. (1974). Equatorial front in the Eastern Pacific Ocean. J. Phys. Oceanogr. 4, 570-578.
- Peterson, R.G., Nowlin, W.D. and Whitworth, T. (1984). Generation and Evolution of a cyclonic ring at Drake Passage in early 1979. J. Phy. Ocea. 12, 712-719.
- Pingree, R.D. and Mardell, G.T. (1981). Slope turbulence, internal waves and phytoplankton growth at the Celtic Sea Shelf-break. Philo. Trans. R. Soc. Lond A302: 663-682.
- Pillsbury, R.D. and Bottero, J.S. (1984). Observations of currents rings in the Antarctic zone at Drake Passage. J. Mar. Res., 42, 853-872.
- Planke, J. (1977). Phytoplankton biomass and productivity in the subtropical convergence area and shelves of the western Indian subantarctic islands. In. Adaptations within Antarctic Ecosystem, (ed. by G.A. Llano), 51-128.
- Pomazanova, N.P. (1980). Divergence of drift currents in the Antarctic sector of the Indian Ocean. Tr. gidromet. Inst. 80, 110-115.
- Rama Raju, D.V. and Somayajulu, Y.K. (1983). Some physical characteristics of the Antarctic and western Indian Oceans. Scientific Report of First Indian Expedition to Antarctic, Tech. Publ. No. 1, 53-61.
- Rao, P. Krishna, A.E. Strong and Koffler (1971). Gulf stream meanders and eddies as seen in satellite infrared imagery. J. Phys. Oceanogr., July 1971, 3(1). (Pp) ?
- Rao, C.V. and Murty, W.S. (1973). Some case studies of vertical circulations associated with oceanic fronts. J. Geophys. Res., 3, 549-557.
- Reid, J.L. and Nowlin, W.D. Jr. (1971). Transport of water through the Drake Passage. Deep. Sea. Res., 18, 51-64.
- Riley, G.A. (1946). Factors controlling phytoplankton populations on Georges Bank. J. Mar. Res., 6, 54-73.

- Ryther, J.H., Menzel, D.W. and Corwin, N. (1967). Influence of the Amazon River outflow in the ecology of the western tropical Atlantic I. Hydrography and nutrient chemistry. J. Mar. Res., 25, 69-83.
- Sarukhanyan, E.I. (1985). Structure and variability of the Antarctic circumpolar current. Amerind Pub., New Delhi, 108 pp.
- Savchenko, V.G., Emery, W.J. and Vladimirov, O.A. (1978). A cyclonic eddy in the Antarctic circumpolar current South of Australia, Results of Soviet-American Observations aboard The R/V Prof. Zubov, J. Phys. Oceanogr., 8, 825-837.
- ☆ Schott, G. (1926). Geographic des Atlantischen Ozeans, 1st ed., Hamburg, (2nd ed., Hamburg, 1944) 438 pp.
- ☆ Schott, G. (1935). Geographie des Indischen und Stillen ozeans. Hamburg, C. Boysen Verlag, 413 pp.
- Seitz, R.C. (1967). Thermostat, the antonym of thermocline. J. Mar. Res., 25, 203.
- Sievers, H.A. and Emery, W.J. (1978). Variability of the Antarctic Polar frontal zone in the Drake Passage Summer 1976-1977. J. Geophys. Res., 83, 3010-3022.
- Stommel, H. (1957). A survey of ocean current theory. Deep Sea Res., 4, 149-184.
- Sverdrup, H.U. (1933). On vertical circulation in the ocean due to the action of wind with application to conditions within an Antarctic circumpolar current. Discovery Rept., 7, 134-170.
- Sverdrup, H.U., Johnson, M.W. and Fleming, R.H. (1942). The Oceans. Their Physics, Chemistry and Biology, Prentice-Hall, Inc., 1-1087.
- ☆ Taljaard, J.J. (1958). Sea temperature observations between Cape Town and SANAE. Notos, 7, 199.
- Taylor, H.W., Gordon, A.L. and Molinelli, E. (1978). Climate characteristics of the Antarctic Polar Front zone. J. Geophys. Res., 9, 4572-4578.

- Tchernia, P. (1980). Descriptive Regional Oceanography. Pergaman Press Ltd., Oxford, 1-253.
- Voorhis, A.D. and Hersey, J.B. (1964). Oceanic thermal fronts in the Sargasso Sea. J. Geophys. Res., 18, 3809-3814.
- Voorhis, A.D. (1969). The horizontal extent and persistence of thermal fronts in the Sargasso Sea. Deep Sea Res., 3, 46-55.
- Welander, P. (1963). Steady plane fronts in a rotating fluid. Tellus, 1, 33-43.
- Wexler, H. (1959). The Antarctic convergence or divergence? In: Atmosphere and Sea in motion, (ed. B. Bolin), 107-120.
- Whitworth, T. III and Nowlin, W.D.Jr. (1987). Watermasses and currents of the Southern Ocean as the Greenwich Meridion. J. Geophys. Res. 92, 6462-6476
- Wietak, Z, Pastuszak, M. and Grelowski, A. (1982). Net phytoplankton abundance in western Antarctic and its relation to environmental conditions. Meeresforschung, 29, 166-181.
- ☆ Witte, E. (1902). Zur Theorie der Stromkabelungen. Gaea, Koln, 484-487.
- Wright, L.D. and Coleman, J.M. (1971). Effluent expansion and interfacial mixing in the presence of salt wedge, Mississippi River delta, J. Geophys. Res., 76, 8649-8661.
- ☆ Wust, G. (1928). Der ursprung der atlantischen Tiefenwasser. z. ges. Erdk. Jubilaums Sonderband, 506-534.
- ☆ Wust, G. (1933). Das Boden Wasser und die Gliederung der Atlantischen Tiefsee, in "Wissenschaftliche Ergebnisse der" Deutschen Atlantiscchen Expedition Meteor, 1925-1927, 1-106.
- ☆ Wust, G. (1935). Die Austbreituny der Antarktischen Boden Wassers Atlantischen and Indischen Ozeans. Z. Geophys., 2, 1-49.

- Wust, G. (1936). Schichtung und Zirkulation des Atlantischen Ozeans. Die Stratosphere wissenschaftl. Erg. Dt. Atlant. Expdn. Meteor., 6, 1925-1921.
- Wyrтки, K. (1960). The Antarctic circumpolar current and the Antarctic Polar Front. Deut. Hydro. z, 4, 153-173.
- Wyrтки, K. (1961). Scientific results of marine investigations of the South China Sea and the Gulf of Thailand. Physical Oceanography of the Southeast Asian Waters, NAGA Report, 21, pp 195.
- Wyrтки, K. (1966). Oceanography of eastern equatorial Pacific Ocean. Annual reviews of Oceanography and Marine Biology.
- Wyrтки, K. (1971). Oceanographic atlas of the International Indian Ocean Expedition, National Science Foundation, Washington D.C., pp 531.
- Wyrтки, K. (1973). Physical Oceanography of the Indian Ocean In: Biol. of the Indian Ocean. (eds. B-zetzchel and S.A. Gerlach), Ecol. Studies, Berlin, Springer Verlag, 3, 18-36.
- Zillman, J.W. (1970). Sea surface temperature gradients South of Australia. Australian Meteorological Magazine, 18, 22-30.

☆ Not referred in original